# Noise source location in the built environment, using a simple microphone array

by

**Michael Latham**

A thesis submitted to the University of Plymouth in partial fulfilment for the degree of

## Doctor of Philosophy



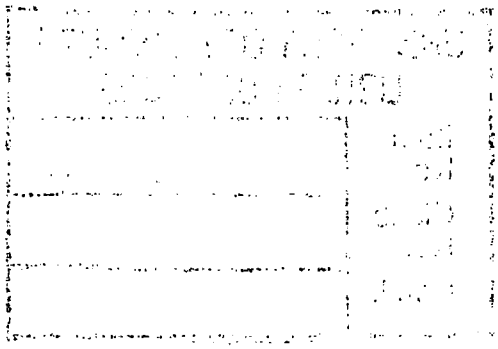



School of Architecture
Faculty of Technology

in co-operation with the University of Salford and Cornwall College

## March 1994

# Abstract

## Noise source location in the built environment, using a simple microphone array.

**Michael Latham**

An inadequate level of noise attenuation provided by a building element is frequently the result of a lack of completeness in the construction. This often invisible fault acts as a noise source in a room, so in order to undertake remedial work the source position must be found. Recently, near field noise intensity measurement has been the popular method for noise source location in buildings. This method of using intensity studies requires a grid of readings to be taken. An alternative method, the one used in this work, employs a different strategy. Here, the source location is identified by direction scanning of time delays at a number of microphones arranged in a regular three-dimensional array.

A novel arrangement of seven microphones, in the shape of a wheel-brace, is used to measure the differences in time taken for the sound waves to travel from a source to the various microphones. The magnitudes of these time differences are combined and converted into the coordinates of the source, relative to an origin which is placed at the centre of the wheel-brace array. The mathematics for this conversion is derived and the errors in the experimental arrangement discussed.

The use of this array for the identification of faults in built structures is explored. A significant contribution is made to the knowledge of noise source location in buildings, since the microphone array is used to demonstrate the location of a noise source irrespective of the direction of the incoming noise.

The use of computerised data collection is described for a budget system, where time was cheap, but equipment expensive. The accuracy of the technique would be improved considerably if state-of-the-art electronics were used to measure the time differences. The feasibility, advantages and potential performance of a modern system, that could be assembled today, is described and discussed.

# Contents

# Figures and Tables

**Chapter 3**



**Chapter 4**



**Chapter 5**



**Chapter 6**

# Acknowledgement

The invaluable assistance of Dr. Martin Williams, of Brüel & Kjær, is gratefully acknowledged. His advice, support and use of equipment in the development of the system used in the research was most appreciated.

Biodata supported the research by demonstrating the newer technology and the latest software for data acquisition.

In particular, Dr. Richard Griffiths must be thanked for his conscientious scrutiny and careful steering of the research throughout its development and fulfilment.

Finally, but not least, my family must be acknowledged for their tolerance and encouragement during the disruption from housing the equipment used for the practical work.

# Author's Declaration

At no time during the registration for the Degree of Doctor of Philosophy has the author been registered for any other University award.

The study has been privately financed, but the initial practical work was funded by the Lockheed International Research Institute.

The programme has been supplemented by assistance from manufacturers and suppliers of equipment, consultancy work and software developers. Several seminars and courses have been attended during the study period.

# PREFACE

This research was considered following a project undertaken in conjunction with the Lockheed International Research Institute of America. At that time, Lockheed was concerned with the recognition and location of aircraft by acoustic means. For this work an acoustic array system had been assembled and computer software developed to analyse and present the data. At the conclusion of the work, the equipment had no immediate use. The current research applied this acoustic array and associated hardware to noise source location in the built environment.

In investigating the break-out of noise, either between spaces in the same building or from buildings, the problem is usually to identify the weak areas in the construction that is allowing the escape of a disproportionate amount of the sound energy. Problems associated with the conversion of old property into sheltered accommodation for the elderly have shown that sound insulation between adjacent flats is extremely important. Where old buildings have been modified, it is not uncommon to find that old chimney areas have been covered with light weight panelling and partition walls erected without much regard for the sound attenuating qualities of the overall structure. As is so often the case, consultants are only approached when problems are noted, usually long after the builders have completed the structure and departed. Any method which could show where voids in partitions have been left without having to make much disturbance to the residents, would obviously be a tremendous boon. Techniques are available, such as sound intensity measurements, but unless there is a proven demand that can ensure the frequent use of such equipment, it is extremely difficult to make an argument for its purchase. In addition, the system requires that a sequence of readings be taken and processed, so that it is not in any way, a real time measurement. From the literature dealing with various techniques employing acoustic arrays, it was concluded that arrays could offer a real time solution to identifying the position of sound peaks on the surfaces of building facades by constructing a scanning device that could produce an acoustic picture of a surface.

This research work does not claim to have produced such a solution, but rather to have established the feasibility of the solution by showing that the equipment needed is now available and the analysis techniques are possible. It is believed that a compact device could be produced that would be a definite diagnostic help, relatively economic to construct and use.

*Chapter 1*

# Introduction

# INTRODUCTION

The investigation of the location of a noise source from an array of microphones is not new. In the First World War, enemy gun positions were located by the use of four 'horns' as the equivalent of the microphone. Defence industry underwater research has produced evidence of the location of sources by the placement of hydrophones. The intention of this research was to use relatively cheap equipment to find imperfections in building elements, such as floors and walls, by the location of noise spots on a surface. Since the start of the work, much has changed. Other research has developed mathematics for analysis of noise from distant sources. Defence research has investigated location of moving vehicles, employing state-of-the-art computer technology. The original equipment used in this work was based upon a computer with 64 k memory and a speed of processing that does not even match many hand held calculators of today. For example, the analogue to digital (A to D) conversion systems have increased in speed and computers have become faster, with more software available for intensive calculation and analysis, but at a cost. This research programme has had to be completed on available equipment and, therefore, any conclusions reached can be expected to be considerably enhanced by more effective and newer equipment.

In parallel with this work, other research teams have made even more striking advances. For instance, D.J.Oldham, of Liverpool University and X Zhao of UMIST, have used acoustic intensitometry to measure the size of the straight through cracks in partitions. Therefore, this research must be seen as an introduction to relatively portable equipment of reasonable cost, that could provide short test methods for identification of acoustic weaknesses in building components of a completed structure.

## History of project - Previous Research

The use of the sound generated by a process to identify its position has been a technique used for a considerable time. Sound ranging was invented by a French Astronomer, Professor Ernest Esclangon, at the beginning of the first World War [Esclangon, Ernest, "L'Acoustique des

Canons et des Projectiles," Memorial de L'Artillerie Française IV, 3, 639 - 1026, Imprimerie Nationale, Paris 1925][65]. The effective detection of enemy artillery was well established in the Second World War and in the Korean conflict. The advantage of acoustical soundings was that they were not capable of electronic jamming and required minimal training of personnel to use the equipment. The major disadvantage was the effect of atmospheric errors. In the 1970's the method was to use six microphones, a waveform recorder with time marker and a communication observer who initiates recording on hearing enemy gunfire. The microphones were normally installed along a straight line at intervals of 1350.4 metres [65].

In 1954 Kenneth Goff [25] discussed the application of an analog correlator, which computed the cross correlation function between two sound pressures for three applications (i) for the location of noise sources, (ii) for the determination of transmission loss and (iii) for the reduction of microphone wind noise. In the paper he points out that the cross correlation function between two nonperiodic signals will have a peak in amplitude, if a component of each signal originates from a common source. The value of the time delay for which this peak occurs equals the difference in time required for the individual components to propagate from the common source to the two points under study. An analog electronic correlator, which was described in a companion paper [67][68], was constructed. By employing the property of the cross correlation function, it was possible to separate the acoustic signals into components according to their points of origin, the transit time from source to a given point and to the frequency. He concluded that correlation provides a practical method for determining the amount of sound contributed to the total acoustic field at a given point by each of several sources. He further concluded that the correlator, by separating the signal transmitted directly through the wall from the flanking signal on the basis of arrival time, was a useful tool for measuring the transmission loss of walls. The correlator in these experiments consisted of recording magnetically upon a revolving drum and using the angular separation of the record and replay head movements to alter the time delay, thus changing the angle through which the drum rotates while the signal is stored upon it. A delay of between -15 and 190 ms was possible. The two signals from the time delay mechanism were applied to a vacuum tube squaring device and the signals integrated by a low pass RC filter. The output of the integrator was applied to plotters having both logarithmic and linear scales. The motion of the paper through the plotters was synchronised with the motor drive that changed the time delay thus enabling the cross

correlation function to be plotted automatically. In considering the transmission loss through panels Goff argued that a continuous signal had the advantage of not requiring control over the source and it was not necessary to deliver a large amount of energy over a short period.

In 1957 Berman and Clay [5] investigated the directional characteristics of a linear array of omnidirectional receiving elements. They concluded that the same directional characteristics can be achieved from the time averaged product of a relatively small number of sensors as with a large number of elements of an additive array. Alternative correlator systems to the additive array, required that the correlator was steered in a mechanical fashion, for instance, steering the correlator in a two receiver correlation system by rotating the axis of the two receivers. In such a case, the finiteness of the source distance does not introduce a directional error. Where mechanical steering is difficult, or impossible, then a time delay steering method must be used and a directional error for sources close to the receivers has to be accepted. A two-receiver steerable correlation system intended to process signals from point sources at a large distance from and in a common plane with the receivers, will give a predicted source direction, which is generally different from the actual source direction, when the source to receiver distance is small. Such was the opinion expressed by Melvin Jacobson [35] in 1958. He excepted the cases of broadside, or end-fire sources, for which the actual and predicted directions are equal, but that apart, the predicted direction is always closer to the broadside than the actual direction.

In the 1960's work on noise sources underwater using hydrophone arrays showed that split beam trackers were nearly optimal for uniformly spaced arrays. Further work was carried out on the arrangement of the sensors to give optimal range and bearing calculations.

Hinich [32], in a paper in 1978, stated "A linear array can detect a plane wave signal at the wrong bearing if the signal wavelengths are shorter than twice the distance between the closest adjacent sensors." This phenomenon is called spatial aliasing and is greatest when the bearing is near endfire. In the paper a solution using a frequency-wavenumber approach is explained.

The paper of Landers and Lacoss [41] explained how they used a triangular array and the use of conventional and maximum likelihood high resolution frequency-wavenumber array analysis techniques for finding the bearing of aircraft from the noise emitted.

A system was developed for the real-time sound source location on full-size jet engines by Billingsley and Kinns, in the Department of Engineering at the University of Cambridge, in

1970's. It consisted of an array of microphones connected to a small digital computer via a sequence of preamplifiers, analog filters and analog to digital convertors. Microphone signals were processed to give on-line displays of time varying source distributions, or statistical averages with respect to position and frequency.

The Acoustic Telescope of Billingsley and Kinns [6], reported in 1976, used 6.35 mm B&K capacitance microphones, type 4135, energised at 150 volts. Their output at 0.15 mV per $\mu$bar from an impedance of 6pF required a high input impedance preamplifier to obtain a flat response down to 30 Hz. The upper limit for the system was 80 KHz. The preamplifier had a gain that could be remotely switched to maintain a reasonable signal in the 100 m cable between the microphones and the centre console. Each preamplifier was housed within a 25.4 mm diameter tube, which formed part of the microphone mounting. The microphone capsule was located at the end of a length of 6.35 mm tube blended to the 25.4 mm tube with a shallow conical section. Individual microphone cables were gathered to a nearby junction box and then connected to the console by two multiple cables. The console had gain controls for each channel, allowing switching in 10 dB steps for recordings of sound pressure level between 60 and 140 dB (relative to $2 \times 10^{-4}$ $\mu$bar). Connections were provided for record and playback to an Ampex FR-1300A 14 channel tape recorder. Signals were passed to an anti-aliasing filter circuit, containing fourteen channels of low pass filters. The signals were converted to digital form by sampling in pairs at 6 $\mu$s intervals and digitised to 8-bit precision. The spread of 36 $\mu$s, over which the samples were collected, had the effect of imparting a slight squint to the telescope. The computer was a CAI LSI-2 with a memory capacity of 48 kB. The analysis software was written within a Fortran framework. The results were stored on disc with a storage capacity of 0.3 Mb. The whole system was transportable, but required mains electricity to drive it.

The analysis used was a simple additive process. Once a data set had been recorded various analysis techniques were used including frequency domain applications [70], and also cross products of partial sums could be used. A mathematical statement of the theory of the acoustic telescope was given.

The statistical errors associated with spectral density estimates were discussed. These were believed to be proportional to a chi-square distribution with $n_f$ degrees of freedom [39], where $n_f$ is twice the number of data segments multiplied by a factor determined by the procedures

for data modification. Also discussed were the effects of environmental defects. It was noted that the theory required that the microphones be as far away as possible from the source region. As the distance increases, however, reflections from remote objects and other sources of extraneous noise become more significant, while wind and temperature gradients , atmospheric absorption and surface roughness increase in importance with the greater distance. Therefore, a compromise distance had to be devised, which showed the advantage of an on-line system to determine optimum conditions with the minimum of delay.

The software was written to offer a diversity of analysis techniques. An initialisation program was run to set up the number of parameters and constants. The program interrogated the user to find such parameters as number and location of microphones, logging speed and the required focal positions. The program allows the user to specify the frequency range required. The processing time for 14 microphones at 129 frequencies was 5 seconds per data segment.

A paper presented in Noise Control Engineering Sept-Oct 1984 detailed an arrangement by Boone and Berkhout for monitoring the sources of industrial noise from a distance [7]. The idea of using an acoustic array in this present research was a development from the use of acoustic arrays for the determination of sources of sound in the jet stream of aircraft engines and in particular, the use of an Acoustic Telescope [6]. In all these cases the concept was to collect data from a number of transducers and then compare the shift in the waves by mathematical analysis, and, hence, calculate the noise source coordinates relative to a given origin. The source in these examples was noise generated within a system rather than a superimposed noise used as a tracer.

In the paper by A.D.Broadhurst [8] the possibility of using an acoustic array for identifying the sound sources within enclosures was described. It was suggested that the array may be useful in studying diffusion and the acoustical sensation of space. It was pointed out that the limitations of the Billingsley Kinns Acoustic Telescope were that;

a) the sources must occur in a straight line

b) the problem of spatial aliases causes confusion

c) the existence of side lobes, again confuses, and

d) the resolution is a function of frequency.

Broadhurst suggested the use of 125 microphones as a reasonable compromise between the number of microphones and the resolution of the system. He further showed that there was

good repeatability of impulse sounds produced by a loudspeaker in an auditorium. It was suggested that the directionality of the system could be of use in overcoming public address system problems. This could be by developing a directional microphone (from the array system) that could be adjusted from some remote situation to change the directional characteristics.

Employing a cubic array of 125 pressure microphones, with a suitable additive processing of the microphone signal data should allow the telescope to be focused in any direction. The directivity patterns indicated that a mean halfpower beamwidth of 32° may be realised in the 1000 Hz octave band. The system could be used to measure the directional distribution of sound field components in auditoria, and the coherence between different reflections, which is a measure of the acoustical sensation of space.

With the present experimental arrangement it was soon realised that the limited computing power and complex mathematics would constrain the project, so the aim became to ignore the possibility of calculations done in real-time. Rather, to determine a simple mathematical basis to allow the time shift information, that could be obtained with reasonable accuracy and resolution, to give the noise source location. This work would concentrate on investigating a practical arrangement that could offer good information at acceptable confidence limits. This led to a number of modifications in the original concept for this work, which will be discussed in the next section.

The paper by Boone and Berkout [7] deals with the construction of a microphone array to produce a directional system. The reason for the system was to produce the equivalent of a highly directional microphone that enabled the noise emission from a source to be measured and analysed. This array allowed the contribution of the different noise sources to be identified and quantified. The microphone needed good directivity - at least to within one or two degrees to effect good separation of the sources under investigation. The directivity of the linear array is obtained simply by adding the output signals of the individual microphones [6]. A disadvantage of the linear array is that to avoid spatial aliasing a large number of microphones is required. The 'sparse microphone' array uses a different mathematical approach [31] so that the separation, based upon the two-dimensional Fourier transform of the space time correlation

functions of the microphone array elements, allows the same resolution for the telescope, with less microphones.

In most of these examples the source of the signal is a continuous noise, so that spatial aliasing is an important feature. The alternative approach is to limit the duration of the signal and measure time delays when the spatial aliasing effect can be eliminated by the geometry of the microphone array. However, in using pulsed sound, one is no longer studying the noise emitted by a source, but rather using the noise burst as a diagnostic tool to investigate the acoustic properties of the medium through which the sound is travelling. In acoustic imaging, short wave or ultra sound is used to achieve the resolution. In the context of this research, a frequency range of 100 to 4000 Hz has been considered, so that small obstacles will be invisible to the collection system.

*Chapter 2.*

# Aims of Research

# Aim of the research

For the Acoustic Consultant involved in solving problems associated with the built environment, the usual difficulty is that problems become apparent after a project is completed. The fact that the cost of remedial work is large, compared with a low initial cost if the problem is anticipated at the design stage, is rarely appreciated. The problems are further compounded by the fact that once a building is completed, exactly how the structure is put together beneath the decorative finish is seldom known.

It has long been believed that if there was a simple technique, which would identify that a problem exists, as well as identify the cause of the problem, then remedial work would be cheaper and probably more cost effective. For example, problems are often encountered in the conversion of large, older property to multi-occupancy. When built, the property is advertised as suitable for retired persons, and the first set of occupants move in and find everything satisfactory. With subsequent changes in tenancy, younger families move in, or some of the elderly residents have young families visiting. Complaints then start because young children tend to move more quickly than the elderly. The sound insulation of the floors is shown to be lacking. The slamming of doors in upstairs flats resounds throughout the entire building. Conversations between the younger relatives and the hearing impaired occupant are enjoyed by all residents.

Undertaking sound insulation measurements, because it is suspected that the fabric of a building is the cause of the complaints about intrusive noise, often shows that the sound transmission loss between floors is well below the required standards. This can be rectified, with stock remedies, such as placing additional floor panels or suspended ceilings. If it were possible to detect whether the problem were due to poor workmanship in that gaps had been left between bricks in a party wall, or that there was sound leakage around a ceiling, then the chance of a satisfactory conclusion would be much higher.

With the advent of sound intensity measurement equipment becoming commercially available in the mid-eighties, such investigations have become possible. Unfortunately, the use of sound

intensity requires that all the measurements are done in the near field, so that measurements are made close to the surface under investigation. A grid of readings is taken and the computer works out the noise contours. The equipment is expensive and the procedure is time consuming.

Studying articles dealing with acoustic imaging and the location of noise sources from a distance, the prospect that it may be possible to construct an acoustic device that works on a similar principle to an optical device was attractive. The acoustic telescope uses a scanning technique. The source of sound coming from an object sends acoustic waves to a device which can process the waves and in an analogous manner to the optical telescope, it can assess the source by focusing upon different points of the surface. The acoustic telescope of Billingsley[6] worked on the basis that the sources under investigation were in a straight line parallel with the axis of the linear array. The acoustic antenna of Berkout and Boone[7] were at a sufficient distance that the sound rays could be considered as reaching the acoustic array as a set of parallel waves. With the normal building problem, the source of the noise is usually tens of metres distant, and the acoustics of the enclosure are such that they will greatly affect the perception of any received acoustic signals.

The initial concept envisaged in the research programme described in this thesis, was to have sufficient microphones to act as the individual elements of a lens, and by introducing time delays at each element , to select a point on the surface and look at the amplitude-time relation of the noise coming from that part of the surface. By using a computer to control the scanning of the lens, sequential data would give rise to a 3-D plot showing the variation of the amplitude of the surface sound in relation to location and time.

This was attempted by using a continuous source of noise, and correlating successive waves from the source. The step between the waves was selected to give a focus at a particular point. All the waves were then plotted in a waterfall diagram. The waves were colour coded to represent the particular element of the lens. A most attractive display resulted, but the interpretation of the information gave no insight into the way the sound was being propagated. The sound waves were produced by the total room acoustics and the standing waves merged

with the progressive waves to create utter confusion. At this stage, the use of a single handclap was considered. This gave rise to more intelligible information and estimations of distance to the source were possible.

It now became apparent that a pulsed source of sound had advantages over continuous sound and because finite distances were involved, then equations had to be derived to calculate the position of the source from the time intervals between the reception of signals. The design of the microphone array was also changed so that the data would enable coordinates to be calculated to pinpoint the source position. The choice of the array geometry had to relate to the availability of microphones and the processing power of the ancillary equipment. It was decided to attempt simultaneous processing of data, rather than sequential, because at that stage it was not appreciated how reproducible the results were over a time period. In the light of the work done, it would be possible to take measurements at a number of locations several metres apart and combine the information so increasing the resolution of the data by effectively increasing the aperture of the telescope.

Once the configuration of the equipment was determined and the effectiveness of the method satisfactorily established, then the practicality of the system had to be evaluated. Looking at a noise such as a signal transmitted through a partition, as in the BS 2750 method for measuring sound transmission loss, then the partition is energised by the sound over its entire surface. If the transmitted sound is observed by the telescope, there are an infinite number of paths by which the sound can reach the microphones. The time delay between these paths is not apparent, because the sources are coherent, and the received wave is going to be an interference pattern of all the waves. In addition, the pattern is complicated by the fact that each wave will have a different amplitude, due to the attenuation effect of the panel. By using a pulsed source of sound, the one piece of information that is apparent, is the start of the pulse at the receptor position. However, the pulse that is received first is not necessarily the sound passing through the weakest part of the panel. If the attenuation of the panel is large - say in excess of 10 dB - then any direct sound paths due to air gaps in the structure or by flanking transmission, will have amplitudes much bigger than the attenuated waves. It should be possible to calculate the attenuation of the panel, as well as determine the source of the start of the strongest pulse, and so estimate the position of the weak link. If the received pulse is only coming through the panel,

then the indications are that the equipment will only locate the first pulse to arrive. Much more elaborate mathematical or statistical processing will be needed to separate and identify the pulses travelling through a common material by different paths.

One approach to the problem that is within the capability of this project, is to use cross correlation techniques in conjunction with auto-correlation to make better estimates of the position of specific waves. The auto-correlation shows the periodicity of the signal even where the source is random. Therefore, where the final wave is due to the interference pattern of a number of superimposed waves, the auto-correlation function should show in the first estimate, the periodicity of the successive waves. By selecting a sine wave of the same frequency and combining it with the signal, modification of the original signal can be achieved. It is then possible to use this information to perform a subtraction of the source wave from the wave received at any microphone location and then to cross correlate to get a better estimation of the wave separations. This technique should work as in the experimental situation where the multiple sources are point sources each emitting the same signal. Where the signal is affected by the transmitting medium and frequency shifts occur as well as large amplitude variations, then the problem is considerably more complicated. This problem will not be considered in any detail in this work.

The aims of this work can be summarised as:

1. To develop a mathematical model for source location using a seven microphone array with variable spacing.
2. To verify by experiment, the mathematical model.
3. To develop a computer program for collection of data and determine coordinates of the source.
4. If the model works, to consider the optimal design for a portable system.

*Chapter 3.*

# The Model

# The selection of a model for the array.

In order to determine the location of a noise source, it is necessary first to define the parameters that will enable the measurement to be made. In the first instance it must be assumed that the source is a point in space that can be defined by the use of the three coordinates x,y and z . These coordinates are measured relative to a point, normally the origin and here the reference point is $m_o$, which is the centre microphone.

The source, S, can be at any point in space, therefore the three coordinates can have negative as well as positive values. It is therefore necessary to define how negative distances can be recognised. From the various references, in particular The Acoustic Telescope of Billingsley and Kinns, it is made clear that a linear array can only distinguish the position of a source along a line. For this a number of microphones is used. For example, in the case of the Billingsley and Kinns Acoustic Telescope, the number was fourteen. If the source is to be defined in a spatial context, then a microphone array must exist in each of the reference planes. From the evidence of Billingsley and Kinns, this would suggest three arrays, each containing fourteen microphones and the arrays mutually perpendicular to each other. Such an arrangement would not necessarily indicate the difference between the negative and positive directions. The array could be modified to have the middle microphone of each array common to all three arrays. This arrangement needs the number of microphones to be an odd number. One research project had used a circular array which enabled determination of the source in a single plane with the ability to distinguish positive and negative directions, but not elevation and depression.

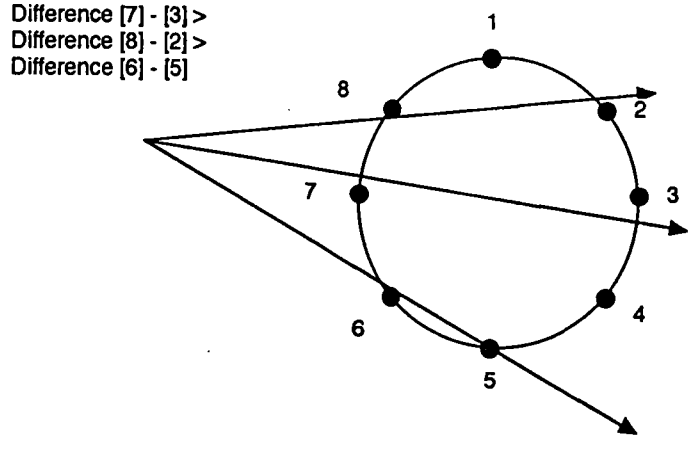


*The Circular Array Figure 3.1*

If the circular model is extended to a spherical model, then any point can be determined by reference to the centre of the sphere, if the surface of the sphere contains the elements of the array. The model can be further simplified, if the array size is reduced to three microphones. This is the smallest number of microphones in an array that can have a centre

reference microphone, and distinguish between a positive and negative direction. The complete model must possess three arrays mutually at right angles to each other and forming the coordinates about the reference microphone, which becomes the centre of the model.

## The origin of the coordinates

The particular frame of reference is for convenience only, but it is based upon accepted mathematical rules. Geometrical space is a mathematical concept to describe physical space. In it, a point has no magnitude and a line has no breadth.

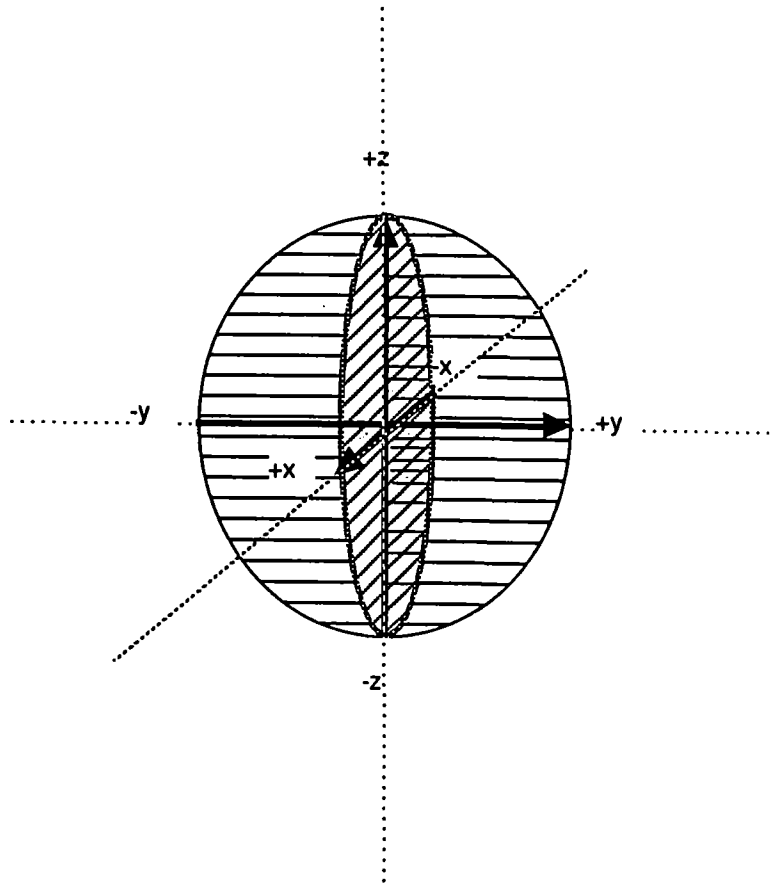


*Position of axes - Figure 3.2*

The choice of coordinates is that of a "right handed" rectangular three dimensional axes. If one was to turn a tap, or screw, or any ordinary threaded device with a right handed twist from the positive direction on the x-axis to the positive direction on the y-axis, the result would be a thrust along the direction of the z-axis.

The three planes determined by the three possible sub-pairs of coordinate axes are called the (x,y), the (x,z) and the (y,z) coordinate planes. Just as the two axes of a single plane divide the entire reference plane into four quadrants, so the three coordinate planes of a three-dimensional set divide all space into eight regions called octants. The octant in which the values of x,y, and z are all positive is known as the first octant. The other octants are not normally numbered.

Given any of the variables x,y and z, then a corresponding point in space $P_1$, is uniquely defined.

## The relation of the array to the coordinates.

The microphone array is based upon the coordinates described above and shown in Figure 3.4. The array comprises of three microphones along each coordinate direction. The higher numbered microphone represents the positive coordinate, the lower numbered microphone represents the negative coordinate and the third microphone is the reference microphone and is common to the three axes. This gives a total of seven microphones.

## Calculation of the position of the source

To find the position of a noise source from the microphone array requires three variables to be determined. They can be either the three coordinates x,y, and z, or the polar coordinates R,θ and φ, as shown in Figure 3.3. A solution could also be obtained from any three of these variables.

The direct measurement of the angular displacements would be possible by mechanical movement of the array. This was not considered an option. Another method is by finding the

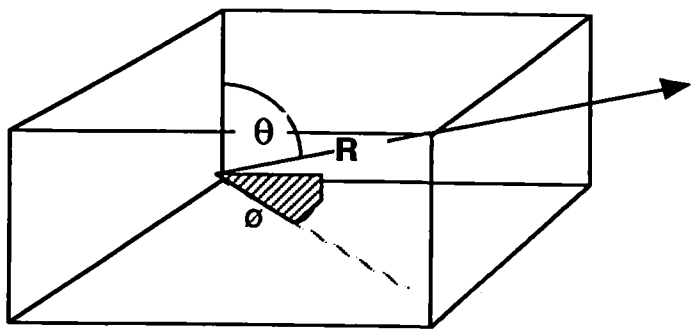


*The polar coordinates - Figure 3.3*

time differences of the signal reaching the various microphones. The limitation of this technique is only in terms of the speed at which data can be captured.

The position of the source will be identified by the angles 'α' the *altitude* and 'ø' the *bearing*. The bearing is the angle made by the projection onto the 'zy' plane, of the line 'R' that joins the reference microphone, $m_o$, to the noise source, 'S'. (See Figure 3.5)

The altitude is the angle between the line 'R' and the projection of 'R' on the (z,y) plane. It is

# Diagram showing position of microphones relative to axes.

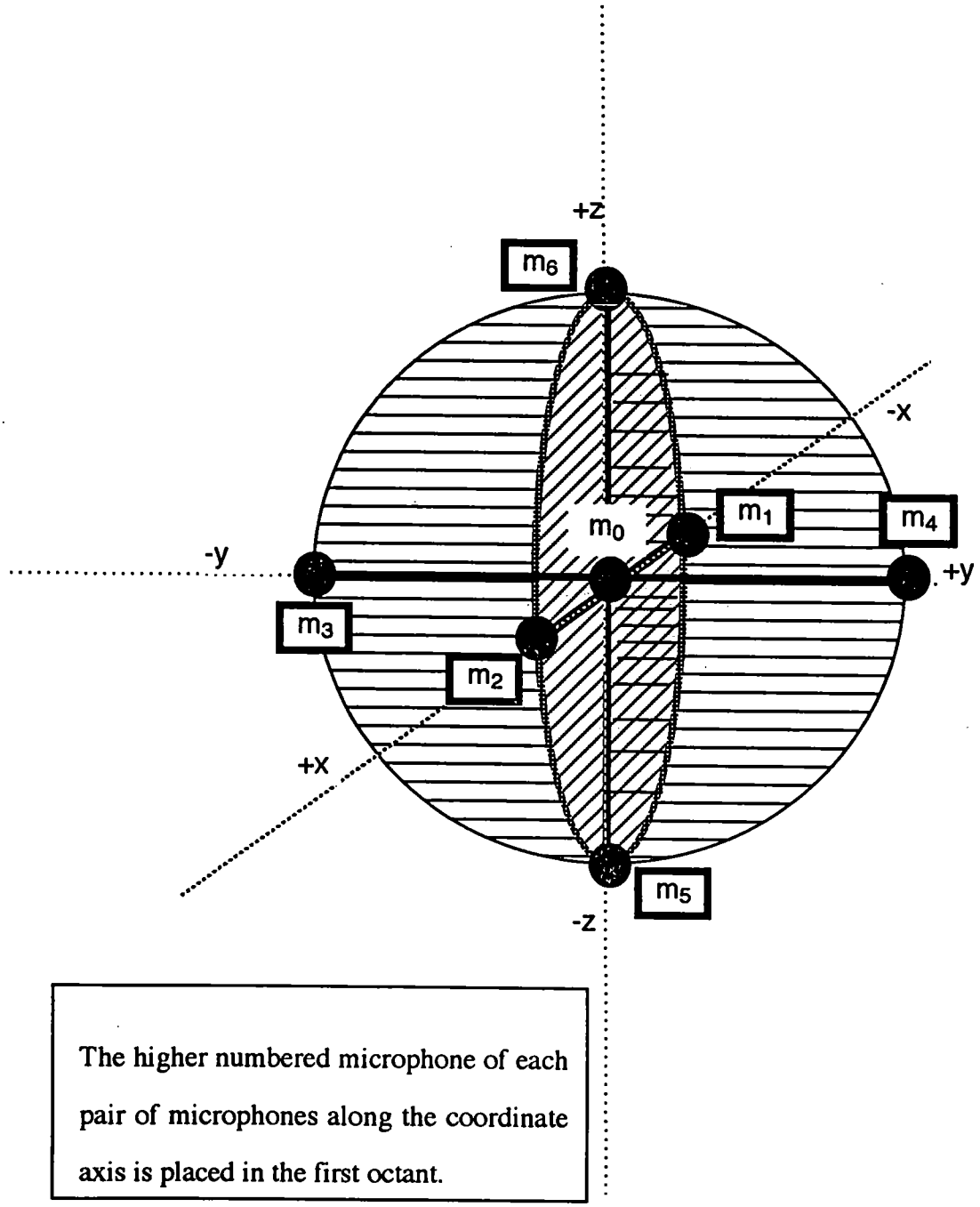


The higher numbered microphone of each pair of microphones along the coordinate axis is placed in the first octant.

*Figure 3.4 - Microphone location*

## Diagram showing the angles that are used in the mathematical equations

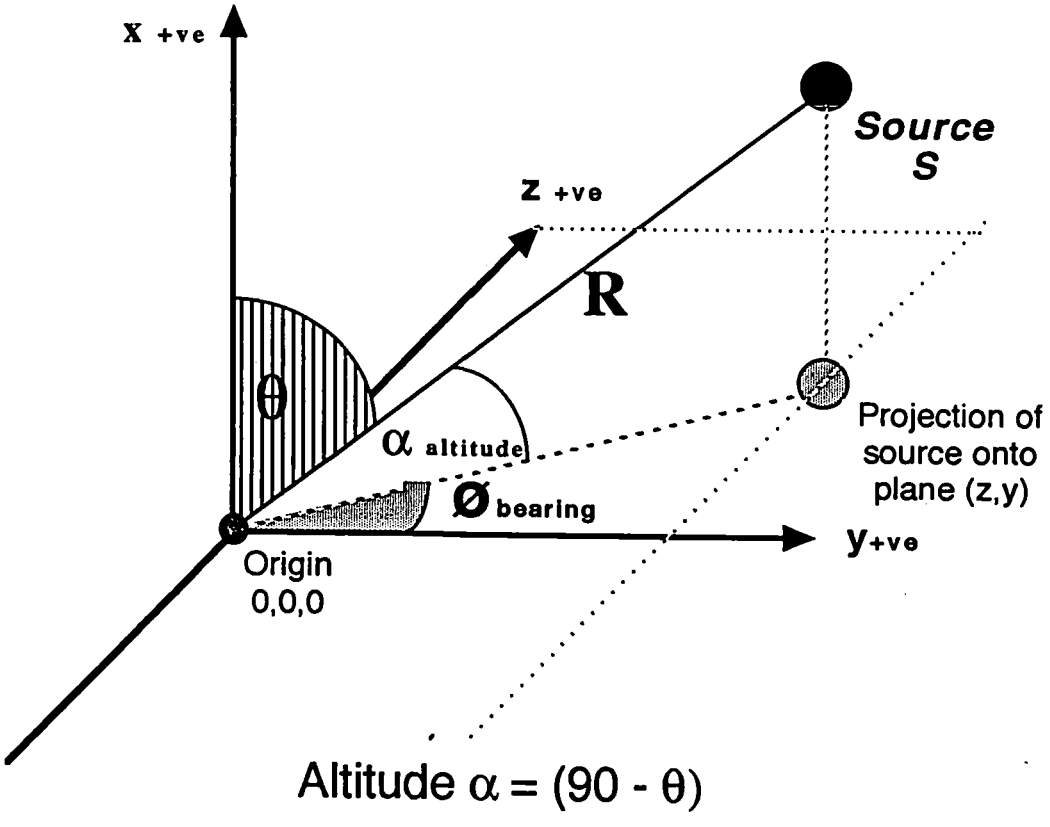


*Figure 3.5 Definition of altitude and bearing*

The angle between the projection onto the (z,y) plane of the line joining the origin (0,0,0) (which is the position of the reference microphone $m_0$), and the source 'S', to the positive 'y' axis is ø. The angle between the 'x' axis and the line joining (0,0,0) to the source is 'θ'

*Chapter 4*

# Mathematical Analysis

# Assumptions used in Mathematical Proofs

The objective was to use a 'wheel-brace' array of microphones as illustrated in Figure 4.1 The convention used to represent the source and the receiver is that of a 'Right-handed' rectangular three-dimensional axes.

The microphone is placed at the origin of the co-ordinates (0,0,0) and the source is at the position $(x_s,y_s,z_s)$ which can also be defined by the polar co-ordinates R,ø and α.

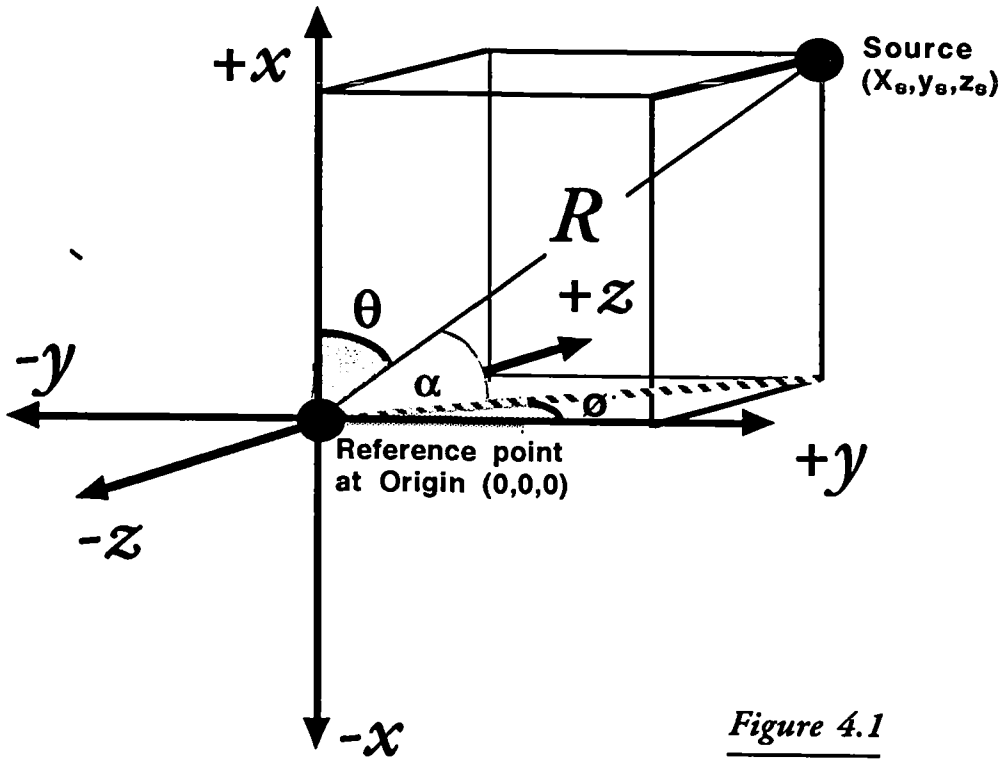


*Figure 4.1*

In order to speed the mathematics, a simple convention will be used. As stated earlier, the even numbered microphones will always be the closest of the linear pair to the source, when the source is in the positive quadrant. For example, the microphone pairs $m_1$ and $m_0$, and $m_0$ and $m_2$ lying parallel to the x-axis, then the sound will arrive at microphone $m_2$ ahead of the sound at $m_0$, while the sound arriving at $m_1$ will be delayed behind $m_0$. Microphones $m_3$ and $m_4$ are on the y-axis, $m_5$ and $m_6$ on the z-axis. The simple assumption underlying the mathematics of this technique is that these time leads and lags can be related to the difference in the distances between source and the microphones.

The microphone arrangement is shown in Figures 4.2 to 4.7. The centre microphone $m_o$ is placed at the origin of the co-ordinates. The microphones $m_1$, $m_2$, $m_3$, $m_4$, $m_5$ and $m_6$ are placed equidistant from $m_o$ along the axes at a distance 'd' metres from $m_o$. As can be seen in Figure 4.3, the distance between the reference microphone $m_o$ and any of the other microphones is a constant value 'd'. The distance 'd' will be referred to as the array 'half-distance'. To determine the source location relative to the microphone array and the co-ordinate origin, three parameters must be determined, R, ø and θ. (See Figure 4.3 for definition of the angles ø and θ).

If the distance from the source 'S' to the microphone $m_2$ is '$l$', then the time lead of the signal at $M_o$ is $(R - l) \div v$, where 'v' is the velocity of sound in air. Similarly, if the distance from the source 'S' to microphone $m_1$ is 'm', then the time lag compared to the noise at $m_o$ is $(m-R) \div v$.

The experimental technique uses bespoke software to determine the time leads and lags at the various combinations of microphones, and these times are converted into distances. The following analysis of the performance of the 'wheel-brace' array is undertaken with these distances. For example, if the time lead at microphone $m_2$ is $t_2$ seconds ahead of the signal at $m_o$, the difference in distance is represented by $x_2$.

Therefore $x_2 = R - l = vt_2$ .....[1]

By a similar argument $x_1 = m - R = vt_1$ .....[2]

By reference to Figure 4.3 and the ΔESG, where EG = 'z' and GS = 'y', then the diagonal of the plane, determined from the Theorem of Pythagoras is $ES = (y^2 + z^2)^{1/2}$ .....[3]

Using the difference between the distances of the source to $m_1$ and to $m_o$ as $x_1$ and $m_2$ to $m_o$ as $x_2$, then $l = R - x_2$ and consequently $l^2 = (R - x_2)^2$ .....[4]

The distance from microphone $m_o$ to 'E' is the distance represented by the 'x' co-ordinate and also the distance from $m_2$ to 'E' must therefore be 'x - d' where 'd' is the distance between the microphones. Therefore the distance between $m_1$ and 'E' is 'x + d'.

From the Δ $m_2$SE, then $l^2 = (x - d)^2 + y^2 + z^2$ .....[5]

By combining equations [4] and [5] $(R - x_2)^2 = (x - d)^2 + y^2 + z^2$ .....[6]

which becomes $R^2 - 2Rx_2 + x_2^2 = x^2 - 2xd + d^2 + y^2 + z^2$

but from Δ OSE, $R^2 = x^2 + y^2 + z^2$ .....[7]

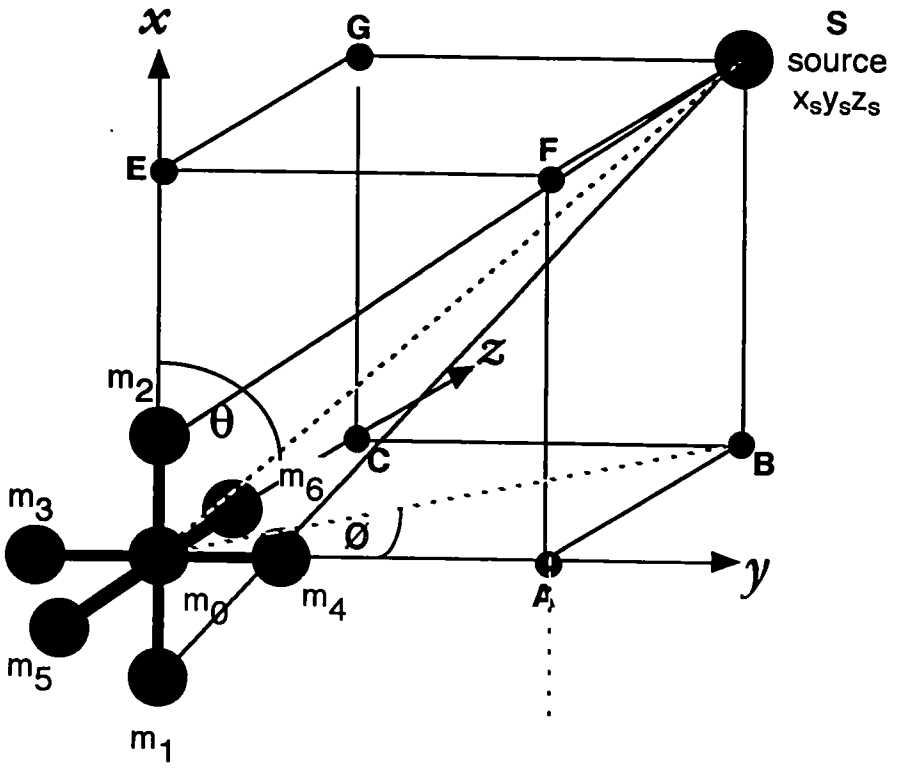


*Figure 4.2*

The reference point is the central microphone - $m_0$ - which is always placed at the origin.

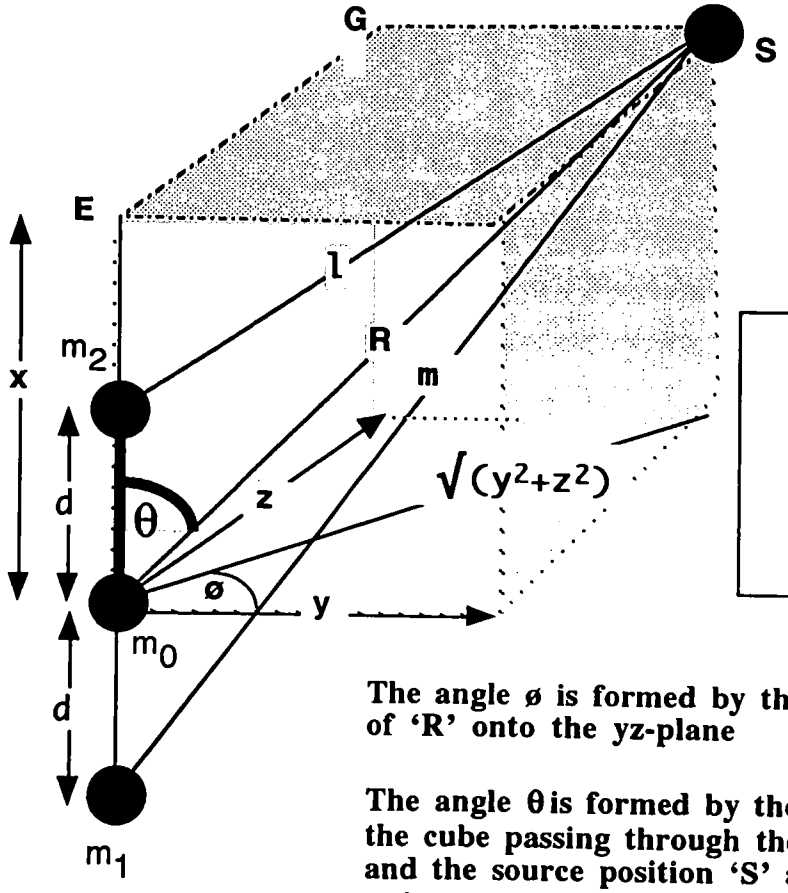


*Figure 4.3*

$R - l = x_2$

$m - R = x_1$

**The angle ø is formed by the projection of 'R' onto the yz-plane**

**The angle θ is formed by the diagonal to the cube passing through the origin 'O' and the source position 'S' and the 'x' axis.**

## *Diagrams of the geometry of the microphone array*

Therefore combining equations [6] and [7] gives $R^2 - 2Rx_2 + x_2^2 = R^2 + d^2 - 2xd$ .....[8]

But the 'x-coordinate' of the source = $R \cos\theta$ .....[9]

From equation [2] $x_1 = m - R$ or this can be written as $m = R + x_1$ .....[10]

Using the cosine rule on $\Delta OSm_1$ gives $m^2 = R^2 + d^2 - 2dR.\cos(180 - \theta)$, or

$$m^2 = R^2 + d^2 + 2dR.\cos\theta$$

which by substituting for 'm' from equation [10] becomes

$$(R + x_1)^2 = R^2 + d^2 + 2dR\cos\theta$$

This can be simplified by re-arranging the terms and cancelling $R^2$

$$2Rx_1 + x_1^2 = d^2 + 2dR\cos\theta \quad \text{.....[11]}$$

By changing equation [10] to use $x_2$ from equation [1], then $l = R - x_2$ and using the cosine rule on $\Delta OSm_2$ gives $l^2 = R^2 + d^2 - 2dR\cos\theta$, which on substituting for '$l$' gives

$$x_2^2 - 2Rx_2 = d^2 - 2dR\cos\theta \quad \text{.....[12]}$$

On adding equations [11] and [12]

$$R = \frac{2d^2 - (x_1^2 + x_2^2)}{2(x_1 - x_2)} \quad \text{.....[13]}$$

On subtracting equations [11] and [12]

$$\cos\theta = \frac{(x_1^2 - x_2^2 + 2R(x_1 + x_2))}{4dR} \quad \text{.....[14]}$$

Moving our attention to the y-axis and the line of the microphones $m_3$, $m_o$ and $m_4$ as shown in figure 4.5, exactly the same analysis can be applied with the following results. The radial distance 'R' is given by the expression

$$R = \frac{(2d^2 - (x_3^2 + x_4^2))}{2(x_3 - x_4)} \quad \text{.....[15]}$$

Using the process to determine cos ø - (see figures 4.5 and 4.7)

$$\cos\phi = \frac{(x_3^2 - x_4^2 + 2R(x_3 + x_4))}{4d(R^2 - x^2)^{1/2}} \quad \text{.....[16]}$$

Using a similar argument to derive sin ø and combining the expression with equation [16] achieves the angle ø via the tangent.

$$\tan(\phi) = \frac{(x_5^2 - x_6^2 + 2R(x_5 + x_6))}{(x_3^2 - x_4^2 + 2R(x_3 + x_4))} \quad \text{.....[17]}$$

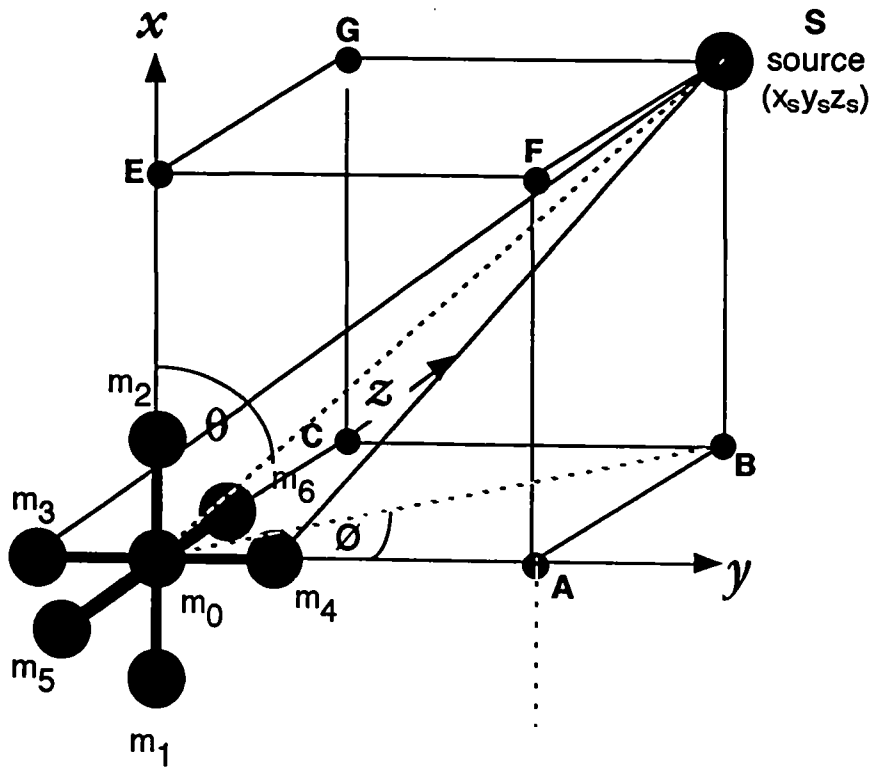


*Figure 4.4*

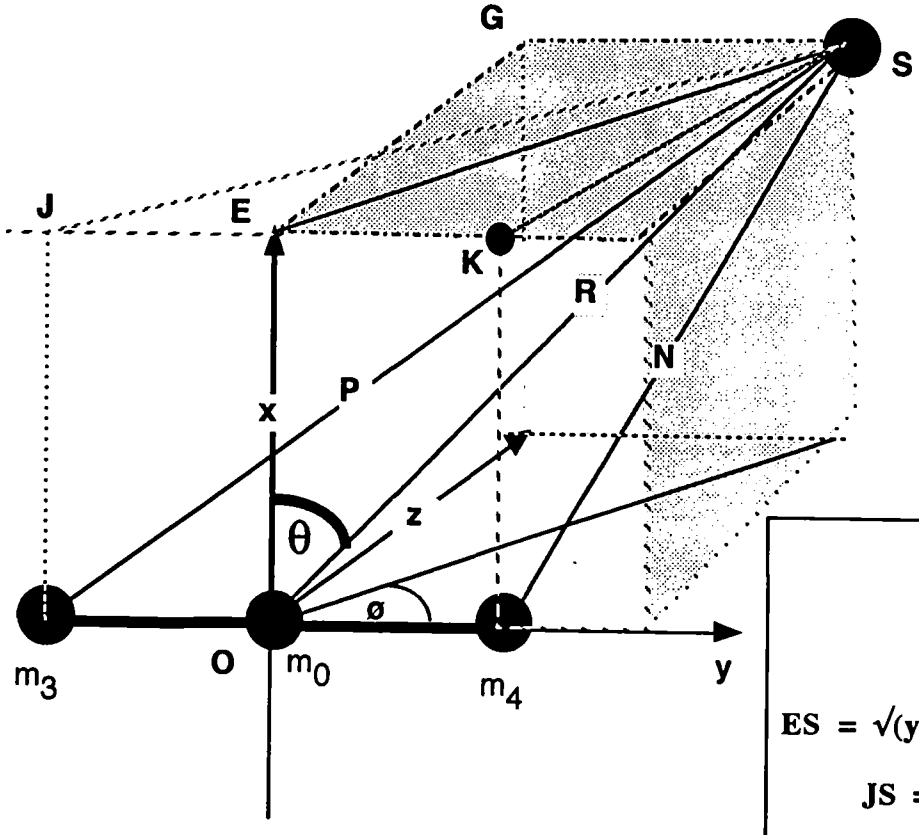


*Figure 4.5*

$P - R = x_3$

$R - N = x_4$

$ES = \sqrt{(y^2+z^2)} = \sqrt{(R^2-x^2)}$

$JS = \sqrt{(P^2 - x^2)}$

$KS = \sqrt{(N^2 - x^2)}$

***Diagram of geometry for microphones $m_3$ and $m_4$***

Figure 4.7 shows the geometry of the microphones $m_5$,$m_o$ and $m_6$, which lie in the line normal to the source plane, the z-axis. Writing Pythagoras' theorem for triangles $m_6$,$m_o$,S and for $m_5$,$m_o$,S and using $T^2 = (z_s + d)^2 + SC^2 = (R + x_5)^2$ .....[18]

and $Q^2 = (z_s - d)^2 + SC^2 = (R - x_6)^2$ .....[19]

Expanding these two equations, remembering that $R^2 = z^2 + SC^2$, and on subtracting equation [19] from [18] we have that $z_s = \dfrac{(x_5^2 - x_6^2 + 2R(x_5 + x_6))}{4d}$ .....[20]

Moreover, adding these equations gives another value for 'R' as

$$R = \frac{(2d^2 - (x_5^2 + x_6^2))}{2(x_5 - x_6)} \quad \text{.....[21]}$$

As an aside, it can be shown from Figure 4.5 that $\cos\theta = (x_s/R)$ .....[22]

and by re-arranging equation [11] and combining with equation [22] .....

$$x_s = \frac{2Rx_1 + x_1^2 - d^2}{2d} \quad \text{.....[23]}$$

If the values of the differences $x_1$, $x_2$, $x_3$, $x_4$, $x_5$, and $x_6$ are determined from the experimental results of the time differences, then three values of 'R' are available from which the mean may be calculated. Moreover, values of $\theta$ and $\phi$ are obtainable from figure 4.1. The coordinates of the source 'S', relative to the origin can be determined since $x_s = R\cos\theta$, $y_s = R\sin\theta.\cos\phi$ and $z_s = R\sin\theta.\sin\phi$. This is an exact analysis of the geometry of the array relative to the source involving the path length differences $x_1$ ... $x_6$, and shows that if the corresponding time differences can be established then source location with this wheel brace array of seven microphones is possible. However, there will be problems in the field associated with the errors involved in measuring the time differences, and, clearly, the values of $z_s$ and the array half dimension, will need to be chosen carefully. Further, when making the calculations, it is important to be able to check the results against alternative measurements. With the present hardware it is easier to measure the (x,y,z) coordinates than the angles of altitude and bearing. It is also useful to have knowledge of the calculated values of the diagonals of the geometric model as a check. Therefore, the following analysis seeks to determine these quantities in terms that can be derived from the time differences.

By re-arranging the terms in equation [11] $\cos\theta = \dfrac{(R + x_1)^2 - R^2 - d^2}{2dR}$ .....[24]

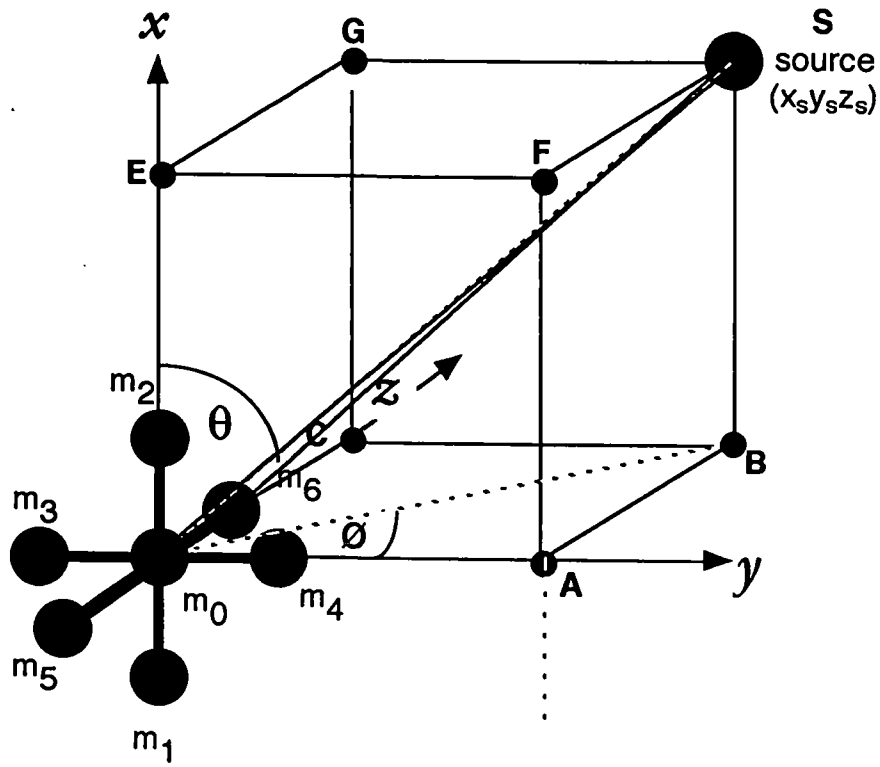


*Figure 4.6*

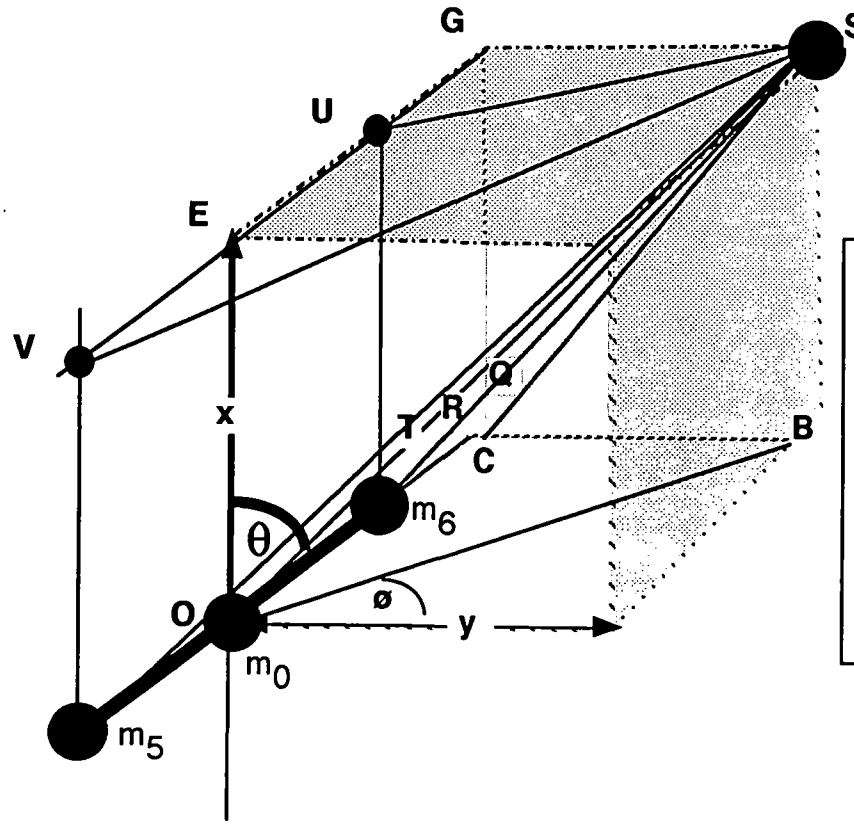


*Figure 4.7*

$T - R = x_5$

$R - Q = x_6$

$VS = \sqrt{(T^2 - x^2)}$

$US = \sqrt{(Q^2 - x^2)}$

***Diagram of geometry for microphones $m_5$ and $m_6$***

and by combining equations [9] and [24]

$$x = \frac{(R + x_1)^2 - R^2 - d^2}{2d}$$

or 'x' is either $x = \frac{2Rx_1 + x_1^2 - d^2}{2d}$ or $\frac{2Rx_2 - x_2^2 + d^2}{2d}$ .....[25]

Combining equations [25] and [8] it is possible to arrive at an expression for 'R'

$$R^2 - 2Rx_2^2 + x_2^2 = R^2 + d^2 - 2xd = \frac{R^2 + d^2 - 2d(2Rx_1 + x_1^2 - d^2)}{2d}$$

or $$-2Rx_2 + x_2^2 = d^2 - (2Rx_1 + x_1^2 - d^2)$$

$$R = \frac{2d^2 - (x_1^2 + x_2^2)}{2(x_1 - x_2)} \quad \text{.....[26]}$$

From the symmetry of the array, it is possible to use similar reasoning on the other microphone pairs, $m_3$ and $m_4$, $m_5$ and $m_6$ to achieve another two equations for 'R'

$$R = \frac{2d^2 - (x_3^2 + x_4^2)}{2(x_3 - x_4)} \quad \text{.....[27]}$$

and

$$R = \frac{2d^2 - (x_5^2 + x_6^2)}{2(x_5 - x_6)} \quad \text{.....[28]}$$

Now consider the microphone pair $m_3$ and $m_4$ (reference Figure 4.5)

$$P = R + x_3 \quad \text{.....[29]}$$

and

$$N = R - x_4 \quad \text{.....[30]}$$

The projection of $m_4$ onto the 'yz' plane containing the source 'S' is at a distance $(N^2-x^2)^{1/2}$

Using the cosine law on the $\Delta$ SEK gives

$$(N^2 - x^2) = d^2 + (y^2 + z^2) - 2d(y^2 + z^2)^{1/2}.\cos \phi \quad \text{.....[31]}$$

Substituting for 'N' from equation [30]

$$(R - x_4)^2 - x^2 = d^2 + (y^2 + z^2) - 2d(y^2 + z^2)^{1/2}.\cos \phi$$

Substituting for $R^2$ as in equation [7] gives

$(R - x_4)^2 = R^2 + d^2 - 2d(y^2 + z^2)^{1/2}.\cos \phi$ which on simplifying gives

$$x_4^2 - 2Rx_4 = ..d^2 - 2d(y^2 + z^2)^{1/2}.\cos \phi \text{ but } R^2 - x^2 = y^2 + z^2$$

therefore

$$\cos \phi = \frac{2Rx_4 - x_4^2 + d^2}{2d(R^2 - x^2)^{1/2}} \quad \text{.....[32]}$$

but from the Δ EGS $\cos \phi = \dfrac{y}{(R^2 - x^2)^{1/2}}$ .....[33]

So by combining equations [32] and [33] the expression for 'y' becomes

$$y = \frac{2Rx_4 + d^2 - x_4^2}{2d} \quad \text{.....[34]}$$

By using the distance to the projection of $m_3$ onto the 'yz' plane containing the source 'S' , the distance JS is seen to be $(P^2 - x^2)^{1/2}$ and by following the reasoning given above, an alternative expression for y is, $y = \dfrac{2Rx_3 - d^2 + x_3^2}{2d}$ .....[35]

Also from the Δ SGE the expression $z = y \tan \phi$ can be obtained .....[36]

To evaluate the term 'z' refer to Figure 4.7 where, as in the previous proof, the projection of the microphones $m_5$ and $m_6$ onto the plane of 'yz' containing the source 'S' gives Δ's USG and VSG where the diagonals US and VS are respectively $(Q^2 - x^2)^{1/2}$ and $(T^2 - x^2)^{1/2}$. The separation between the time for the signal to reach $m_5$ and $m_o$ is $x_5 = T - R$ and for the time interval between $m_o$ and $m_6$ is $x_6 = R - Q$.

Therefore $Q = R - x_6$ .....[37]

$T = R + x_5$ .....[38]

Using the cosine rule for Δ EUS gives

$$Q^2 - x^2 = d^2 + y^2 + z^2 - 2d\sqrt{y^2 + z^2}\cos(90-\phi) \quad \text{.....[39]}$$

From equation [7] and the fact that $R^2 - x^2 = y^2 + z^2$ allows equation [39] to be simplified to

$$(R - x_6)^2 = d^2 + R^2 - 2d(R^2 - x^2)^{1/2}\cos(90 - \phi)$$

or $\cos(90 - \phi) = \dfrac{x_6^2 - d^2 - 2Rx_6}{-2d\,(R^2 - x^2)^{1/2}}$ .....[25]

but from Δ ESG $\cos(90 - \phi) = \dfrac{z}{(R^2 - x^2)^{1/2}}$ .....[40]

therefore $z = \dfrac{2Rx_6 + d^2 - x_6^2}{2d}$ .....[41]

By following the above method and using the expression for $T = R + x_5$, the alternative equation for 'z' can be shown to be

$$z = \frac{2Rx_5 - d^2 + x_5^2}{2d} \quad \text{.....[42]}$$

## Summary of Equations used to determine Co-ordinates

$$R = \frac{2d^2 - (x_1^2 + x_2^2)}{2(x_1 - x_2)} \quad \text{or} = \frac{2d^2 - (x_3^2 + x_4^2)}{2(x_3 - x_4)} \quad \text{or} = \frac{2d^2 - (x_5^2 + x_6^2)}{2(x_5 - x_6)} \quad \text{Equations (i)}$$

$$x = \frac{2Rx_1 - d^2 + x_1^2}{2d} \quad \text{or} \quad = \frac{2Rx_2 + d^2 - x_2^2}{2d} \quad \text{Equations (ii)}$$

$$y = \frac{2Rx_3 - d^2 + x_3^2}{2d} \quad \text{or} \quad = \frac{2Rx_4 + d^2 - x_4^2}{2d} \quad \text{Equations (iii)}$$

$$z = \frac{2Rx_5 - d^2 + x_5^2}{2d} \quad \text{or} \quad = \frac{2Rx_6 + d^2 - x_6^2}{2d} \quad \text{Equations (iv)}$$

$$\text{Tan } \phi = \frac{z}{y} \quad \text{Equation (v)} \qquad \cos\theta = \frac{x}{R} \quad \text{Equation (vi)}$$

LEGEND

| | |
|---|---|
| Equation (i) = | Equations 26, 27 and 28 |
| Equation (ii) = | Equation 25 |
| Equation (iii)= | Equations 34 and 35 |
| Equation (iv)= | Equation 41 and 42 |
| Equation (v) = | Equation reference figure 4.8 |
| Equation (vi)= | Equation 9 |

*{Note that Equation [20] = Equation [41] + Equation [42]}*

***Table 4.1***

The source can be located from R, ø and θ only, using the following equations.

$$R = \frac{2d^2 - (x_1^2 + x_2^2)}{2(x_1 - x_2)} \qquad \cos\theta = \frac{(x_1^2 - x_2^2 + 2R(x_1 + x_2))}{4dR} \qquad \tan\phi = \frac{(x_5^2 - x_6^2 + 2R(x_5 + x_6))}{(x_3^2 - x_4^2 + 2R(x_3 + x_4))}$$

The equations given in Table 4.1 provide extra detail for use in evaluation of results and the critical analysis of practical data.

# Determination of the inherent error due to finite time interval used in the analogue to digital sampling

In the following calculation, the arrangement assumes that the source of the noise signal is at one corner of a rhombohedron and the reference microphone is at a diagonally opposite corner.

By reference to Figures 4.8 and 4.9 the arrangement of the microphones is shown as a series along each of the three mutually perpendicular axes. From the three diagonals of the figure and the fact that the separation of the microphones is a constant - represented by 'd' - then the use of Pythagoras' Theorem enables the distance to each microphone to be calculated.

From Figure 4.8:

The diagonal which is the diagonal for the plane ZY, $OB = \sqrt{(z^2 + y^2)}$ ..... [43]

The diagonal for the plane defined by the axes ZX and represented by AS is

$$AS = \sqrt{(x^2 + z^2)} \quad \text{..... [44]}$$

The diagonal for the plane defined by XY is CS, $CS = \sqrt{(x^2 + y^2)}$ ..... [45]

To calculate the distance to microphones m4 and m3, where the distances from

$$E \text{ to } m_o = x; \quad A \text{ to } m_0 = y; \quad C \text{ to } m_o = z$$

$$E \text{ to } m_2 = x - d; \quad A \text{ to } m_4 = y - d; \quad C \text{ to } m_6 = z - d$$

$$E \text{ to } m_1 = x + d; \quad A \text{ to } m_3 = y + d; \quad C \text{ to } m_5 = z + d$$

then the radial distance R is

$$m_0 \text{ to } S = \mathbf{R} = \sqrt{(AS^2 + y^2)} \quad \text{..... [46]}$$

$$m_3 \text{ to } S = \sqrt{[(y+d)^2 + AS^2]} \text{ and } m_4 \text{ to } S = \sqrt{[(y-d)^2 + AS^2]} \quad \text{..... [47]}$$

$$m_1 \text{ to } S = \sqrt{[(x + d)^2 + OB^2]} \text{ and } m_2 \text{ to } S = \sqrt{[(x - d)^2 + OB^2]} \quad \text{..... [48]}$$

$$m_5 \text{ to } S = \sqrt{[(z + d)^2 + CS^2)} \text{ and } m_6 \text{ to } S = \sqrt{[(z - d)^2 + CS^2]} \quad \text{..... [49]}$$

From the above equations it is possible to construct a spreadsheet to calculate the distances between microphones and source for any set of co-ordinates, either positive or negative. The angles ø and θ can also be found.

$$ø = ACOS\,(y/OB) \text{ and } \theta = ACOS\,(x/R) \quad \text{..... [50]}$$

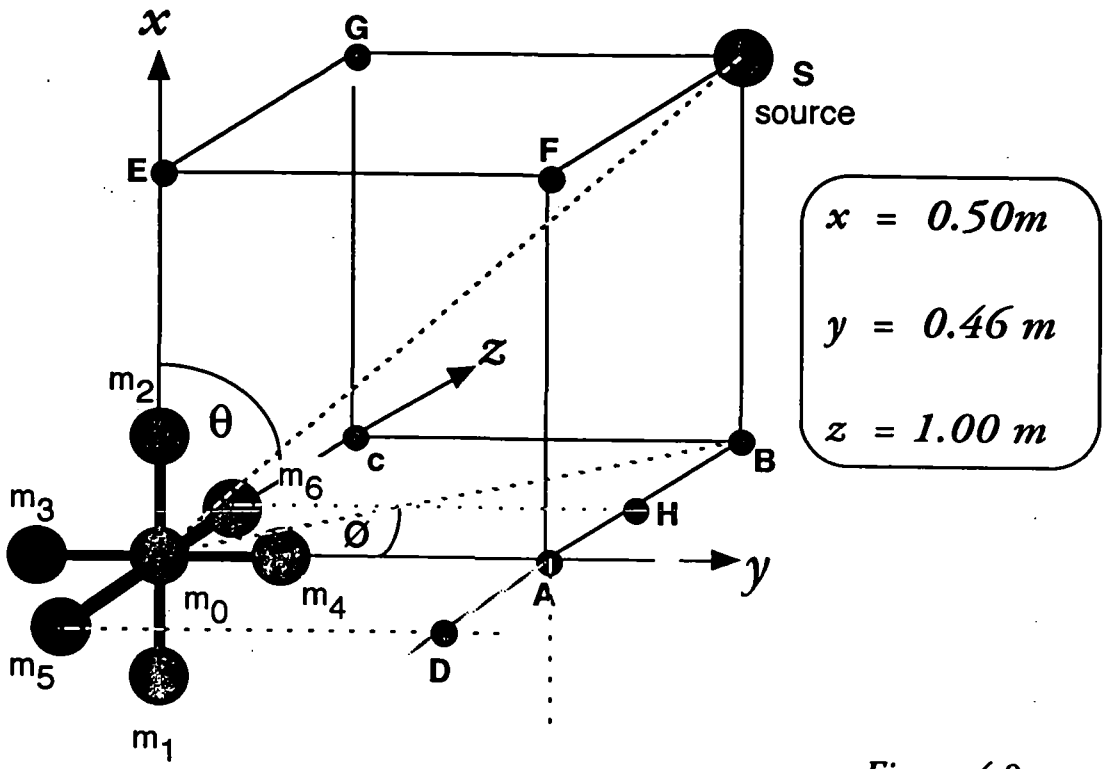


*Figure 4.8*

The reference point is the central microphone - $m_0$ - which is referred to as point 'O' in all the mathematics.

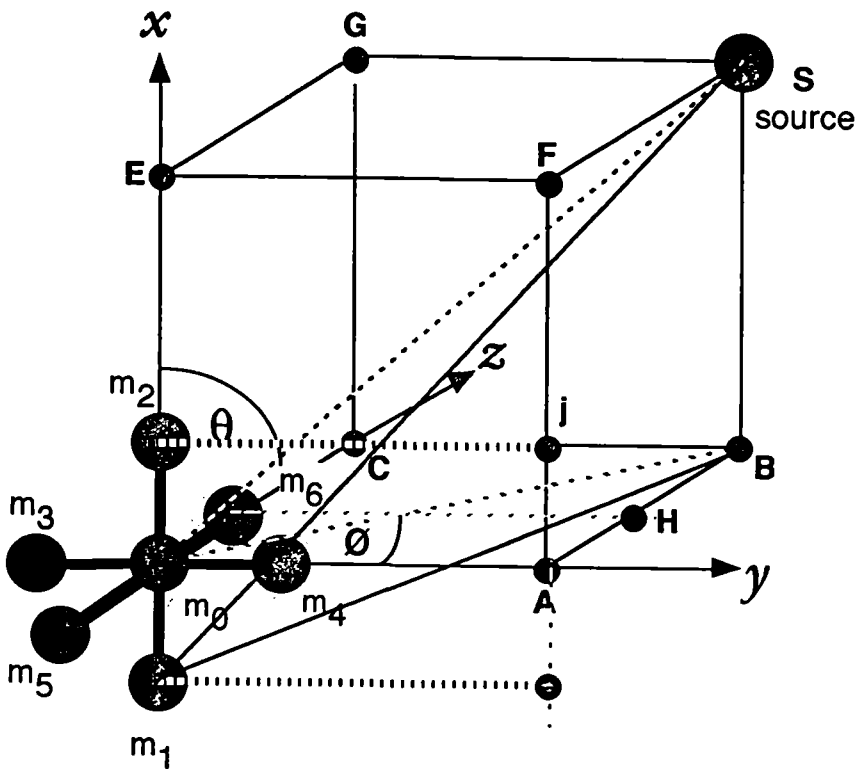


*Figure 4.9*

The reference point is the central microphone - $m_0$ - which is referred to as point 'O' in all the mathematics.

By calculating the distances and then converting the distances into units of time, it is possible to compare results obtained in practical work with the theoretical prediction. Because the units of time determined by the A to D convertor are 20 $\mu$S units, then unless the time interval is a whole number of 20 $\mu$S units, an error will be introduced.

The spreadsheet makes the calculation by working out the actual distances between microphones and source, using a value for the speed of sound derived from equation [51], relating velocity of sound to the absolute temperature. The reference velocity of sound was taken as 344 m/s at 21 °C and then finding the nearest whole number of 20 $\mu$S intervals. In this calculation 0.5 and below are converted to the lower whole number.

$$\frac{V_1}{V_2} = \sqrt{\frac{(T_1 + 273)}{(T_2 + 273)}} \quad \text{..... [51]}$$

The whole number values of the time intervals were then used to calculate the distances between the microphones.

| | | | | |
|---|---|---|---|---|
| **Separation of microphones** | 0.28 m | **Distance 'R' between source and reference microphone** | 1.209 m | |
| **'X' co-ordinate** | 0.50 m | **Time interval in 20$\mu$S intervals between mo & S** | | |
| **'Y' co-ordinate** | 0.46 m | **Interval between m1 and S** | 20 | |
| **'Z' co-ordinate** | 1.00 m | **Interval between m2 and S** | 13 | |
| **Temperature at which measurements occurred** | 20 ° C | **Interval between m3 and S** | 19 | |
| **Velocity of sound** | 343.41 m/s | **Interval between m4 and S** | 11 | |
| | | **Interval between m5 and S** | 35 | |
| | | **Interval between m6 and S** | 32 | |
| **Calculation of 'R'** | | **Calculation of 'x'** | | **Calculation of % Error** |
| For x1 and x2 | 1.352 | For x1 | 0.515 | |
| For x3 and x4 | 1.220 | For x2 | 0.530 | **Mean 'x' = 0.523 Error 'x' = 4.53%** |
| For x5 and x6 | 1.230 | **Calculation of 'y'** | | |
| Mean value of 'R' | 1.2674 | For x3 | 0.481 | |
| % error | 4.83% | For x4 | 0.472 | **Mean 'y' = 0.476 Error 'y' = 3.57%** |
| **Calculation of Angles** | | **Calculation of 'z'** | | |
| θ | 65.6 ° Error 0.5% | For x5 | 1.051 | |
| ø | 65.6 ° Error 0.1% | For x6 | 1.049 | **Mean 'z' = 1.050 Error 'z' = 4.99%** |

***Table 4.2 - Calculation showing inherent errors.***

The time window introduces an error into the calculated values. The above table illustrates the size of this error. Experimental errors are considered later.

From the table of results, Table 4.2, on page 42, it is apparent that there is an error introduced into the calculation by the finite size of the time intervals. In the table, values of '$x_s$', '$y_s$' and '$z_s$' were taken as 0.5, 0.46 and 1.00 metres respectively. These were selected as they corresponded to the dimensions used in one of the practical arrangements to be described in detail later. The practical problem of determining $x_s$,$y_s$,$z_s$ with a tape measure will be discussed later (see page 80). The table calculates the microphone distances from the source using the assumption that the microphone and source are at opposite ends of the diagonal of a rhomboid. This enables all the distances to be calculated using Pythagoras' Theorem. From this information the difference in distances to each microphone was calculated. The distances were converted to the unit of time measurement, that is 20 $\mu$S values. In every case these were decimal values, but the practical equipment can only make measurements to the nearest whole number.

The distances between the microphones and the source was then recalculated using the modified times. The distance between the reference microphone $m_o$ and the source was then calculated by each of the derived equations for 'R'. The values were averaged and the difference between the average value of 'R' and the value determined from the geometry of the arrangement was used to calculate the percentage error. Similar calculations were used to find the errors in determining the co-ordinates, '$x_s$', '$y_s$' and '$z_s$' .

The final figures in the table show that with the co-ordinates selected, the error is below 5%. However, when values are used allowing 'z' to vary from 0.0 to 1.7 metres, while 'x' and 'y' were kept to their original values, the error oscillates between positive and negative values and can be as high as 20%. [See Figure 4.10]. Anomalous results are achieved when the variation in the values of, say, x1 and x2, become equal, due the 'rounding-up' procedure. The difference can become zero, which as a divisor, gives an infinite value. If the separation of the microphones is doubled, then the range of error is less for larger values of 'z', but ultimately the magnitude of the error becomes excessively large. [See Figure 4.11]

The minimum error will occur when one axis of the array is in line with the source. This is the 'end fire' position. When the array is arranged in this form, the separation in the time intervals is the time taken to travel between the successive microphones, 'd'. In the system described 'd'

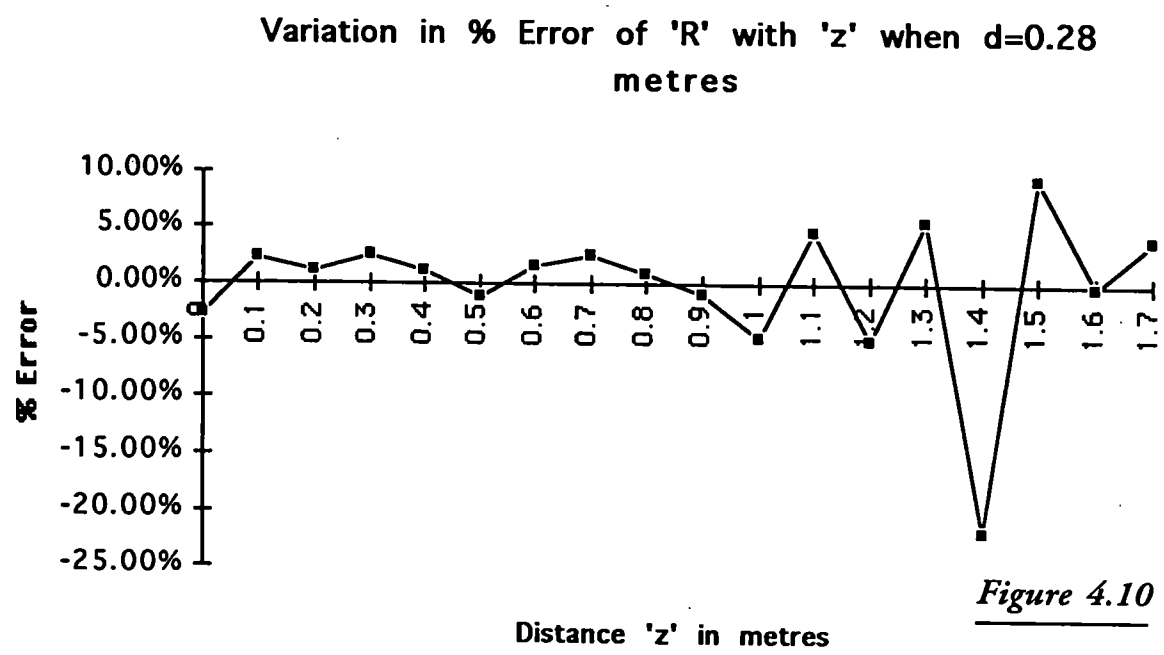


*Figure 4.10*

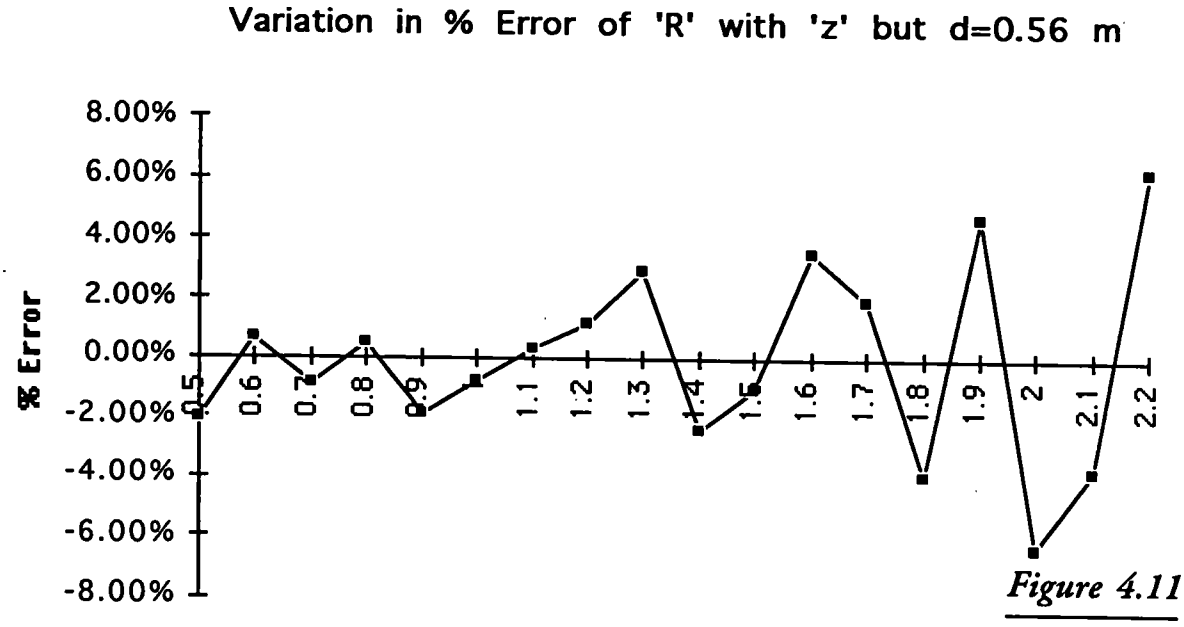


*Figure 4.11*

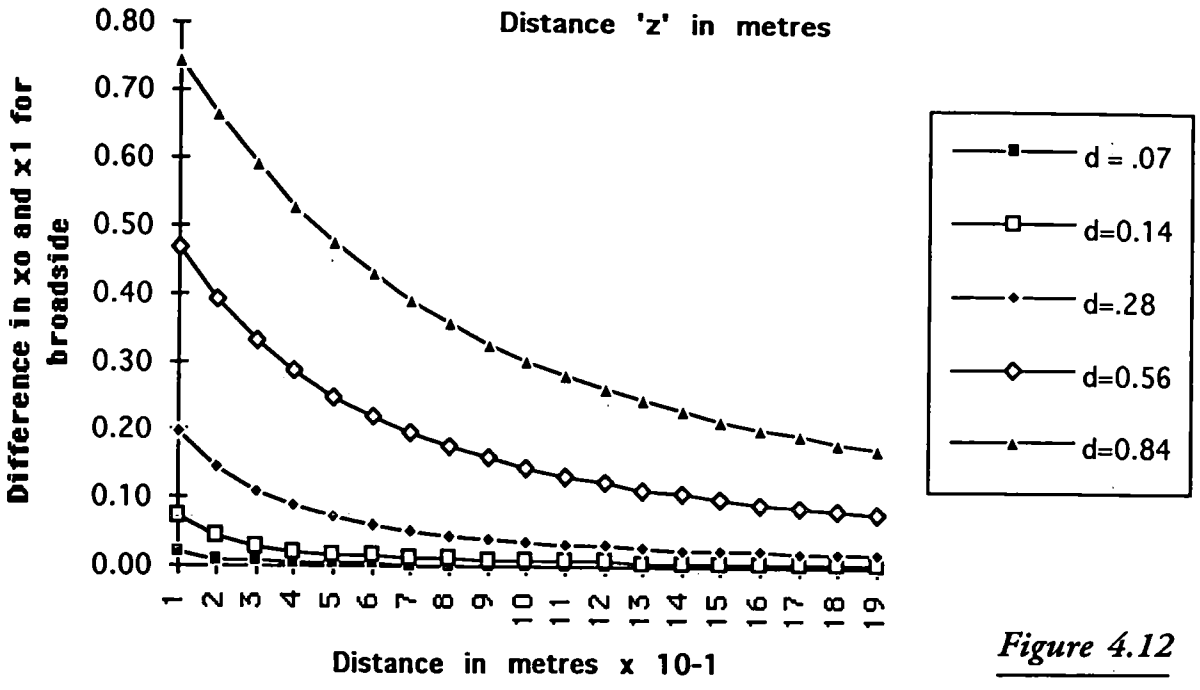


*Figure 4.12*

is 0.28 m and therefore the time interval in 20 $\mu$S units is

$(0.28 \times 10^6) \div (344 \times 20) = 40.69 = 41$ units to the nearest whole number assuming the velocity of sound to be 344 m/s.

It follows that errors may be reduced by increasing the separation of the microphones, but the equipment itself becomes unwieldy, as a consequence, and would not be capable of use inside an ordinary room.

When the array is in the 'broadside' position, Figure 4.13(a), then the two microphones will be equidistant to the source. The reference microphone and the source will be on the normal to the microphone axis. In this arrangement, the separation of the time intervals between the sound reaching either microphone and the reference microphone will be at the smallest value. Therefore, the accuracy of measurement will be the least, or the potential error the greatest. In Figure 4.12 a graph of the difference in the time intervals, $x_1$-$x_0$, is shown as a plot against the distance between the source microphone and microphone $m_1$ for different separation of the microphones 'd'. As the distance to the source increases, so the difference between the times decreases until, when the source is effectively at infinity, the separation in distance becomes d sin $\theta$ where $\theta$ is the angle of incidence of the sound waves - see Figure 4.13 (b). When the sound waves are parallel to each other and normal to the array, then the value of '$\theta$' is 0°, and there is no difference in arrival time.

If all the co-ordinates change, that is, the 'x', 'y' and 'z' at the same time, then the variation in the error of measuring 'R' is proportionately greater.

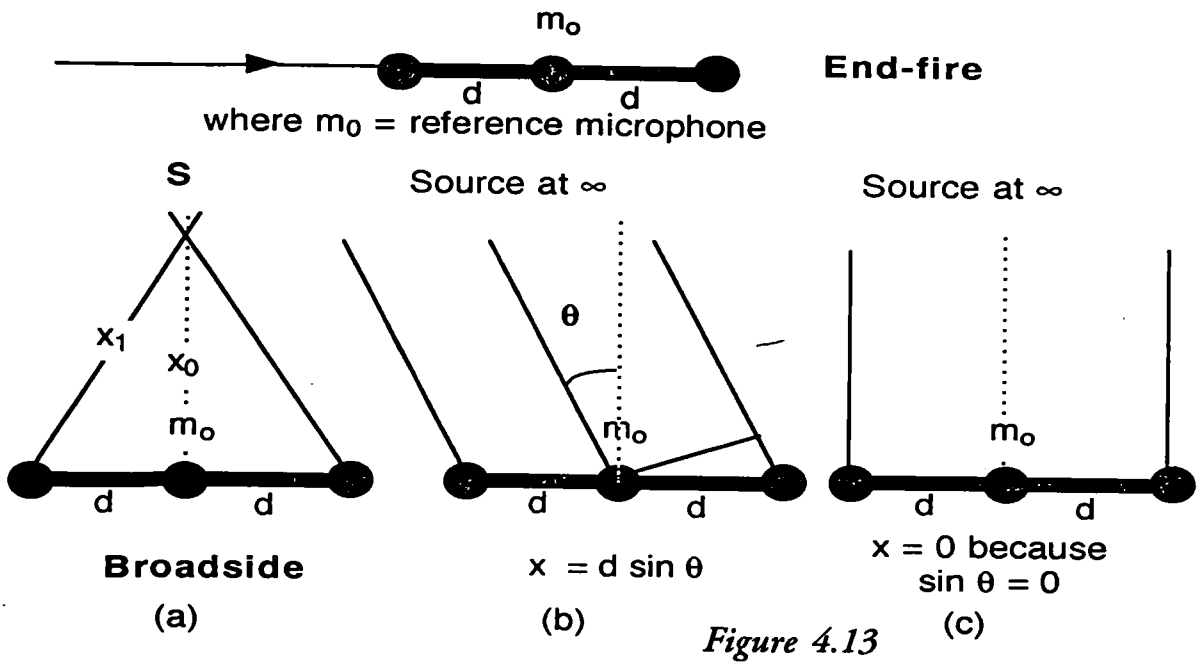


*Figure 4.13*

*Chapter 5*

# The Hardware - The Experimental Arrangement

# Apparatus

At the start of this research, the various references had shown that a number of models were available upon which the experimental equipment could be based. However, there were three constraints that had to be accepted:

1) A certain amount of equipment was readily available

2) The cash for further improvements in equipment was strictly limited, and

3) Computation facilities were restricted to the hardware already purchased.

It was accepted that the scope of the research was to investigate fundamental concepts and establish the feasibility of the project. It would also show that if applied with the current equipment available, then significantly better accuracy in the location of sources would be possible and also the speed of processing would enable 'real time' evaluation of the results.

The original Rolls Royce Acoustic Telescope equipment became available. This consisted of a set of 8 amplifier cards in one box together with a set of preamplifiers designed to use B&K $^1/_2$ inch microphone capsules. With this arrangement each microphone was on a separate lead and each amplifier had a separate meter to monitor input. The output from these preamplifiers was fed into an A to D conversion unit produced by Biodata. The information was output to computer and stored on disk as a 12 bit binary record. The analysis was done using an Apple ][e 64K microcomputer. The analysis was a program written in basic (Applesoft) for cross correlation

The analogue to digital conversion was made simultaneously by eight identical analogue to digital CH12 modules[1]. The output from each microphone was fed to its appropriate card. After the signal was digitised the data was sequentially transmitted to the computer. It was decided that each record should be 4096 bits. The computer was an eight bit machine whereas the A to D card was 12 bit. Data was converted to 8-bit format for recognition by the computer and the collection software routine dealt with the conversion as part of the capture and save operation. The processing was achieved using a compiled basic program that accepted a keyboard command instructing how many channels were used and 'poking' the digitised data

[1] CH12 is the reference to the BIODATA module

output to a memory location in the computer. The data was stored as a binary file on disc. The data was plotted and the waveform compared to that produced on a storage oscilloscope. This served as a check that the wave plotting routine of the computer was giving an accurate representation.

The approach used in this research is similar to that of locating dislocations in a rock mass. In the work of Redfern and Munson [72] , the technique was to use a linear regression method and a reiterative process to find a best fit solution. In this research, a geometric analysis has been used. The velocity of the wave has to be known. Since the time shift between waves is calculated, either by the visual displacement of waves, or by the use of a normalised cross correlation, the start of the signal is important.

The clarity of the signal is important to the current research, since the noise source data recorded must have a clearly defined start to assist in the analysis process.

# Description of Apparatus

The apparatus can be considered as six modules that are interlinked.

1. Source of noise
2. Microphones and assembly
3. Amplifiers
4. Analogue to Digital conversion (A/D)
5. Computer
6. Printout

The modular nature of the arrangement has allowed flexibility in the approach to the acquisition of data . As new equipment comes onto the market, it is possible to interface it with the existing arrangement. The limitation to this is, of course, the cost of new equipment. Therefore, the arrangement, although having undergone several modifications, still consists of devices that would be regarded as obsolete if the project were starting in 1993. The most obvious is the choice of the Apple ][e computer. This machine was nearing the end of its commercial acceptability at the commencement of the project. It does, however, offer a substantial advantage, even today, provided that speed and memory capacity are not the prime requirements. It has up to four slots available for inserting special boards, and it incorporates a straightforward, though quite sophisticated, form of BASIC programming language. This allows alterations to be effected quickly and relatively painlessly. Newer computers offer the data acquisition in real time with dedicated software for analysis. The advantages of this are obvious, but from the investigative point of view, the ability to modify techniques was, and is, still regarded as of prime importance.

# Source

The mechanism chosen to represent a noise source was a small loudspeaker. It was necessary for the source to be small so that the largest dimension of the loudspeaker should be approximately a tenth of the distance between the source and any microphone. The power output of the speaker was not critical. Provided the noise level of the signal burst was at least 10 dB above background, there was no complication due to addition of noises. The small size

of the source allowed the assumption that the centre of the loudspeaker corresponded to the point of the noise generation. The loudspeaker was supported on a metal stand and its position could be adjusted vertically over the height of the stand.

## Microphones and assembly.

The microphones were selected to match the rest of the equipment and offer reliability. The choice originally was to use miniature capacitance microphones with preamplifiers designed and made as part of the work. Following the practical problems associated with these microphone preamplifiers, it was decided that the more expensive B&K 4133 12 mm microphone capsules should be employed. The preamplifiers were ones that had been developed for use with the Rolls Royce Acoustic Telescope by Rolls Royce and were found to be satisfactory. The system was designed for use at a considerable distance from the main amplifiers. From reference to the paper of Billingsley and Kinns, which describes the system used by Rolls Royce, the microphones used in the original telescope were 6.35 mm B&K type 4135. By the time the equipment was used on this project, the termination for the preamplifiers had been changed to take the 12 mm B&K capsule. The fittings and associated cable for the 100 m extension were still in place. The control of the input gain from the preamplifiers was entirely from the amplifier unit.

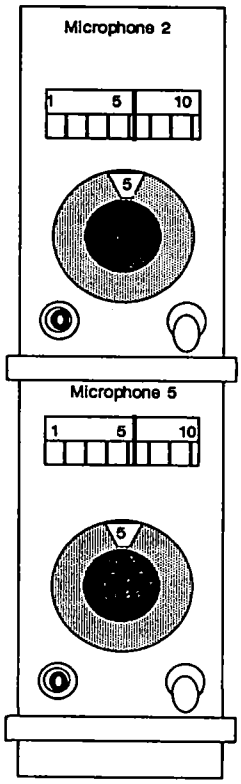


*Figure 5.2*

## Amplifiers.

The amplifiers were connected to the microphones via a multiplug at the rear of the case. Each microphone card (see Figure 5.2) pushed into a socket in the case.

The amplifier board contained a display showing the signal input voltage, a dial to alter the gain in 10 dB steps, a BNC output plug and a switch to insert or isolate the filter. A separate power supply with switchable outputs for the heater elements, is

placed to the side of the amplifiers. The amplifiers were designed to give a flat response from 80 kHz down to 30 Hz.

At the start of the research extensive testing was performed to check the compatibility of the amplifiers to the rest of the system and to find whether any phase shifts were introduced. This testing was carried out by replacing the microphone capsule with a jack socket and feeding a signal from a sine wave generator into all channels simultaneously. The signals were recorded on the computer disk and analysed by plotting the waves on a pen plotter. No phase shifts were observed between the channels. By altering the signal input, the amplifiers were matched for gain and calibrated in terms of switch setting against dB.

## The Analogue to Digital Conversion

The analogue to digital conversion unit was purchased from Biodata limited. The system comprised a main frame containing the circuitry necessary for complete IEEE-488 bus operation and a number of modules to transfer data between the bus and the computer. The MICROLINK™ interface has a standard connector of the IEEE-488 bus mounted on the back panel of the enclosure. This was used to connect the unit to an IEEE-488 card in slot 4 of the computer.

The MICROLINK interface is fully bus compatible. The system acts on the IEEE-488 bus as a single device with a single address - the PRIMARY ADDRESS. The control module in the mainframe of the MICROLINK recognises the primary address of the device when it is sent by the controller. The primary address is a number between 0 and 30, and in the MICROLINK interface the primary talk address and primary listen address are the same. The individual modules are accessed through a secondary address. To send data or commands to a particular module, the controller or computer sends out an extended two byte listen address, the first byte is the primary address of the MICROLINK interface and the second byte is the secondary address of the module within the interface. The interface similarly expects an extended talk address when data is got from a particular module. Flexibility is achieved through the use of secondary addressing. There is only one connection to the IEEE-488 interface bus, and within the MICROLINK interface there is another, internal bus, which connects the mainframe to each of the modules.

The MICROLINK mainframe consists of the instrumentation case, its back panel and two

modules - the Power and Control modules. These are located on the lefthand side of the case. The back panel holds the mains input socket, the fuses and the IEEE-488 socket. The power module has three light emitting diodes. These should all be lit when the supply is normal. The control module has the primary address switches and 2 light emitting diodes. These diodes light when the unit is addressed as either a talker or listener.

The modules used in this work were

a) Time base module TB,

b) Comparator module CMP, and

c) the A to D modules CH12.

The Time Base (TB) module is the heart of the transient capture system. It provides all the sample timing, the starting and stopping facilities necessary for transient capture. Only one time base was used. It possesses one red LED which lights when its address is received. In order to initiate the capture of a transient signal, a trigger signal is required. This can be from one of three sources -

i) the Comparator Module (CMP),

ii) a front panel digital input or,

iii) from the software.

The trigger has no effect until the two control signals, ARM and RUN, have been received from the software. When the RUN command is set, the CH12 modules take and store samples at each sample pulse, but the trigger inputs will have no effect until the ARM is also set. This enables pretrigger capture of data. (From reference to the tables of experimental data, it can be observed that usually there are at least 400 samples before the commencement of the triggered event). The amount of pretrigger data that can be stored is determined by the setting of a slide switch on the module in conjunction with the software commands. There are four possible block sizes, namely 512, 1024, 2048 and 4096. The number of blocks to be counted before the trigger, is set by the software. This means that the system is collecting data as pretrigger information, and the number of blocks counted allows a variety of pretrigger configurations. In the experiments conducted here, the trigger was initiated by the signal of the white noise generator. The timebase is controlled by a software command that allocates an 8 bit byte reference to be sent during the set up. Bits 5 and 6 set the arm and run commands.

# The CMP module

The CMP module provides the facility for triggering the transient capture system from a defined point on the analogue waveform. The front panel of the unit has two BNC sockets - one is for the analogue input and one for the digital output pulse. The front panel also has a red LED which flashes when the trigger threshold has been passed. The CMP determines the type of triggering and the level at which the trigger occurs. It also sets the input voltage range.

# CH12 module - A to D conversion

The CH12 module provides the amplification, 12 bit conversion and sample storage for the transient capture system. The front panel of the unit has a BNC socket for the analogue input. There is one CH12 module for each channel of data input. Again there is a red LED that lights when the module is addressed. The output data from the sample and hold device is taken to a 12-bit A-D convertor. This has software selected ranges of 0 to 10 volts or -5 to +5 volts. The A-D takes readings at each sample pulse received from the time base module and stores it in memory. Since the 12 bit reading is stored as two 8 bit bytes, the remaining four bits are used for the 4 digital status inputs which are recorded with each sample. The data is stored at memory locations by the address counter and the address is incremented in such a way as to store the data in a sequential time series. When the end of the memory is reached the address counter returns to the beginning and continues to store samples. This continues as long as the time base sends out pulses. The effect is that the address counter is always pointing to the chronologically earliest record. When the transient has been captured, the time base ceases to send out pulses and resets its RUN control. The data can be read from memory provided the RUN is not set. The data can be read all at once, or in sections, and can be re-read if necessary.

The status inputs control the gain of the amplifier, and whether the system is polar or bipolar. The gain is set from within the software with a maximum gain of 50. The maximum sample rate for the CH12 is 50 KHz (or 1 sample every 20 $\mu$s). The maximum errors are given as:

| | |
|---|---|
| Initial offset error | ±0.5 LSB |
| Max. offset change with temperature | ±2 LSB |
| Initial full scale cal. | ±0.5 LSB |
| Max. linearity error | ±1 LSB |

The CH12 modules used had 16k memory and there were 8 modules. Seven of the modules were used to monitor the microphone inputs. The eighth module was connected to the trigger from the white noise source. This gave a digital record of the actual signal sent to the loudspeaker and proved useful when multiple sources were used as it gave a comparison between the signal transmitted and received.

# The Computer

As stated previously the computer was an Apple ][e with 64 kB of onboard memory and two $5^1/_4$ inch disk drives. The IEEE-488 card was fitted to slot 4, a dot matrix printer was connected to slot 1, and a pen plotter connected to slot 2. Various additional memory devices have been used, but the one found most useful was an ICE 10 MB hard disk.

The computer was driven using a software routine written in BASIC by the author. The acquisition of data from the A to D equipment was based upon software supplied by Biodata. The computer presents a series of questions requiring the set-up information for the A-D system. This includes the number of channels in the system, the gain of the amplifier and the trigger level. The data supplied is written to disk as a text file, and the A-D left armed and awaiting the trigger signal. The trigger is supplied by the start of the noise from the loudspeaker. The pretrigger information allows a large number of samples to be taken prior to the signal of interest. From this data, electronic noise from microphones, or acoustic noise within the environment, can be determined. By setting the input signal to saturate the system and setting the trigger level to 75%, the start pulse rises very quickly and minimises the confusion that can arise from a low level signal.

The data is stored on the A-D and the software then initiates the transfer, writing the data directly to a memory location on the computer from which it is transferred to the disk. Each channel is sequentially down loaded. This procedure takes time, mainly for the storage to disk. It was decided that this was of little importance in the experimental arrangement, but for on-site work, it would be advantageous to do the analysis from the data stored in the computer. The Apple ][ does not have enough memory space to contain the eight sets of 4096 samples and provide memory for the program. The analysis programmes, such as cross correlation and wave plotting, use programmes that have been compiled. A total analysis of one set of records can take as long as 30 minutes.

# Determination of the Time Intervals

The seven microphones were attached to a framework that held the microphones in constant reference to each other. The individual microphone saddles were capable of small adjustments. The separation between the microphone capsules was selected as 0.28 metres. The sound source was chosen to represent a point source. It was a loudspeaker of 0.025 m diameter attached to a stand, so that its position relative to the microphone array could be maintained for the duration of a measurement, but easily changed for successive investigations.

The measurements of the position of the sound source were made using a tape measure. The use of a jig (figure 6.5) and a set of strings between the microphones and the stand for the noise source, enabled a reasonably accurate measurement to be made. The greatest problem was being sure that the 90° angles were correct. Small variations in the angles made a significant variation to the measured distances. (A description of the use of the jig to measure the coordinate positions is given on page 71).

In order to minimise the error in the determination of the (x,y,z) coordinates using the measurement of the time delay between the microphones, the position of each pair of microphones on the three axes was interchanged. The results gave no significant difference. As the process of changing the microphones was time consuming, the practice was dropped. In the same context, the acquisition of the data at all microphones simultaneously was regarded as essential, but experimentation showed that because the arrangement was static, the time differences recorded at the microphone pairs was extremely stable. It follows that for the type of measurement being undertaken in this study, sequential measurements are acceptable.

The analogue to digital conversion system was activated by a trigger signal obtained from the connection to the loudspeaker. The line output from the white noise generator is parallelled with the output connector to the loudspeaker. This was fed to the eighth amplifier card. The gain of the amplifier was reduced to the minimum value. The output from this amplifier was fed to the trigger input of the A to D and also input into the number 8 A to D convertor to record the trace corresponding to the start of the noise burst from the loudspeaker. By using this signal as the trigger, rather than the signal from any of the microphones, prevents extraneous captures

due to noise in the laboratory.

The determination of the time differences was made by comparing the start of the noise burst in each of the stored results from the microphone array. Two methods were used to determine these quantities. The first technique was to plot the trace for each microphone and compare the trace with the reference microphone. Figure 5.2 shows such a comparison. A special software package was created that allowed the trace to be annotated with the number of microsecond intervals that elapsed from the start of the noise burst. The comparison relied upon a visual match being established between the waves for the beginning of the trace. Where there was a sudden rise in level, the procedure was relatively easy, but often the start of the trace was difficult to determine. A characteristic that clearly identified the point at which the noise burst arrived at each microphone, was used as the origin to read the time difference from the computer graph and recorded by moving a cursor over the trace. The method provided a very useful indication of the time intervals, but the variability in positioning the cursor on identical events for the different microphones caused poor repeatability of measurements.

The alternative method was to use a normalised cross correlation technique. This uses the time averaging of a number of successive points and determines how closely related are the graphs from the calculation of the correlation coefficient. The nearer the coefficient is to unity (irrespective of the algebraic sign) the greater is the correlation. The number of points in the records could be adjusted, so that only the initial sound burst was used. This prevented any of the reflected sounds influencing the calculations, so eradicating any room effects on the measurements. This technique proved to give some extremely consistent measurements.

The program for determining the correlation coefficients was designed to quote the correlation coefficient and the corresponding time interval while plotting the correlation curve on the screen. In this way it was a straightforward matter to find the time intervals by correlating the signals stored from each microphone in turn, with that obtained from the reference microphone, $m_o$. It was found convenient to use the visual method to obtain a coarse correlation, thus enabling the mathematical correlation to be speeded by knowing the approximate time for the start of the signals for each microphone.

The values so obtained were in the form of 20 $\mu$S intervals. These values were converted into distances using the velocity of sound for the air temperature in the room at the time of measurement. This was performed using a computer spreadsheet. The velocity of sound at 20°C was entered from a set of standard tables, and the velocity calculated for actual temperatures

(Example of the spreadsheets are given in the appendices on pages 142 and 143).

All the information was stored on disc. This also allowed a multiple plot of the waveforms to be downloaded to a plotter.

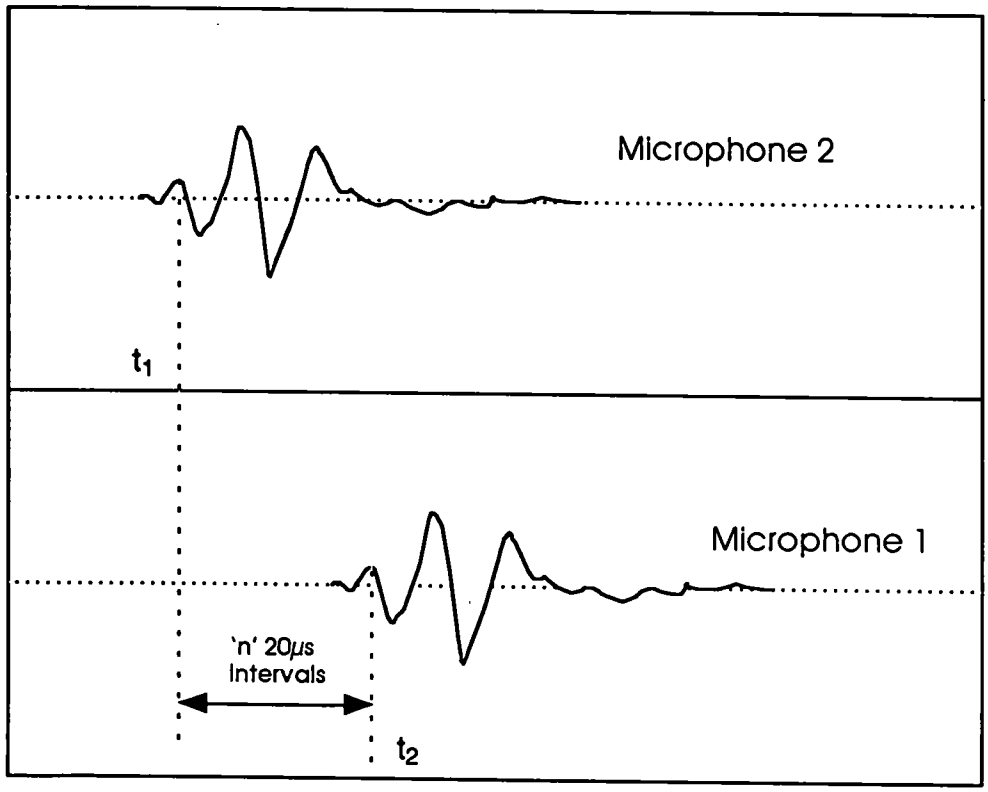


*Figure 5.3 Graphical determination of time interval*

# Connection Diagram of Practical Apparatus

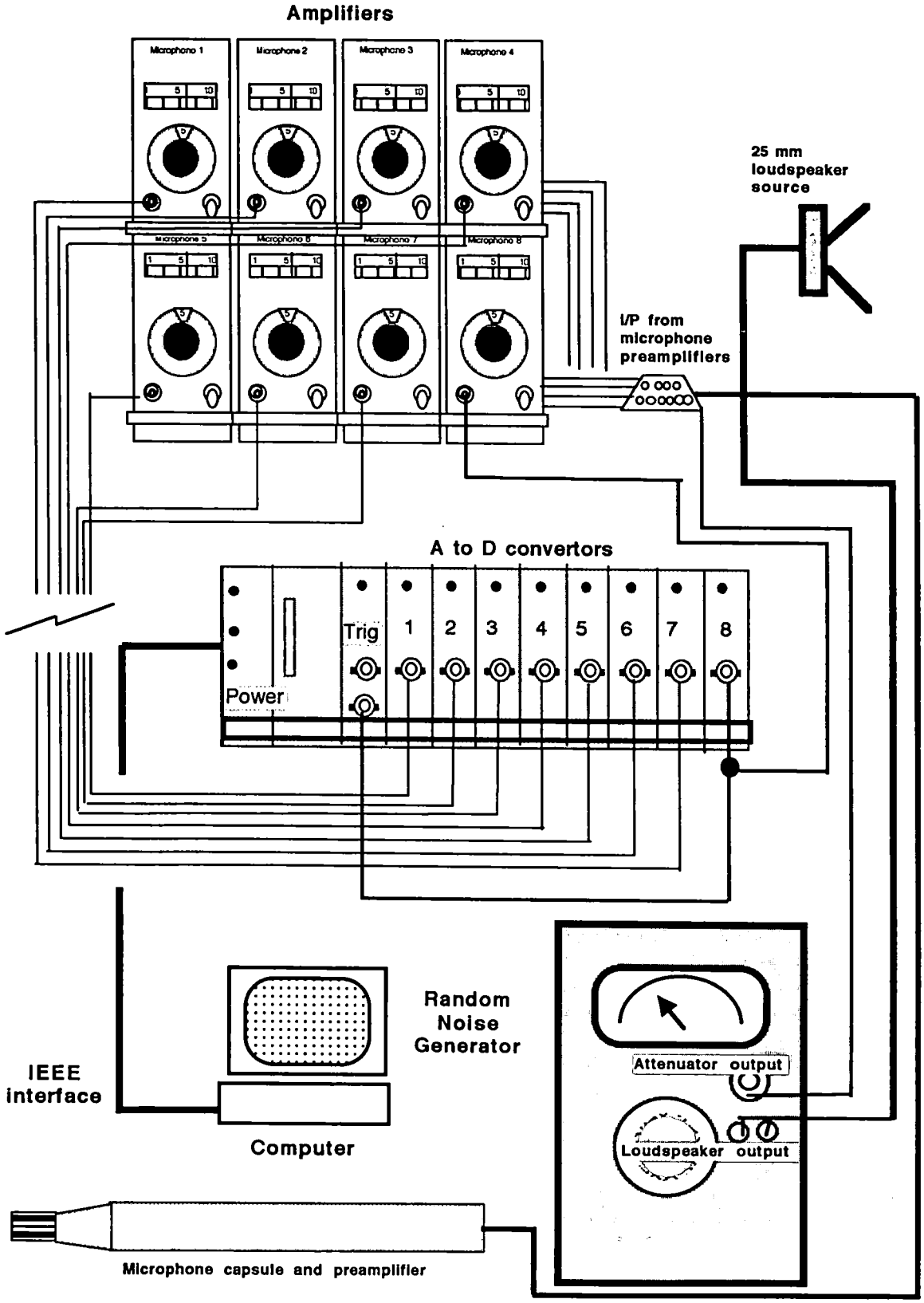


*Figure 5.4*

*Chapter 6*

# Data Acquisition,

## Treatment and Analysis

# Acquisition of Data

## Special Software

The software for acquiring the data from the analogue to digital convertor was written in Applesoft Basic. The program is designed to set the equipment, trigger the collection and store the data.

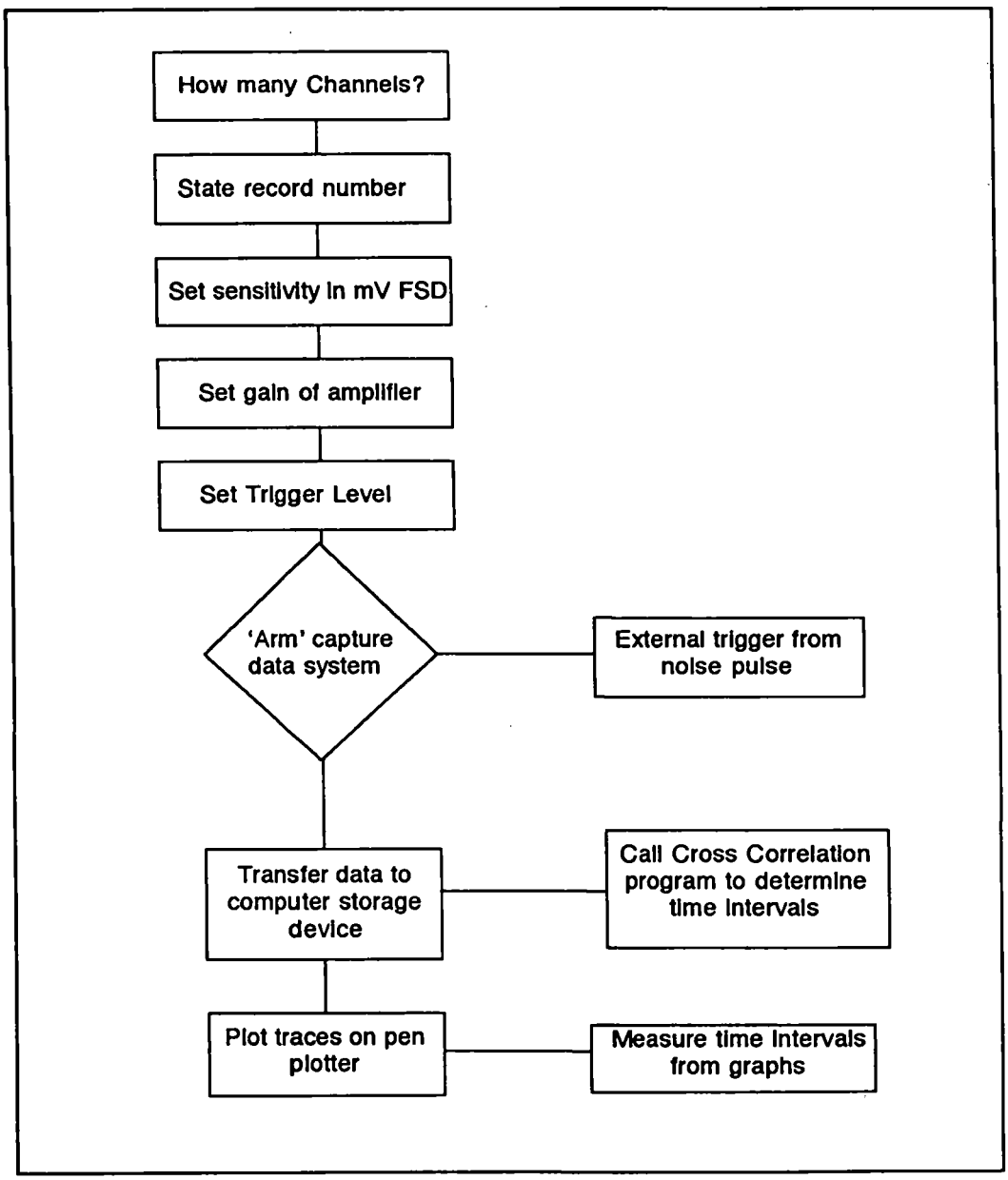


*Figure 6.1*

The system is first initialised by information sent through the software. The voltage range, the amplification of the amplifier and the trigger setting are all performed by sending bytes to the

A to D card. This is performed by creating a special software routine that asks for the various settings and records all the information onto a disk. The A to D is 'armed' which causes the 'clock' to start running. This ensures that an amount of pretrigger information is acquired. The size of the memory available for the recorded data is set by micro switches on the A to D cards. The pretrigger data is determined from within the software. The information being received by the input is recorded continuously until a data 'run' is sent. The recorded data is then stored so that a number of bytes of memory are reserved with the information of the signal prior to the 'run' request being received.

The data is stored simultaneously on each of the A to D cards connected to a microphone. At the completion of the store routine the computer initiates the downloading of the data to disc. This is a sequential action. Each piece of data is named according to a code that stores the date and the microphone number together with another code to identify which record is being stored on a particular date.

The signal sent to the loudspeaker is split. One component drives the loudspeaker, while the second goes to a separate amplifier, the output from which triggers the data capture. A number of readings can be taken for each source position.

The data stored on disk can be processed in a number of ways. It is often convenient to plot the traces on to a single graph. Such a printout gives a visual indication of the time intervals, and therefore enables a commonsense check on the lead and lag times at each microphone.
(See appendices, page 151)
Cross correlation provides a mathematical technique to determine the similarity between waveforms. Where the sound waves originate from more than one source, the plots of the complex waves patterns are impossible to use to determine the time lapses for the separate sources. The theory of the cross correlation method used is explained in the next section.

# Correlation

The correlation coefficients of two random variables, in some sense indicates how closely related the two variables are. In a quantitative sense, the correlation is a measure of the linear relationship between two variables.

A basic indication of the correlation between two variables x and y, is the sum of the products $\sum xy$. In actual computation, time averaging is used.

Given two series of data, $x_1$ - $x_n$ and $y_1$ - $y_n$, then let $\overline{x}$ be the mean of x and $\overline{y}$ the mean of y.

$$\overline{x} = \frac{1}{N} \sum_{n=1}^{N} x_n$$

The deviations from the average can be written as $\partial x_n = x_n - \overline{x}$ and $\partial y_n = y_n - \overline{y}$

If another average of the products of N deviations is taken

$$C_{xy} = \frac{1}{N} \sum_{n=0}^{N} \partial x_n \partial y_n$$

The quantity $C_{xy}$ is the measured covariance between x and y. The correlation coefficient, $\rho_{xy}$, is a normalised version of the covariance, which is the covariance divided by the product of the standard deviations of x and y, which are $\sigma_x$ and $\sigma_y$

$$\rho_{xy} = \frac{C_{xy}}{\sigma_x \sigma_y}$$

The values of x an y are said to be highly correlated because $-1 \leq \rho_{xy} \leq 1$, when

$$|\rho_{xy}| \approx 1$$

# The use of Correlation in Signal Processing

In the application of cross correlation processing, the features whose similarities are being assessed are usually in the form of a sampled series of values. The values are not time dependent. That is, although the value occurred at a certain time, it will not vary or be affected by time either before or after the event of capture. The process of determining similarity between sets of data may become apparent, however, if a time shift is introduced between the values being compared. Because at the start of the analysis, the time lag for maximum similarity is unknown, then the process of correlation must take place for all possible values. Thus, a general covariance function is required.

Given two time dependent signals, x(t) and y(t), the time averages are

$$\bar{x} = \frac{1}{T}\int_0^T x(t)dt \quad and \quad \bar{y} = \frac{1}{T}\int_0^T y(t)dt$$

The deviations from the means are

$$\delta x(t) = x(t) - \bar{x}$$

$$\delta y(t) = y(t) - \bar{y}$$

If, for instance, the similarity between the input, say x(t) and the response, say y(t), is separated by the time '$\tau$' it is to be expected that y(t + $\tau$) will correlate with x(t), for a particular value of $\tau$. The general covariance function :

$$C_{xy}(\tau) = \frac{1}{T}\int_0^T \left[x(t) - \bar{x}\right]\left[y(t+\tau) - \bar{y}\right] \quad \text{..... [52]}$$

It is assumed that x and y are time-invariant variables, so that $\bar{x}$ and $\bar{y}$ do not depend upon t, and that $C_{xy}$ is a function of the time difference only. The normalised correlation coefficient becomes

$$\rho_{xy}(\tau) = \frac{C_{xy}(\tau)}{\left(\sigma_x \sigma_y\right)}$$

Using equation [52], putting y =x and $\tau = 0$ then $C_{xx}(0) = \sigma_x^2$ and similarly $C_{yy}(0) = \sigma_y^2$ then the normalised correlation coefficient becomes

$$\rho_{xy}(\tau) = \frac{C_{xy}(\tau)}{\left\{C_{xx}(0)C_{yy}(0)\right\}^{1/2}} \quad \text{.....[53]}$$

# Cross Correlation Chart

Figure 6.2 below shows a cross-correlogram.

This is a plot of the cross correlation coefficient $\rho_{xy}$ between the data from microphone [$m_2$] and the reference microphone [$m_o$]

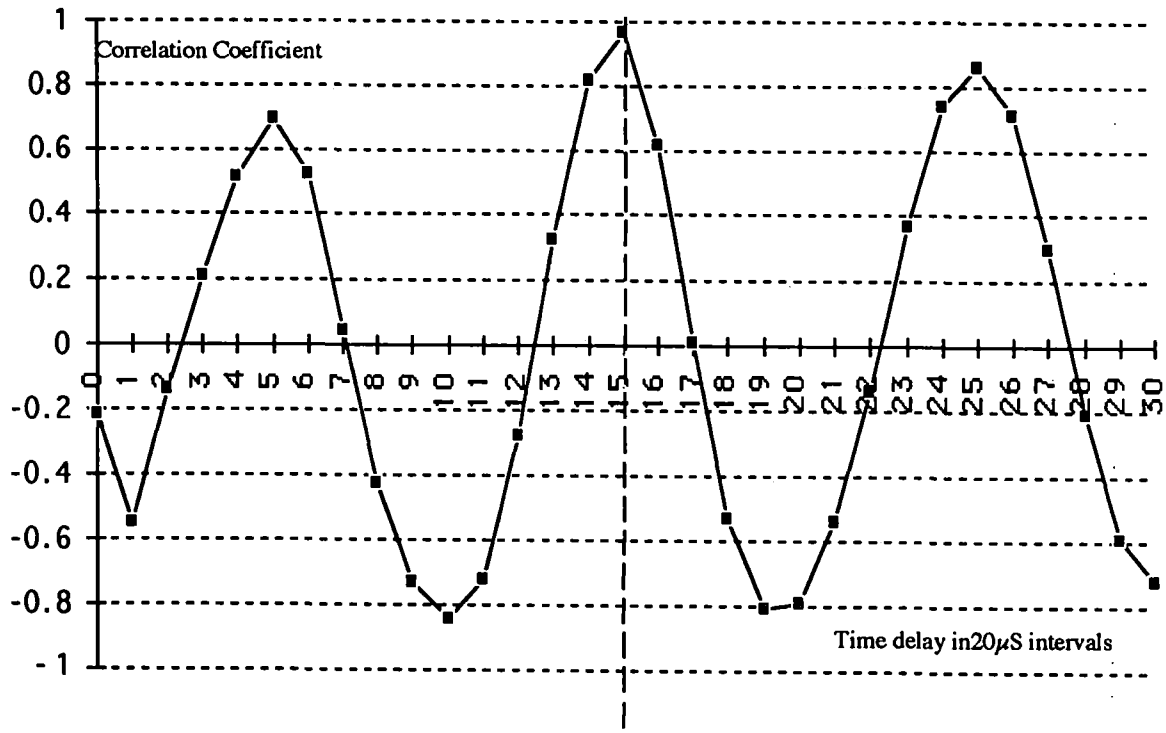


*A Cross-correlogram - Figure 6.2*

The trigger was set for 75%, the voltage range for 500 mV and the gain for 10.

The number of data samples averaged was 20, with the first sample occuring 620 time intervals or 12.4 mS after the start of the storage of data. It is seen in figure 6.2 that the maximum correlation coefficient was 0.97 at the time delay ($\tau$) of 15 x 20 $\mu$S, or 0.30 mS

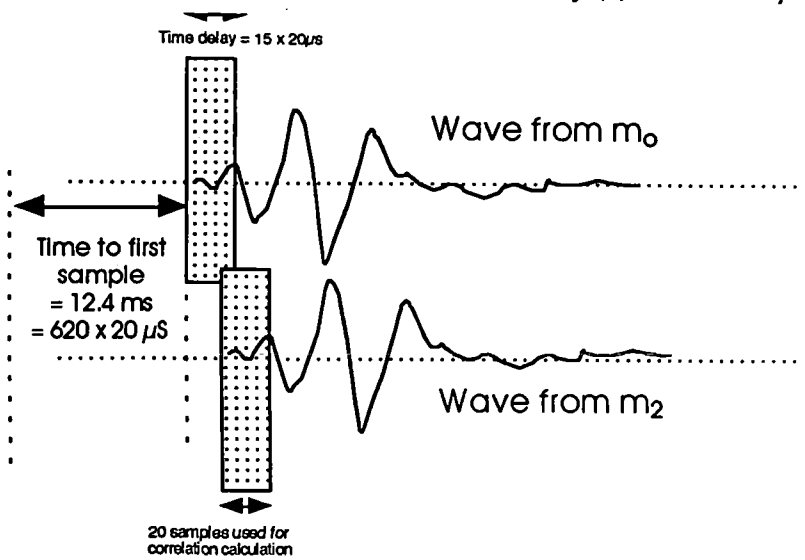


*Figure 6.2b*

# Auto-correlation

Auto-correlation examines the similarity within a single process as a function of the time for which the process is executed. In other words, a cross-correlation between x(t) and x(t + $\tau$) is sought which is a correlation between two elements of the same signal separated by the time $\tau$. Following the earlier argument and modifying equation [53] the normalised auto-correlation coefficient $r_x(\tau)$ is given by

$$r_x(\tau) = \frac{R_x(\tau)}{R_x(0)} = \frac{\int_0^T x(t)x(t+\tau)dt}{\int_0^T x^2(t)dt}$$

The importance of the Auto-correlation function is that, in addition to providing information about the behaviour of x(t) in the time domain, it can, indirectly, give information about the frequency domain behaviour of $x$.

The auto-correlation is nearly zero except for a sharp peak at $t = 0$ for a wide-band noise. This shows that the behaviour of x is unrelated to the events at any other instant. A sinusoidal function shows a correlation function that persists over an infinite range of time lags and the similarity persists no matter what the time lag. The rate of decay of $R_x$ gives an indication of the bandwidth. A narrow band signal, such as a sine wave, has a persistent auto-correlation function, whereas a broadband signal has a $R_x(t)$ that goes rapidly to zero as $t$ goes away from the origin.

Cross correlations provide information about the phase difference of the two functions correlated. Also the magnitude of the cross correlation increases with the amplitude of either function. When two sinusoids with the same frequency are correlated, the result is a sinusoid with the same frequency and a phase which is the phase difference of the two functions correlated. It is consequently possible to extract information about a periodic signal buried in extraneous noise by cross-correlation. The amplitude and phase of the signal can be found by correlating the mixture with a sinusoid of the same frequency. Any function can be considered

as a linear combination of sinusoids, that is, a Fourier Series. A Fourier Transform of a cross correlation is a cross-spectrum and can give information about amplitude and phase relationships. This information is usually found from a FFT or Fast Fourier Transform. The FFT is an algorithm or calculation procedure for obtaining the Discrete Fourier Transform (DFT) with a greatly reduced number of arithmetic operations compared with the direct evaluation. [71]

The error involved in cross correlation can be investigated by considering the term

$$x = A \sin(\omega t + \phi)$$

and measuring values over the interval [0,T]. To estimate the auto-correlation $R_x(\tau)$ the equation is integrated to give

$$R_x(\tau) = \frac{1}{T} \int_0^{T-\tau} x(t)x(t+\tau)dt$$

which becomes

$$R_x(\tau) = \frac{T-\tau}{2T} A^2 \cos\omega\tau - \frac{A^2 \cos[\omega(T-\tau)]}{4\omega T} \sin(\omega\tau + 2\phi)$$

[Reference P.187 Digital Methods for Signal Analysis (3)]

In order to minimise the error in cross correlation, the term $1/\omega T$ should be kept small, where T is the length of the sample interval, In general, the error is related to $1/BT$ where B is the bandwidth.

# The effect of altering the number of samples used in determining the cross correlation coefficient

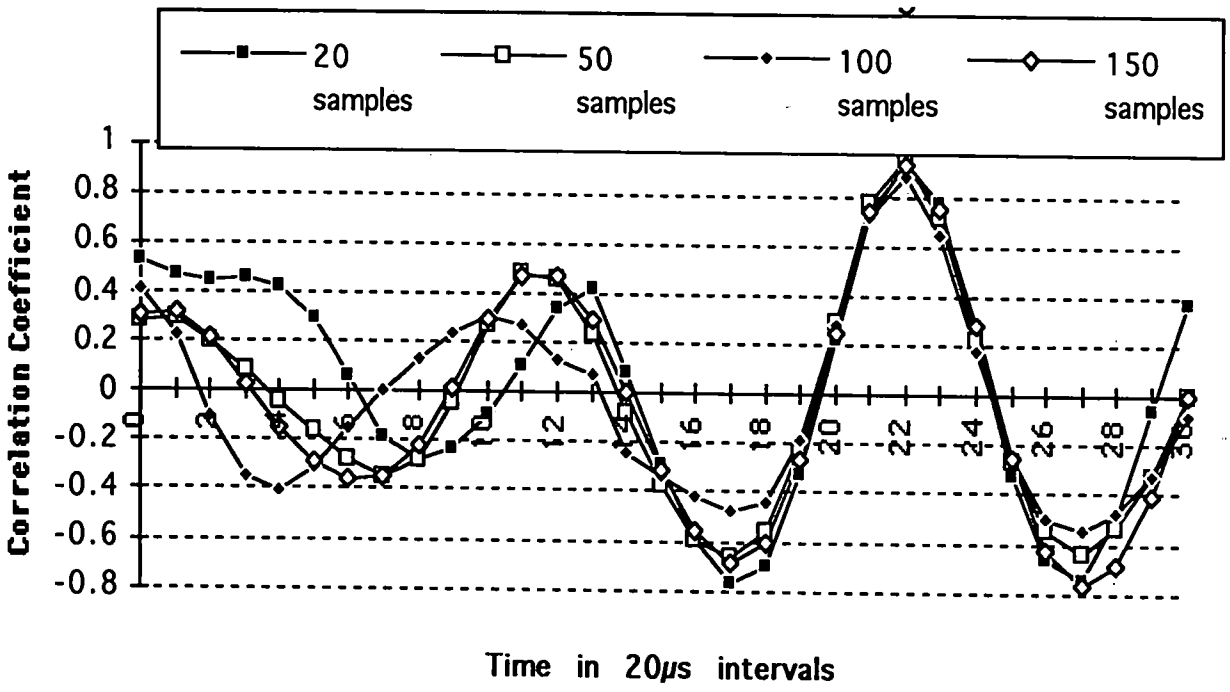


*Figure 6.3*

Figure 6.3 shows the correlation coefficient plotted as a function of the time intervals for different numbers of samples.

The graph, figure 6.3 shows the correlation of data collected from a single point source. The size of the sample being processed is changed, but the time at which the highest correlation occurs remains constant.

# Determination of the bandwidth

From an examination of the auto-correlation of a signal, the filter bandwidth can be estimated. The delay time 't' (which is the product of the number of sampling intervals between two points and 20$\mu$S) is measured at the point where little significant change is occurring in the correlogram, and the filter bandwidth is taken as the reciprocal of this period[3]. The explanation also comes from the analysis of a sin $x/x$ relation which is similar to the auto-correlation. The bandwidth is $1/T$, where $T$ is the period.

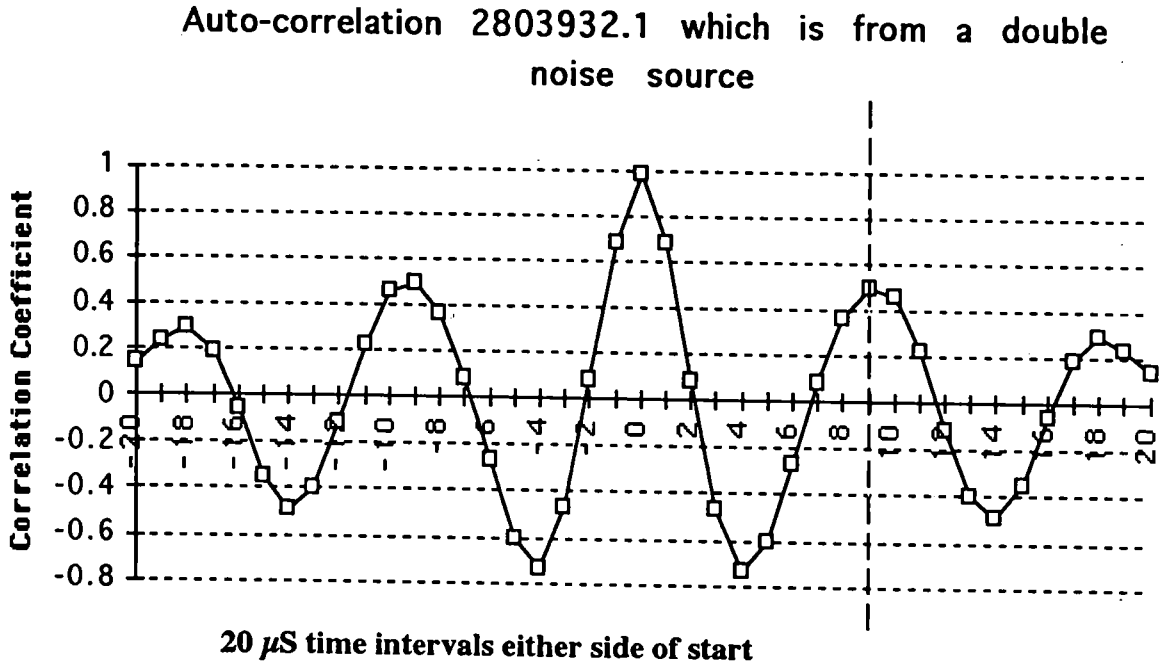


*Figure 6.4*

This graph shows that the second maxima either side of the first, occurs at 9 x 20$\mu$S, and therefore the bandwidth is $\frac{1}{(9\times 20\times 10^{-6})}$ = 5560 Hz

This shows that the source used for these experiments, produces noise that lies between a pure tone and a broadband signal.

The autocorrelation function has application to the built environment. It enables periodic signals buried in noise to be detected. It will also detect the presence of echoes within a signal. Such echoes create the acoustic 'colour' of the sound in an auditorium.

# Experimental validation

From the earlier discussion, summarised in Table 4.2 on page 42, it has been shown that a percentage error in the location of a noise source is bound to occur due to the limitations of the A to D sampling. The reader will recall that this electronic apparatus for the analogue to digital signal capture has a finite window 20 $\mu$S wide. In order to ascertain how closely the practical measurements would match with the theoretical predictions, a test procedure was developed. This consisted of constructing the wheel brace microphone array. It was decided that the microphones and their associated preamplifiers should be mounted sufficiently permanently, that it would be easy to relocate the apparatus for different practical requirements. This was achieved by constructing a wooden frame that was bolted together with screws and butterfly nuts. The main frame was a cross made from 50 mm by 12.5 mm timber, jointed at the intersection to give a flush fit. The vertical piece was grooved in order to register with the horizontal timber and then bolted to a fixed saddle that held the reference microphone. The preamplifiers were located in Terry Clips. This allowed lateral adjustment. The extremities of the timber were slotted with a router, so that wooden saddles could be attached and moved to give the required separations. The whole frame was mounted on parallel aluminium rods of an optical bench, which allowed a degree of movement of the complete array in the direction of the $m_5$, $m_o$ and $m_6$ microphones, the 'z' axis, and supported the array above ground level.

The microphone array was positioned in front of a small loudspeaker, so that the coordinates were approximately x = 0.5 m, y = 0.46 m and z = 1.0 m. The loud speaker was connected to a white noise generator. The loudspeaker was a small 0.025 m diameter device. The smallness enabled it to be perceived as a point source for the distances between source and microphones that were being used. The signal was initiated by operating a push button switch. The duration of the signal was controlled purely by the speed at which the switch could be operated, but the length of the signal recorded was determined by the record length setting of the A to D apparatus. No matter how quickly the switch was operated, the signal was always of longer duration than could be accommodated in the memory of the A to D. The significance of this will be discussed later, when dealing with the identification of a single event from a series of events.

The start of the trace was the only part used in the analysis. By considering the start of the trace only, and by using only the first hundred records of the 20 $\mu$S interval samples, no spurious signals were detected due to reflections from parts of the equipment or items within the room. The wave form was consistent for all the microphones. Any records where the start of the trace was difficult to decide were discarded. The need to reject records was minimised by setting the trigger level for 70% on the rise portion of the curve. This tended to produce a significant voltage at the start of the signal so that the first maxima could be clearly identified.

The experimental programme has been divided into five sections,

1, The source in the positive octant

2, The source in any octant.

3, The source within the half distance of the array. [The mathematics suggests that odd behaviour in errors may be observed].

4, Multiple sources, and finally,

5, Single source and two microphone system, instead of seven microphones.

These will now be described.

# Source in positive octant

**Experimental Programme - Section 1**

The first test was with the loudspeaker, the source, placed in the positive quadrant. Before describing the source location studies, using the wheelbrace array of microphones, the method for determining the source position coordinates in the laboratory, using a tape measure, will be discussed. The measurement of the source position, the '$x_s$','$y_s$' and '$z_s$' co-ordinates proved to be problematic because of the practical difficulty in recognising the 90° angles, without recourse to surveying instrumentation. It was solved by the use of cotton threads and a jig, (Figure 6.5), based upon a protractor to align the measurement positions. The jig consisted of a protractor with 3 mm dowels glued to the 0°, 90° and 180° positions and a reference dowel placed at the centre. The device was attached to the frame by 'terry-clips' and centred on the microphone $m_6$ (along the horizontal line CC′ in Figure 6.6). A cotton thread was attached to the bottom of microphone $m_6$ and the end stand of the support rail, passing the 90° and reference dowels. This indicated the axis of the microphones $m_5$ $m_0$ and $m_6$. A second horizontal thread (BB′), was fitted between two stands at 90° to the CC′ line, shown in Figure 6.6, (the thread

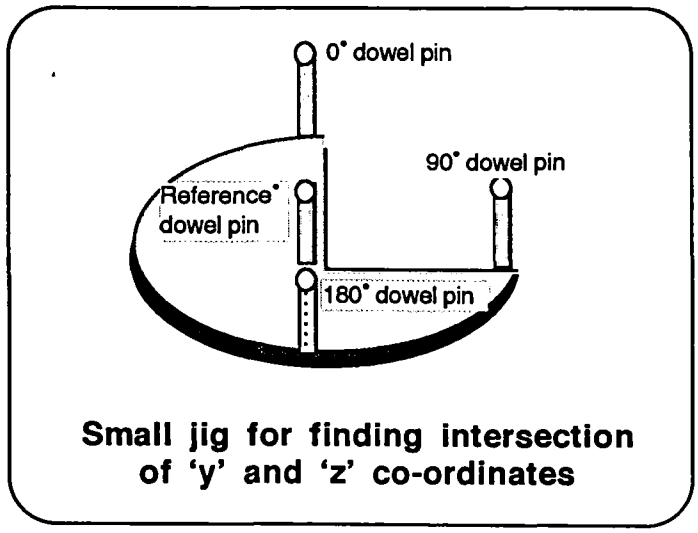


*Figure 6.5 the jig*

was aligned with the 0°, reference and 180° dowels). The jig used to align this thread with the plumb line, which was suspended from the loudspeaker support , and allowed to hang in front of loudspeaker, just touching the speaker edges. (Shown in figure 6.6 as AA´, the vertical plumb line). Measurements were made to the centre, or reference pin, of the protractor from

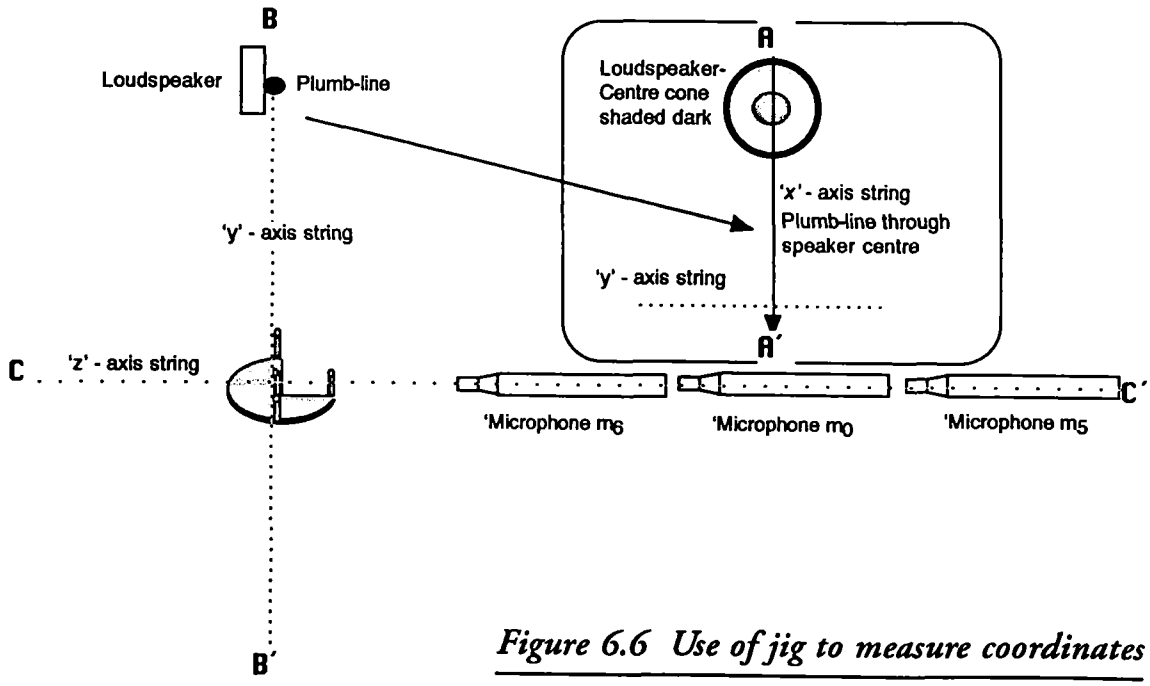


*Figure 6.6 Use of jig to measure coordinates*

the front edge of microphone $m_0$ for the 'z' coordinate. The 'y' coordinate was measured from the reference pin of the jig, to the intersection of the threads at the base of the plumb line. The 'x' coordinate was measured from the centre of the cone of the loudspeaker (shown as the darker shading in Figure 6.6), to the intersection of the plumb line (AA´) and the 'y' coordinate

string (BB'). It was assumed that the source of the noise originated at the geometric centre of the loudspeaker and that the point of reception of the sound was the centre of the circular end of the microphone. Returning to the microphone array detection of the source position, measurements were made of the distances from the loudspeaker to each of the microphones by recording the signals arriving at each microphone.

A set of readings were taken over a period of days that is, the equipment was shut down and re-started several times over the measurement period. The records were stored to disc and the discs retained for further analysis as required. Of the records, 10 sets have been presented in Tables 6.1 and 6.2. The sets of data were obtained by creating sequential bursts of noise. Each disk is capable of storing 3 sets of data from 8 channels of information. Each data set is accompanied by a text giving the experimental set up of each record.

| Time delay interval in 20 $\mu$s units between m0 and other microphones | | | | | | | |
|---|---|---|---|---|---|---|---|
| Record Number | m1-m0 | m2-m0 | m3-m0 | m4-m0 | m5-m0 | m6-m0 | to Source |
| **1803932** | 22 | 15 | 19 | 11 | 34 | 30 | 180 |
| **1803934** | 22 | 14 | 20 | 11 | 34 | 30 | 185 |
| **1803935** | 22 | 15 | 20 | 11 | 34 | 30 | 180 |
| **1803936** | 22 | 15 | 20 | 11 | 34 | 30 | 175 |
| **1903931** | 22 | 15 | 19 | 11 | 34 | 30 | 182 |
| **1903932** | 22 | 15 | 19 | 11 | 34 | 30 | 182 |
| **1903933** | 22 | 15 | 20 | 11 | 34 | 30 | 184 |
| **1903934** | 22 | 15 | 19 | 11 | 34 | 30 | 180 |
| **1903935** | 22 | 15 | 20 | 11 | 34 | 30 | 181 |
| **1903936** | 22 | 15 | 20 | 11 | 34 | 30 | 180 |
| | | | | | | | |
| | | | | | | | |
| Mean | 22 | 14.9 | 19.6 | 11 | 34 | 30 | 180.9 |
| Std.Dev. | 0 | 0..32 | 0.51 | 0 | 0 | 0 | 2.73 |
| 95% Confidence Level | 22±0 | 14.9±0.6 | 19.6±1.0 | 11±0 | 34±0 | 30±0 | 180.9±5 |

***Table 6.1 - Details of measurements***

The signs ascribed to the time intervals are all positive when the source is in the positive octant. This occurs because of the definition of the time interval. If the sound arrives at the even numbered microphone before reaching the reference microphone, $m_o$, then the time interval is positive. Similarly, if the sound arrives at the reference microphone, $m_o$ before it arrives at an odd numbered microphone, the interval is also positive. This convention is built into the mathematical formulae. The algebraic sign indicates leads and lags with respect to the microphone nearest the source when the source is in the positive octant - microphone $m_6$ - and not to the reference microphone.

The experimental data obtained is shown in Tables 6.1 and 6.2. The tables show ten sets of data collected over a period of two days. The set of figures shown in table 6.1 is the information gained from the cross correlation of the waves. Each record consists of a trace of the noise history received by each microphone. A special program was created to display two wave traces simultaneously on the computer screen. The waves displayed were selected from the data to show the start of the noise pulse. The program allows the trace to be drawn in one of three options.

a) One pixel to each data point

b) Five pixels to each data point

c) Ten pixels to each data point.

The options allow the magnification of the waves and a greater precision in placing a cursor over the start of the noise pulse. For the first two waves displayed, the first wave is always from the data collected by the reference microphone. The position of the cursors is recorded as the number of data points from the start of the data record and the difference between the cursors is shown. This difference between the cursors is the time difference in the waves reaching the respective microphones. The difference is expressed in 20 $\mu$S time intervals. The remaining waves are then displayed in pairs and the computer records the time differences for each wave with respect to the reference microphone. This technique depended upon a visual selection of a reference point, on which the cursor was placed. The main use of this technique was to identify the approximate location of the start of the noise pulse. This information was used to combine the data from the reference microphone and each of the other microphones in turn. The time delay at the position of the maximum correlation coefficient was the value used to

substitute into the equations for the determination of the source coordinates 'x,y,z'.

The average value from the ten records was calculated. The standard deviation and the 95% confidence level for the ten values shows that the readings are very consistent. The results support the view that similar results would be obtained if readings were taken from the six microphone positions in sequence, rather than taking simultaneous readings. Where variations occur in the results, it is usually due to approximating answers to 0.5 of a time period. Such an approximation occurs where the correlation coefficient is at its maximum value for two adjacent time periods.

Knowing the temperature in the room, the velocity of sound can be calculated using the standard value at 20°C = 343.5 m/s calculated from the quoted value of 331.3 m/s at 0°C in the Open University Science Data Book edited by R.M.Tennent. From the time delays, remembering that a delay can be either positive or negative, the difference in distance travelled from the source to the various microphones, as well as the distance to the reference microphone, was calculated.

For example, the time delay between noise arriving at microphone $m_1$ and at the centre microphone $m_0$, was 22 time units.

This means that microphone $m_1$ is 22 x 343.5 x 20 x $10^{-6}$ m, or 0.151 m further away from the source than the centre microphone $m_0$.

Table 6.2 lists the distance intervals between the reference microphone, $m_0$, and the other microphones. The 95% confidence levels are shown based upon the standard deviation of the ten measured time intervals for each microphone position. The calculated values of 'R' with 'x','y' and 'z', are shown, determined by using the equations from the Table of Equations, Table 4.1, on page 38. The 95% confidence level is based upon the two readings for each coordinate and the three readings for the distance of the source to reference microphone distance 'R'. The actual distance between the various microphones and the source is expressed from the combination of the mean calculated value for 'R' and the difference in distance $x_n$,

| Calculation of Co-ordinates using the equations in Table 4.1 and the practical data from Table 6.1 | | | | | | | |
|---|---|---|---|---|---|---|---|
| **Record** | **Difference in distance, xn, in metres between source to reference microphone, m0, and source to other microphones** | | | | | | |
| | *x1* | *x2* | *x3* | *x4* | *x5* | *x6* | *R Source* |
| 1803932 | 0.15 | 0.10 | 0.14 | 0.08 | 0.23 | 0.20 | 1.22 |
| 1803934 | 0.15 | 0.10 | 0.14 | 0.08 | 0.23 | 0.20 | 1.26 |
| 1803935 | 0.15 | 0.10 | 0.14 | 0.08 | 0.23 | 0.20 | 1.22 |
| 1803936 | 0.15 | 0.10 | 0.14 | 0.08 | 0.23 | 0.20 | 1.19 |
| 1903931 | 0.15 | 0.10 | 0.13 | 0.08 | 0.23 | 0.20 | 1.24 |
| 1903932 | 0.15 | 0.10 | 0.13 | 0.08 | 0.23 | 0.20 | 1.24 |
| 1903933 | 0.15 | 0.10 | 0.14 | 0.08 | 0.23 | 0.20 | 1.25 |
| 1903934 | 0.15 | 0.10 | 0.13 | 0.08 | 0.23 | 0.20 | 1.22 |
| 1903935 | 0.15 | 0.10 | 0.14 | 0.08 | 0.23 | 0.20 | 1.23 |
| 1903936 | 0.15 | 0.10 | 0.14 | 0.08 | 0.23 | 0.20 | 1.22 |
| **Average** | **0.15** | **0.10** | **0.14** | **0.08** | **0.23** | **0.20** | **1.23** |
| **95% confidence level** | **0.15± 0** | **0.10±0** | **0.137 ±0.009** | **0.08±0** | **0.23±0** | **0.20±0** | **1.23± 0.04** |
| **Calculation of R** | 1.3 | 1.12 | 1.15 | **Mean R** | | **1.19±0.2** | |
| **Actual distance = (Mean R)±x** | **1.33±0.2** | **1.08±0.2** | **1.32±0.2** | **1.11±0.2** | **1.42±0.2** | **0.98±0.2** | **1.19±0.2** |

| **Angles** | | | | | |
|---|---|---|---|---|---|
| | | | **Calculation of 'x'** | 0.53 | 0.55 |
| | | | **Mean 'x'** | **0.54 ± 0.03** | |
| **Bearing** | | **Altitude** | **Calculation of 'y'** | 0.45 | 0.46 |
| ø | θ | α | **Mean 'y'** | **0.45 ± 0.01** | |
| **64.1°** | **62.6°** | **27.4** | **Calculation of 'z'** | 0.94 | 0.93 |
| | | | **Mean 'z** | **0.93 ± 0.01** | |

***Table 6.2***

taking account of the algebraic sign due to the lead or lag of the signal. The 95% confidence level shown for these measurements, is found from the sum of the error for the difference in distance plus the error for 'R'. It is noticeable that the error in the calculation of 'R' is high compared with the other measurements. The significance of this is dealt with in detail in Chapter 7.

This analysis gives the experimentally determined coordinates of the source, using the wheel brace microphone array, as:

$$x = 0.54 \pm 0.03 \text{ m} \quad y = 0.45 \pm 0.01 \text{ m} \quad z = 0.93 \pm 0.01 \text{ m}$$

Turning now to the coordinates of the source, as determined by the tape measure, and using the jig shown in Figure 6.5 gave

$$x = 0.56 \pm 0.01 \text{ m} \quad y = 0.47 \pm 0.01 \text{ m} \quad z = 0.96 \pm 0.01 \text{m}$$

The error for each coordinate is expressed as the 95% confidence limit where the confidence limit is related to the standard deviation, $\sigma$, and calculated as $x \pm 2\sigma$. This is based upon the assumption that the values would fit on a normal distribution curve.

It is of interest to note that the expected problems with errors in measurement were thought to lie in the recording of the time intervals, whilst the measurement of distances with a tape measure would be straight forward. In reality, the tape measured results have proven to be the more problematic. For instance, when the equipment was originally set up, the distances for the coordinates were thought to be :

$$x = 0.50 \text{ m} \quad y = 0.46 \text{ m} \quad \text{and } z = 1.0 \text{ m}$$

After the first set of measurements, when the measured time intervals were found not to agree with the predicted values, the coordinates of the loudspeaker were re-measured with the tape measure. This time the results were :

$$x = 0.59 \text{ m} \quad y = 0.46 \text{ m} \quad \text{and } z = 0.95 \text{ m}$$

At this stage it was considered necessary to implement a better system for ensuring that the distances measured were truly at right angles, so the jig arrangement (Figure 6.6) was put into use.

This produced values for the coordinates of :

$$x = 0.56\ m \quad y = 0.47\ m \quad \text{and } z = 0.96\ m$$

The accuracy with which the tape measure can be used does not reflect the error obtained from placing the tape measure at the wrong angle. The measurements of the distance from the source to the microphones is a more accurate measure than the tape measured values of the coordinates 'x,y,z'. The reader will recall Table 4.2 page 42 showed the theoretical errors possible, expressed as a percentage. Table 6.3 shows the theoretical errors possible for the experiments reported in Table 6.1. The figures produced from the experimental method fall inside the expected error from the calculation based upon the geometry of the array and source. The values of $x_3$ for microphone number 3, vary compared with the other microphone time intervals. The time intervals range between 19 and 20, 20$\mu$S periods. The figures in Table 6.1 are averaged and the time interval is taken as 19.6 units. The calculation in Table 6.3 converts all time intervals to the nearest whole number, as the time window for the A to D conversion is restricted to increments of one whole 20$\mu$S period. In Chapter 7, the consequence of altering the practical reading to eliminate the fractional time interval will be further discussed. Suffice it to say at this stage, the overall accuracy of the practical measurements is a function of the coordinate distances, so that the error in the estimation of the distance 'R' affects the determined values of 'x','y' and 'z'.

Table 6.3a shows the calculated values of the co-ordinates and angles using the coordinates determined by measurement with a tape measure. With the existing equipment, there was no possibility of being able to measure the angles ø, θ on the experimental model with any accuracy, other than measuring the horizontal distance between $m_0$ and the source, [the diagonal of the 'YZ' plane shown in figure 4.2 as the line OB], and using this distance with the measured 'R' value to find the cosine of 'θ'. Therefore, the measured results are compared with the results calculated from the geometry of the arrangement. It must be accepted that any errors involved in the measurement of 'x', 'y' or 'z' will be reflected in the calculated angle. The radial distance between the source and the reference microphone, R is 1.22 m according to the tape measurement; OB (the measured horizontal diagonal, or the projection of 'R' onto the 'y,z' plane) is 1.08 m. (See Column [4], Table 6.4 for measured values)

Therefore the altitude angle, α, which is 90-θ, can be determined since,

$$\cos(90-\theta) \text{ is } 1.08/1.22, \text{ or } \theta \text{ is } 62.3^\circ \text{ and the altitude, } \alpha \text{ is } 27.7^\circ.$$

| | | | | |
|---|---|---|---|---|
| **Separation of microphones** | 0.28 m | **Distance 'R' between source and reference microphone** | 1.21m | |
| **'X' co-ordinate** | 0.56 m | **Time interval in 20μS intervals between mo & S** | | |
| **'Y' co-ordinate** | 0.47 m | **Interval between m1 and S** | 22 | |
| **'Z' co-ordinate** | 0.96 m | **Interval between m2 and S** | 15 | |
| **Temperature at which measurements occurred** | 20 ° C | **Interval between m3 and S** | 19 | |
| **Velocity of sound** | 343.41 m/s | **Interval between m4 and S** | 11 | |
| | | **Interval between m5 and S** | 34 | |
| | | **Interval between m6 and S** | 30 | |
| **Calculation of 'R'** | | **Calculation of 'x'** | | |
| For x1 and x2 | 1.28 | For x1 | 0.55 | |
| For x3 and x4 | 1.22 | For x2 | 0.56 | **Mean 'x' = 0.55**<br>**Error 'x'=1.04%** |
| For x5 and x6 | 1.09 | **Calculation of 'y'** | | |
| Mean value of 'R' | 1.20 | For x3 | 0.45 | |
| % error | 0.96% | For x4 | 0.45 | **Mean 'y' = 0.45**<br>**Error 'y'=3.10%** |
| **Calculation of Angles** | | **Calculation of 'z'** | | |
| θ | 62.4 °<br>Error<br>0.0% | For x5 | 0.96 | |
| ø | 64.6 °<br>Error<br>0.6% | For x6 | 0.94 | **Mean 'z' = 0.95**<br>**Error 'z'=1.51%** |

## *Theoretical Time intervals calculated from coordinates - Table 6.3a*

*The data in this chart is from calculating the time intervals, using the (x,y,z) values measured with a tape.. It should be noted that the geometric calculation suggests that the time interval to the third microphone should be 19 x 20μS intervals as opposed to the 19.6 x 20μS averaged value. (See Table 6.1)*

From the measured values of the coordinates, the bearing, ø, is ATAN (z/y) or 64.2°.

The values for the angles from the experimental data, that is, using the time differences obtained with the wheel brace array of microphones, and substituting the results into the equations summarised in Table 4.1 page 38, gives

$\theta = 62.6°$ $\quad ø = 64.1°$ (See columns [3] & [4] Table 6.4)

(This is a difference of 0.5% for 'θ' and 0.7% for 'ø')

***Table 6.3b comparison of tape measurements***

| Measurement | Source Co-ordinates in metres | | |
|---|---|---|---|
| | 'x' | 'y' | 'z' |
| First measurement | 0.50 | 0.46 | 1.00 |
| Second measurement | 0.59 | 0.46 | 0.95 |
| Measurement using Jig Fig.6.6 | 0.56 | 0.47 | 0.96 |
| Standard deviation | 0.046 | 0.006 | 0.026 |
| 95% confidence level | 0.55±0.09 | 0.46±0.01 | 0.97±0.05 |

There are errors in measuring the coordinates using a tape measure. There is a degree of uncertainty in deciding the position of the source on the loudspeaker and the point of reception on the microphone. The error has been estimated at ± 0.01 m. This does not make any allowance for the error in choosing the correct 'line' to measure, but does attempt to allow for the uncertainty of from where the measurements should be taken. There is a greater error in measuring the coordinates $(x_s,y_s,z_s)$, than in measuring the distances between the various microphones and the source.

The errors and problems encountered in finding the values of (x,y,z) using a ruler or tape measure, will also occur in projecting the source position onto the partition, from the values derived by the experimental determination of the coordinates. If it is difficult to be sure the axes are at right angles, it will be difficult to locate the source as a practical exercise from the coordinates. For this work, the problem has been mitigated by illustrating the position of the source graphically, using the computer to plot the positions. The plots use the various derived values, such as those obtained for 'x,y,z' from the time difference calculations, and the values of 'x,y,z' from the geometry of the measured coordinates. The spread of these points on the graphs such as figures 6.5, 6.6, 6.7 and 6.10 indicates the circle of confusion in precisely locating - pinpointing - the source in space, from the measurements made.

The values for the distances between the various microphones and the source can be determined in a number of ways. Table 6.4 places the various alternatives in a way that comparisons can be made.

Column [1] uses the measured coordinates obtained with a tape measure. The figures were used in a calculation based upon the geometry of the array. The values for the distances obtained are mathematically correct provided the original coordinates were measured with a 90° angle between them.

Column [2] uses the experimentally determined value for the source to reference microphone distance, R. This is available because the signal fed to the loudspeaker is recorded by the number 8 A to D convertor. The distance between the source and the reference microphone can be calculated from the time at which the signal was sent to the loudspeaker and the time the signal was received by the reference microphone. The average value is shown from the ten results recorded in Table 6.2. The value of 'R' is combined with the values for the differences in distance between the various microphones and the source to give a totally experimentally determined value of source to microphone distances. These values are affected by the time window constraints.

Column [3] uses the calculated value of 'R' from substituting the difference in distance values, obtained experimentally as the time differences between microphones and the reference microphone, into the derived equations (equations [1]) quoted in Table 4.1 on page 38. The value of 'R' used is the mean value of the three calculated values. Note that the 95% confidence level for the calculated mean gives a variation on 1.19 of ± 0.2 compared with the value of 'R' obtained directly from the experimental readings of 1.23 ± 0.04 (see last column of Table 6.2).

Column [4] uses the tape measured values for all quantities except the angles. The angles are calculated from the measured distances of the diagonals.

Comparison of Column [1] and [4] is an indication of the accuracy with which the coordinates were measured. If column[1] differs from column[4] to any great extent, it creates the suspicion

| Comparison of Measured Distances and Experimentally Determined Distances | | | | |
|---|---|---|---|---|
| Microphone distance | Calculation using x=0.56 y=0.47 z=0.96 (Tape measured values of coordinates) [1] | Distance using measured 'R' ( = 1.23 ) plus measured difference in distances xn. See Table 6.2 [2] | Distances found from Table 6.2 (Mean R=1.17) plus measured difference in distances xn [3] | Distances measured with tape [4] |
| d1 | 1.36 | 1.38 | **1.33** | 1.37 |
| d2 | 1.11 | 1.13 | **1.08** | 1.15 |
| d3 | 1.34 | 1.37 | **1.32** | 1.35 |
| d4 | 1.13 | 1.16 | **1.11** | 1.13 |
| d5 | 1.44 | 1.47 | **1.42** | 1.45 |
| d6 | 1.00 | 1.03 | **0.98** | 1.02 |
| Source | 1.21 | 1.23 | **1.18** | 1.22 |
| x | 0.55 | 0.57 | **0.55** | 0.56 |
| y | 0.45 | 0.48 | **0.45** | 0.47 |
| z | 0.95 | 0.97 | **0.93** | 0.96 |
| Diagonal XY | 0.73 | | | 0.74 |
| Diagonal XZ | 1.12 | | | 1.15 |
| Diagonal ZY | 1.07 | | | 1.08 |
| ø | 64.3° | 63.7° | **64.1°** | 64.2° |
| α | 27.6° | 27.7° | **27.4°** | 27.7° |
| θ | 62.4° | 62.3° | **62.6°** | 62.3° |

## *Comparison of Measurement - Table 6.4*

*Notes: Column [1] is derived from entering the measured coordinates obtained with a tape measure, into the equations derived from the geometry of the array arrangement. The values of 'x,y,z' shown in this column differ from the inputted values because of the rounding up of time differences due to the finite values of the time window.*

*Columns[2] &[3] differ due to the choice of 'R' - measured or calculated.*

*Column [4] comes from the physical measurement of the separations between source and microphones using a tape measure.*

that the coordinate was incorrectly measured with the tape. The numbers in column [1] are R± the small differences in the distances travelled between the microphones. The experimentally determined value of 'R' has shown to be very reliable. The figures in Table 6.4 suggest that the measurement of the coordinates using the jig arrangement was successful, since the variation between columns 1 and 4, is never more than 3%.

Comparison of columns[2] and [4] in Table 6.4, indicates the accuracy with which the microphone array can measure the distances with the finite time window of 20$\mu$S. The maximum error is 2.5%.

Comparison of columns[3] and [4] show the effect that the calculated value of 'R' has upon the estimation of the distances. Bearing in mind the error due to the variation in the three calculated values of 'R', the maximum error is 6% between the calculated distances and the measured distances.

The significance of the variation in the value of 'R' is discussed in Chapter 7. A further point that emerges from these figures relates to the averaging of values in 'x3' of Table 6.2. It has been stated that the finite time window allows only integer measurements of time difference. The time difference for microphone (3) varied between 19 and 20 time intervals and the calculations have been based on the average values. Table 6.5 shows what happens when the value is taken as either 19 or 20 time intervals. This will be further discussed under Chapter 7.

Comparison of source to microphone distances when Mic.3 is taken as 19 or 20 time intervals

| Distance between source and microphone | Using 19 x 20 $\mu$S for microphone No.3 | Using 20 x 20 $\mu$S for microphone No.3 | Tape measured values |
|---|---|---|---|
| d1 | 1.37 | 1.32 | 1.37 |
| d2 | 1.12 | 1.07 | 1.15 |
| d3 | 1.35 | 1.31 | 1.35 |
| d4 | 1.14 | 1.09 | 1.13 |
| d5 | 1.45 | 1.40 | 1.45 |
| d6 | 1.01 | 0.96 | 1.02 |

***Changing time interval from 19 to 20 units - Table 6.5***

# Diagrammatic Representation of the Spatial Distribution of the Coordinates.

The following diagram is intended to show the amount of scatter between the predictions of the coordinates from the various methods of calculation. Table 6.4 gives four alternative sets of coordinates. The circle containing these points shows the range over which the coordinates are spread.

The diagram contains a sketch illustrating which plane contains the graphical information. The four 'x,y' coordinates are shown in the upper chart and the four 'z,y' coordinates in the lower chart. The respective planes are shaded to distinguish them. The 'x,y' points are in the vertical plane as seen if the observer were at the position of the reference microphone and looking towards the source. The 'zy' points are in the horizontal plane, viewed from the same perspective.

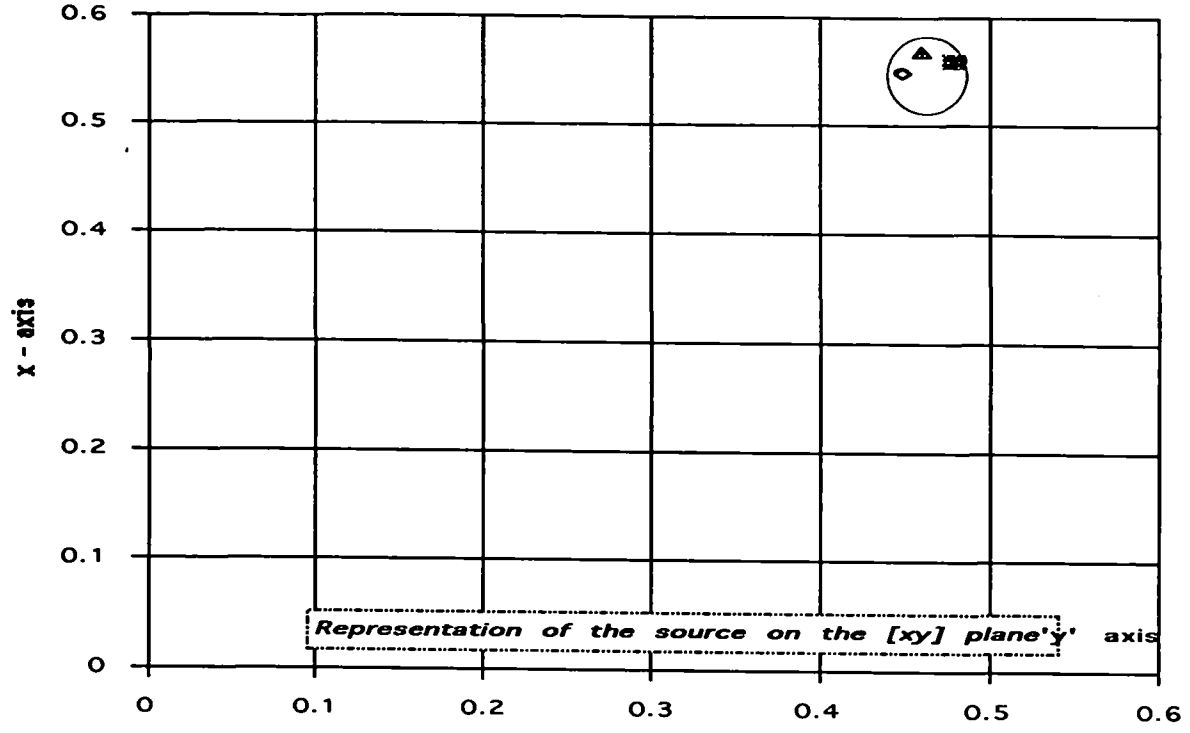


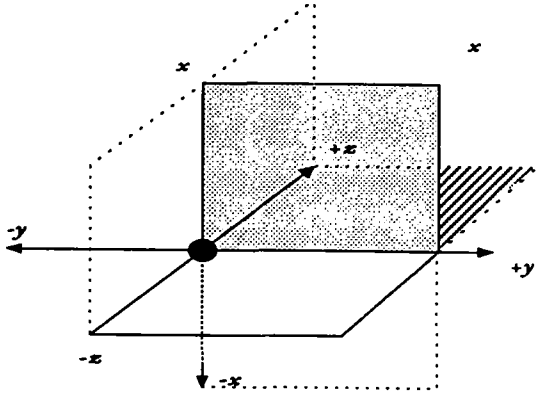


The charts are located in the positive quadrants of the (x,y) and (y,z) planes. The planes are shown shaded in the diagram.

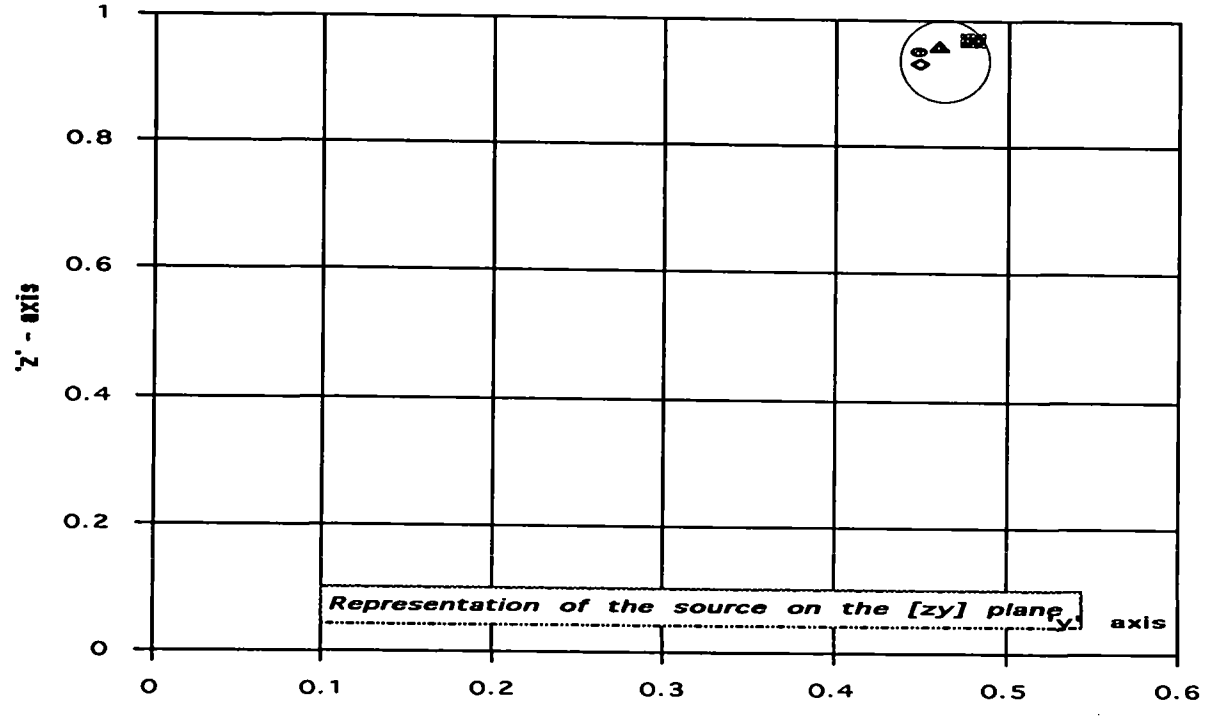


*Figure 6.5*

# Source placed in any octant.

**Experimental programme - Section 2.**

The equations for calculating the position of the source automatically indicate whether the source is in front or behind the reference microphone from the convention used in measuring the time separation. If the time taken for the sound to reach the even numbered microphones is shorter that the time taken to reach the odd numbered microphones, then the source is in the positive octant. The various combinations indicate in which octant the source lies. This enables a 'lookup' table to be created and incorporated in the calculation sheet.

Let the distance to the source from any microphone be $d_x$, where x = the microphone number, then the following illustrate the sign convention adopted in the mathematical analysis

If $d_2 < d_1$ and $d_4 < d_3$ and $d_6 < d_5$ then all coordinates ..... +ve

If $d_2 > d_1$ and $d_4 < d_3$ and $d_6 < d_5$ then [x] coordinate ..... -ve

If $d_2 < d_1$ and $d_4 > d_3$ and $d_6 < d_5$ then [y] coordinate ..... -ve

If $d_2 < d_1$ and $d_4 < d_3$ and $d_6 > d_5$ then [z] coordinate ..... -ve

If $d_2 > d_1$ and $d_4 > d_3$ and $d_6 > d_5$ then [xyz] coordinates ..... -ve

If $d_2 > d_1$ and $d_4 < d_3$ and $d_6 > d_5$ then [xz] coordinates ..... -ve

If $d_2 < d_1$ and $d_4 > d_3$ and $d_6 > d_5$ then [zy] coordinates ..... -ve

If $d_2 > d_1$ and $d_4 > d_3$ and $d_6 < d_5$ then [zy] coordinate ..... -ve

In addition to determining in which octant is the source, the calculation of the angles gives further clarification. Unfortunately, the sign of the angles can cause confusion. If all the coordinates are negative, then the calculation of ø is positive because

$$\tan\phi = \frac{-z}{-y}$$

If $ø_c$ is used to represent the calculated angle, then a table can be created to relate the calculated angle to the true angle ø.

If coordinate 'y' is +ve and coordinate 'z' is +ve ..... $ø = ø_c$

If coordinate 'y' is -ve and coordinate 'z' is +ve ..... $ø = 180 - ø_c$

If coordinate 'y' is -ve and coordinate 'z' is -ve ..... $ø = 180 + ø_c$

If coordinate 'y' is +ve and coordinate 'z' is -ve ..... $ø = 360 - ø_c$

The calculated values for θ do not require any 'lookup' tables because θ is the ACOS (x/R) and R is always positive. Therefore, the change in the sign of 'x' is sufficient to indicate whether the position of the source is above or below the y-z referenceplane and the angle ø provides the rest of the required information to determine the noise source location.

The random placement of a source was used to investigate the validity of the test method. An independent observer placed the source and its location was determined using the array. For this exercise, a single set of readings was used. The potential error in the determination of the coordinates was accepted.

Table 6.6 shows the experimental data obtained from this test. The algebraic signs of the 'x,y,z' coordinate values show that the source was in the negative 'x' octant, the positive 'y' octant and the negative 'z' octant. That is, the source was below the reference plane and behind the microphone array. The calculated angle, $ø_c$ is negative and is the value for the angle measured in a clockwise direction of rotation from the reference line, which is the positive part of the 'y' axis. The true value of 'ø' is 360 - ATAN(z/y), as indicated previously.

The values for the coordinates as found using a tape measure were:

'x' = -0.35 m  'y' = 0.62 m and 'z' = -1.08 m

From these measurements, the angles $\alpha$ and $\phi$ were calculated as follows

$$\text{Measured } \phi_c = ATAN\left(\frac{z}{y}\right) \text{or } 60.1^\circ$$

but the bearing, $\phi$, is 360 - 60.1 or 299.9°

$$\theta = \text{ACOS}\left(\frac{x}{R}\right) \text{or } 105.7^\circ$$

$$\therefore \text{ the altitude } = -15.7^\circ$$

The values for the coordinates from the wheel brace array were

x = -0.31 y = 0.59 and z = -1.02 m

For a prediction of the location of the source based upon a single set of readings, the results are commendably close to the tape measured values - see Table 6.7.

| Time delay interval in 20 $\mu$s units between m0 and other microphones - Random Placement of Source | | | | | | | |
|---|---|---|---|---|---|---|---|
| Record Number | m1-m0 | m2-m0 | m3-m0 | m4-m0 | m5-m0 | m6-m0 | to Source |
| | | | | | | | |
| 805930 | -6 | -14 | 23 | 15 | -32 | -35 | 185 |
| | | | | | | | |
| Mean | -6 | -14 | 23 | 15 | -32 | -35 | 185 |
| Std.Dev. | N/A | N/A | N/A | N/A | N/A | N/A | N/A |
| 95% Confidence Level | N/A | N/A | N/A | N/A | N/A | N/A | N/A |

***Results for random location Table 6.6***

| Calculation of Co-ordinates using the equations in Table 4.1 and the practical data from Table 6.6 | | | | | | | |
|---|---|---|---|---|---|---|---|
| **Record** | **Difference in distance, xn, in metres between source to reference microphone, m0, and source to other microphones** | | | | | | |
| | *x1* | *x2* | *x3* | *x4* | *x5* | *x6* | *R Source* |
| 805930 | -.041 | -0.095 | 0.16 | 0.10 | -0.22 | -0.24 | 1.26 |
| **Average** | -.041 | -0.095 | 0.16 | 0.10 | -0.22 | -0.24 | 1.26 |
| **95% confidence level** | N/A | N/A | N/A | N/A | N/A | N/A | N/A |
| **Calculation of R** | 1.34 | 1.12 | 1.28 | **Mean R** | | **1.24±0.22** | |
| **Actual distance = (Mean R) ± x** | **1.20** | **1.34** | **1.40** | **1.14** | **1.02** | **1.48** | **1.24** |

| Angles | | | | | |
|---|---|---|---|---|---|
| | | | **Calculation of 'x'** | -0.32 | -0.30 |
| | | | **Mean 'x'** | **-0.31±0.01** | |
| **Bearing** | | **Altitude** | **Calculation of 'y'** | 0.60 | 0.57 |
| **ø** | **θ** | **α** | **Mean 'y'** | **0.59±0.04** | |
| | | | **Calculation of 'z'** | -1.02 | -1.02 |
| **299.9°** | **104.4°** | **-14.4** | **Mean 'z** | **-1.02±0.004** | |

***Results for random placing - Table 6.7***

Note: The term (R±x) allows for the lead or lag effect in the signal reaching the respective microphones.

| Comparison of Measured Distances and Experimentally Determined Distances | | | | |
|---|---|---|---|---|
| Microphone distance | Calculation using x=-0.35 y=0.62 z=-1.08(negative) (Tape measured values of coordinates) [1] | Distance using measured 'R' ( = 1.26 ) plus measured difference in distances xn. See Table 6.7 [2] | Distances found from Table 6.7 (Mean R=1.24) plus measured difference in distances xn [3] | Distances measured with tape [4] |
| d1 | 1.25 | 1.22 | **1.20** | N/A |
| d2 | 1.40 | 1.36 | **1.34** | N/A |
| d3 | 1.45 | 1.42 | **1.40** | N/A |
| d4 | 1.18 | 1.16 | **1.14** | N/A |
| d5 | 1.07 | 1.04 | **1.02** | N/A |
| d6 | 1.53 | 1.50 | **1.48** | N/A |
| Source | 1.29 | 1.26 | **1.24** | N/A |
| x | -0.35 | -0.31 | **-0.31** | -0.35 |
| y | 0.62 | 0.60 | **0.59** | 0.62 |
| z | -1.04 | -1.04 | -1.02 | -1.08 |
| Diagonal XY | 0.71 | | | N/A |
| Diagonal XZ | 1.13 | | | N/A |
| Diagonal ZY | 1.24 | | | N/A |
| ø | 300.5° | 299.9° | 299.9° | N/A |
| α | -16.0° | -14.4° | -14.4° | N/A |
| θ | 106.0° | 104.4° | 104.6° | N/A |

## *Comparison of measurements for Random Placing - Table 6.8*

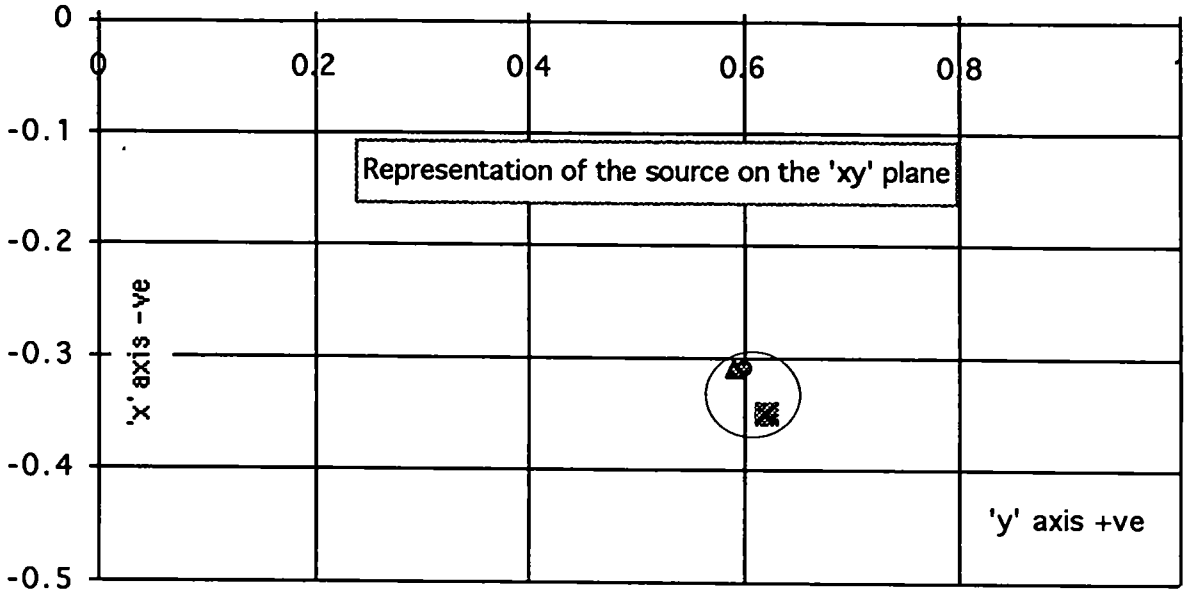


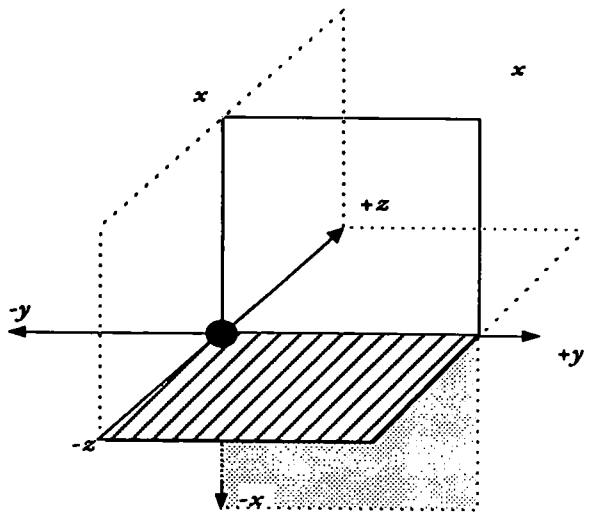


**Random placement of source** - the origin represents the reference microphone

The charts are located in the negative planes as indicated by the shading in the diagram.

*Figure 6.6*

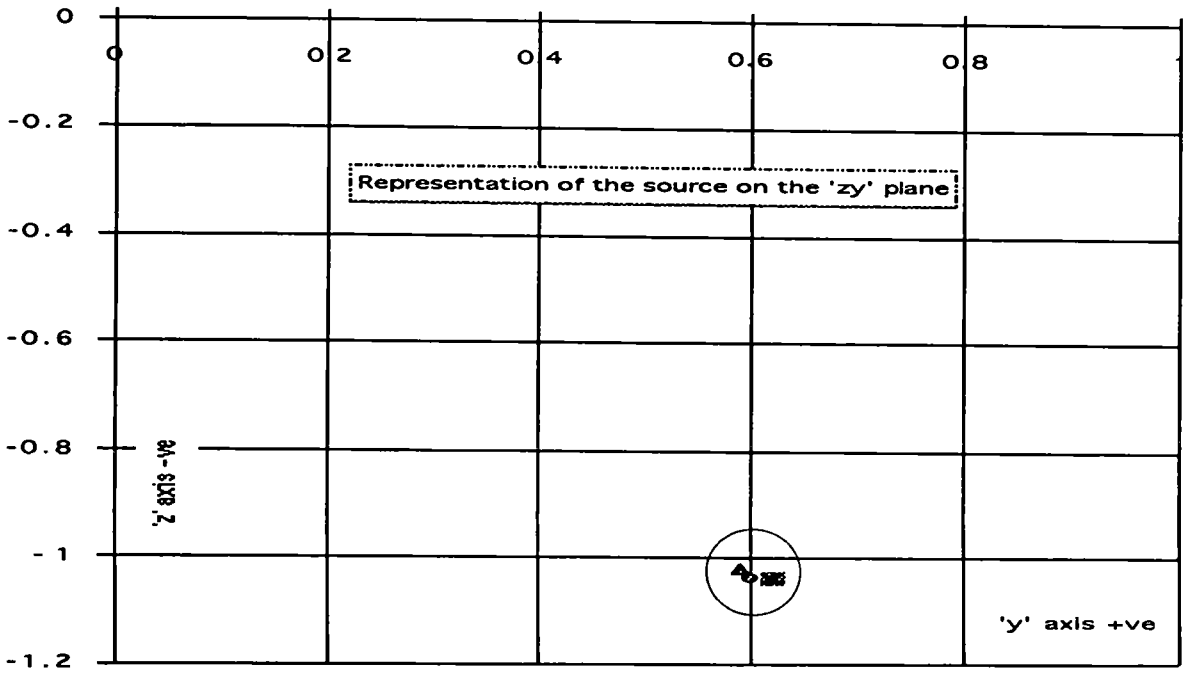

# Source in the all negative octant

**Experimental Programme - Section 3**

When the source coordinates are all negative, as in Table 6.9, the calculated value for the bearing, $\phi_c$ is 55.2°. The calculated angle is positive because the two coordinates that define the tangent of the angle are negative. From the list of angles (bottom of page 85), where both coordinates are negative, then the true angle is $180 + \phi_c = 235.2°$.

The value of $\theta$ at 100.8° indicates that the source is

100.8 - 90 = 10° below the horizontal. This is expressed as the altitude '$\alpha$' = -10.8°

**Time delay interval in 20 $\mu$s units between m0 and other microphones - Source Placement in Negative Octant**

| Record Number | m1-m0 | m2-m2 | m3-m0 | m4-m4 | m5-m0 | m6-m6 | to Source |
|---|---|---|---|---|---|---|---|
| 1509932 | -3 | -12 | -17 | -26 | -32 | NA | 184 |
| 1509933 | -3 | -12 | -18 | -26 | -32 | -35 | 185 |
| 1509934 | -3 | NA | -18 | -27 | -32 | -34 | 184 |
| 1509935 | -3 | NA | NA | -27.5 | -32 | -34 | 184 |
| 1509936 | -3 | -12 | -18 | -26 | -32 | -34 | 184 |
| | | | | | | | |
| Mean | -3 | -12 | -17.7 | -26.5 | -32 | -34.2 | 184.2 |
| Std.Dev. | 0 | 0 | 0.5 | 0.71 | 0 | 0.5 | 0.9 |
| 95% Confidence Level | -3±0 | -12±0 | 17.7±1.0 | -26.5±1.4 | -32±0 | -34.2±1.0 | 184.2±0.9 |

*Table 6.9*

The measured values for the coordinates were:

x = -0.27 m  y = -0.62 m  and  z = -1.04 m

The calculations shown in Table 6.10 introduce some interesting facts that will be dealt with more fully under the discussion in Chapter 7. The calculation of the distance'R', between the source and the reference microphone, shows that the three alternative values for 'R' to be 1.22, 0.91 and 1.83 m. When the 95% confidence level is calculated, the extent of the variation is 1.32 ± 0.92. Converting this to a percentage, suggests that a difference of 70% can exist between readings. Since the calculation of the coordinates depends upon the value of 'R' then the values of the coordinates determined from the calculation of the practical results will have a large possible error.

The respective values for the coordinates are compared in Table 6.11. The four columns of Table 6.11 allow some informative deductions. Columns [1] and [2], which calculate distances

| Calculation of Co-ordinates using the equations in Table 4.1 and the practical data from Table 6.9 | | | | | | | |
|---|---|---|---|---|---|---|---|
| **Record** | **Difference in distance, xn, in metres between source to reference microphone, m0, and source to other microphones** | | | | | | |
| | *x1* | *x2* | *x3* | *x4* | *x5* | *x6* | *R Source* |
| **1509932** | -0.020 | -0.08 | -0.116 | -0.177 | -0.22 | NA | 1.25 |
| **1509933** | -0.02 | -0.08 | -0.123 | -0.177 | -0.22 | -0.24 | 1.26 |
| **1509934** | -0.02 | NA | -0.123 | -0.184 | -0.22 | -0.23 | 1.25 |
| **1509935** | -0.02 | NA | NA | -0.187 | -0.22 | -0.23 | 1.25 |
| **1509936** | -0.02 | -0.08 | -0.123 | -0.177 | -0.22 | -0.23 | 1.25 |
| **Average** | -0.02 | -0.08 | -0.12 | -0.18 | -0.22 | -0.24 | 1.26 |
| **95% confidence level** | -.02±0 | -0.08±0 | -0.12 ±0.007 | -0.18 ±0.009 | 0.22±0 | -0.23 ±0.009 | 1.25± 0.009 |
| **Calculation of R** | 1.22 | 0.91 | 1.83 | **Mean R** | | **1.32±0.92** | |
| **Actual distance = (Mean R) ± x** | **1.30** | **1.40** | **1.20** | **1.50** | **1.10** | **1.55** | **1.32** |

| **Angles** | | | | | |
|---|---|---|---|---|---|
| | | | **Calculation of 'x'** | -0.24 | -0.26 |
| | | | **Mean 'x'** | **-0.25±0.03** | |
| **Bearing** | | **Altitude** | **Calculation of 'y'** | -0.68 | -0.77 |
| **ø** | **θ** | **α** | **Mean 'y'** | **-0.72±0.12** | |
| **235.5°** | **100.8°** | **-10.8** | **Calculation of 'z'** | -1.08 | -1.06 |
| | | | **Mean 'z** | **-1.07±0.03** | |

***Table 6.10- Practical results***

*All readings have been used because of the variation in calculated values of 'R'. (Refer to discussion)*

| Comparison of Measured Distances and Experimentally Determined Distances | | | | |
|---|---|---|---|---|
| **Microphone distance** | **Calculation using x=-0.27 y=-0.62 z=-1.04 (Tape measured values of coordinates)** [1] | **Distance using measured 'R' ( = 1.25 ) plus measured difference in distances xn. See Table 6.10** [2] | **Distances found from Table 6.10 (Mean R=1.32) plus measured difference in distances xn** [3] | **Distances measured with tape** [4] |
| **d1** | 1.21 | 1.23 | **1.30** | 1.20 |
| **d2** | 1.33 | 1.34 | **1.40** | 1.30 |
| **d3** | 1.13 | 1.13 | **1.20** | 1.10 |
| **d4** | 1.40 | 1.44 | **1.50** | 1.40 |
| **d5** | 1.02 | 1.04 | **1.10** | 1.00 |
| **d6** | 1.48 | 1.49 | **1.55** | 1.46 |
| **Source** | 1.24 | 1.25 | **1.32** | 1.22 |
| **x** | -0.31 | -0.23 | **-0.24** | -0.27 |
| **y** | -0.72 | -069 | **-0.73** | -0.62 |
| **z** | -1.22 | -1.02 | -1.07 | -1.04 |
| **Diagonal XY** | 0.67 | | | 0.71 |
| **Diagonal XZ** | 1.07 | | | 0.99 |
| **Diagonal ZY** | 1.21 | | | 1.10 |
| **ø** | 239° | 235° | 235° | 239° |
| **α** | -12° | -10° | -11° | -13° |
| **θ** | 102° | 100° | 101° | 103° |

***Table 6.11 - Comparison of results for all negative readings***

Note: *Column [1] is derived from entering the measured coordinates obtained with a tape measure. The values of 'x,y,z' shown in this column differ from the inputted values because of the rounding up of time differences due to the finite values of the time window.*

from the geometry of the array and the distances from the experimentally determined value of the separation 'R', show much similarity. This suggests that the values for the coordinates were correctly measured. Comparison of columns [2] and [4], which compare the calculated values to the measured values, show differences of 3%, which is similar to the worst comparisons of columns [1] and [2]. This again suggests that the measured values for the distances and the calculated values for the distances are in reasonable agreement. When the values obtained from the experimental results, together with the calculated value of 'R', see column [3], are compared with any of the columns, there are as much as 7% variations in values.

This suggests that the distances derived from the calculations are not very reliable. The calculations shown in column [1] add further information to this view. The coordinates obtained from the tape measurements were substituted into the geometric equations to predict the values of the time intervals - see Table 6.12. The coordinates were calculated from the results by converting the arithmetic quantities of the time intervals to the nearest integer. The calculation shows that a difference of between 14 and 17% will occur in the values of the coordinates determined from the two methods. This variation is due to the time window limitations.

| | | | | |
|---|---|---|---|---|
| **Separation of microphones** | 0.28 m | **Distance 'R' between source and reference microphone** | 1.209 m | |
| **'X' co-ordinate** | -0.27 m | **Time interval in 20$\mu$S intervals between mo & S** | | |
| **'Y' co-ordinate** | -0.62 m | **Interval between m1 and S** | -4 | |
| **'Z' co-ordinate** | -1.04 m | **Interval between m2 and S** | -13 | |
| **Temperature at which measurements occurred** | 20 ° C | **Interval between m3 and S** | -17 | |
| **Velocity of sound** | 343.41 m/s | **Interval between m4 and S** | -23 | |
| | | **Interval between m5 and S** | -33 | |
| | | **Interval between m6 and S** | -35 | |
| **Calculation of 'R'** | | **Calculation of 'x'** | | |
| For x1 and x2 | 1.20 | For x1 | -0.28 | |
| For x3 and x4 | 1.43 | For x2 | -0.34 | **Mean 'x' = -0.31 Error 'x' = 14.8%** |
| For x5 and x6 | 1.73 | **Calculation of 'y'** | | |
| Mean value of 'R' | 1.45 | For x3 | -0.72 | |
| % error | 17.3% | For x4 | -0.73 | **Mean 'y' = -0.72 Error 'y' = 16.8%** |
| **Calculation of Angles** | | **Calculation of 'z'** | | |
| θ | 102.3 ° Error 0.3% | For x5 | -1.23 | |
| ø | 210.7 ° Error 0.2% | For x6 | -1.21 | **Mean 'z' = -1.22 Error 'z' = 17.3%** |

## *Table 6.12 - Theoretical time intervals calculated from measured coordinates*

*Note - the predicted time intervals do not agree with the measured intervals in this table.*

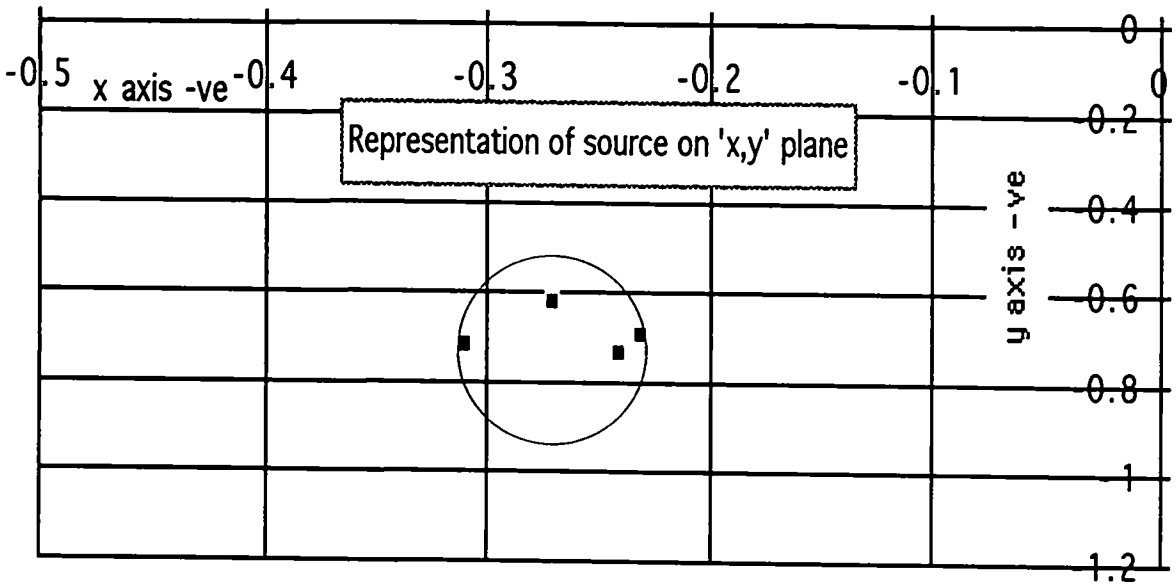


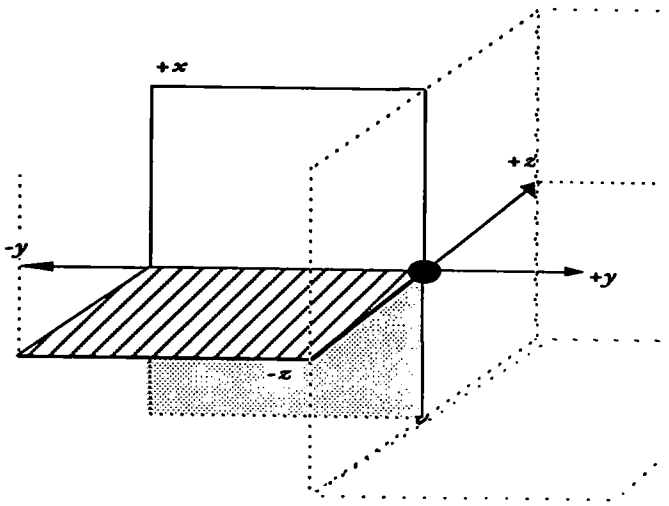


**Source in all negative octant** - The charts are located in the negative planes of the 'x', 'y' and 'z' coordinates as shaded in diagram.

*Figure 6.7*

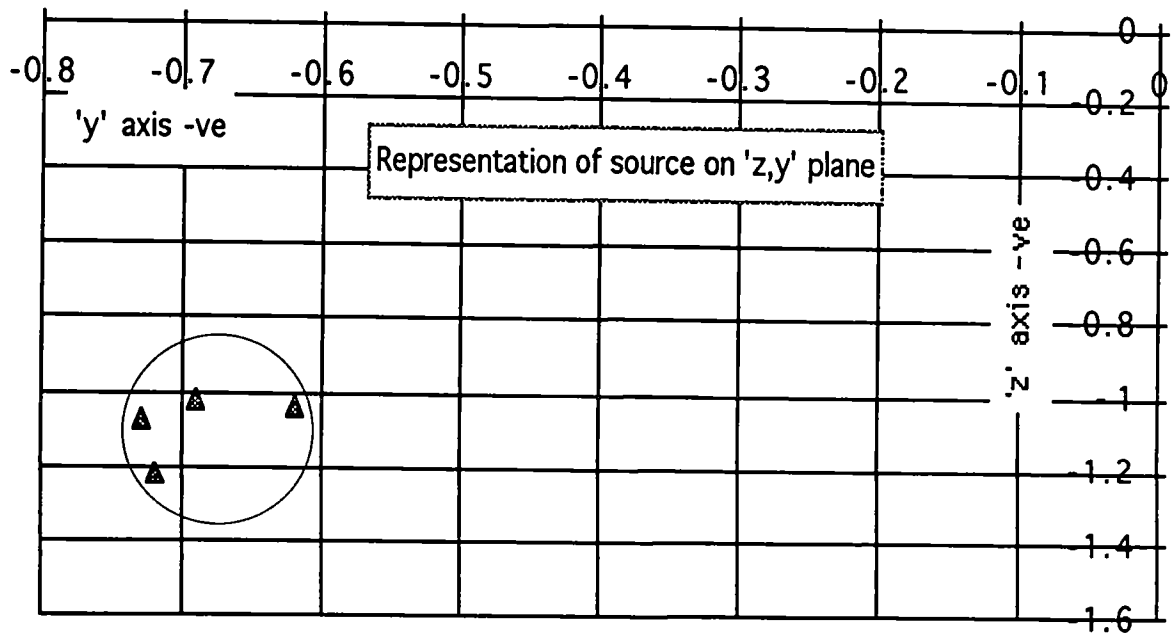

# Source placed within array half distance.

**Experimental Programme - Section 4**

The source was placed so that the 'z' coordinate was positive, whilst both the 'x' and 'y' coordinates were negative. The value of at least two of the coordinates, 'y' and 'z', was considerably less than the 0.28 metres separating the microphones. The results are shown in Table 6.13. A number of problems become apparent. The size of the source loudspeaker is no longer a point source with respect to some of the microphones. Also the arrangement supporting the microphones can cause interference patterns. The sound waves coming from the vents at the back of the loudspeaker reach some microphones sooner than the waves from the front of the loudspeaker. This makes it difficult to measure the distance with a tape measure because of the shape of the loudspeaker back. In general, it has been assumed that the greater signal is coming from the holes at the back of the speaker frame and that these coincide with the pulses from the front of the speaker. In general terms, the equipment is well able to cope with the problems, but although the time difference information is clearly seen and determined from the wave traces, the use of the cross correlation technique is more dubious. The correlation process works provided a very small number of records is averaged. The necessary distinction between the pre-trigger signal and the start of the pulse is clear. The wave beyond the first ten or so records starts to change visibly and attempting correlations with records

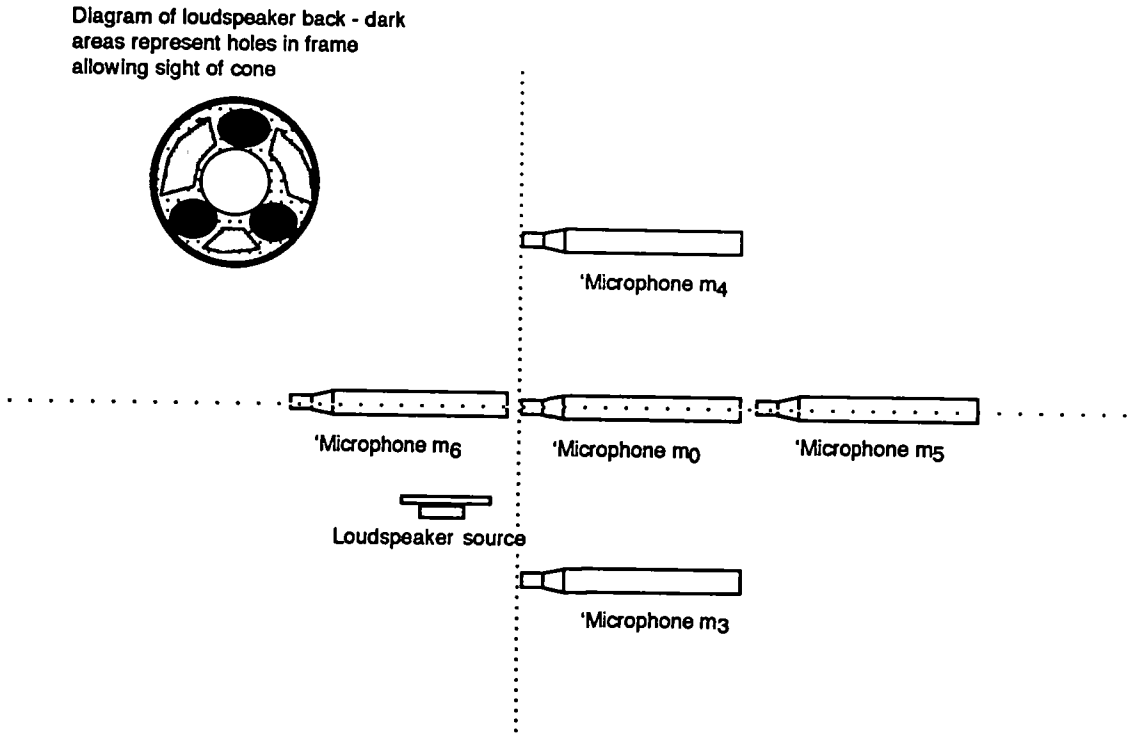


*Figure 6.8 - Placement of source within array half distance*

beyond this point is difficult. The phenomena varies between the microphones, the microphones nearest the source showing the worst results. From table 6.15, the average values for the (x,y,z) coordinates obtained from experiment, are shown as

-0.31, -0.18 and +0.09.

The coordinates obtained using a tape measure were

-0.29, -0.19 and 0.09.

Table 6.13 shows that the recorded values for the time intervals reflect the difficulties of the cross correlation by being more variable than the results obtained with other arrangements. In contrast, the calculated values for the coordinates show only small variations, including the three values for 'R'. This is dealt with further under Chapter 7. The comparison of the columns in Table 6.15 shows the agreement between the calculated distances in column [1] and the calculated distances using the experimentally measured value of 'R' in column [2]. This suggests that the measured coordinates using a tape measure were accurate. The agreement between columns [1], [2] and [4] further verify this. The calculated results from the time differences in column [3] all show high values. This is because the calculated value of 'R' is 0.05 m greater than the distance measured.

The measurement of the angles in this octant again shows some deviation from the calculated result. The actual calculated value, $\phi_c$ is -24.1° because the coordinate 'y' is negative. In accordance with the statement on page 85, ø is 180 - 24.1 or 155.9°.

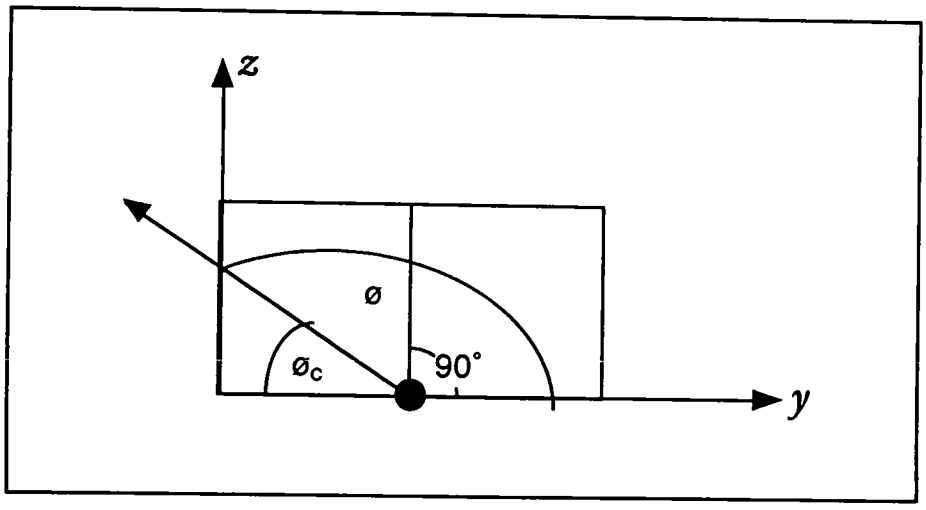


*Figure 6.9- Diagram of angle calculation*

| Time delay interval in 20 $\mu s$ units between m0 and other nicrophones - Source Placement within half beam width | | | | | | | |
|---|---|---|---|---|---|---|---|
| Record Number | m1-m0 | m0-m2 | m3-m0 | m0-m4 | m5-m0 | m0-m6 | [illegible] |
| 280993 | -22 | -38 | -5 | -28 | 21 | -5 | 55 |
| 2809932 | -22 | -35 | -5 | -28 | 21 | -6 | 52 |
| 2809933 | -24 | -35 | -2 | -26 | 20 | -6 | 53 |
| | | | | | | | |
| Mean | -22.6 | -36 | -4 | -27.3 | 20.7 | -5.7 | 53.3 |
| Std.Dev. | 1.15 | 1.73 | 1.73 | 1.15 | 0.6 | 0.6 | 1.5 |
| 95% Confidence Level | -22±2.3 | -36±3.4 | -4±3.4 | -27.3±2.3 | 20.7±1.1 | -5.7±1.1 | 53.3±3 |

*Table 6.13 - Results for source within array half distance*

| Calculation of Co-ordinates using the equations in Table 4.1 and the practical data from Table 6.13 | | | | | | | |
|---|---|---|---|---|---|---|---|
| Record | Difference in distance, xn, in metres between source to reference microphone, m0, and source to other microphones | | | | | | |
| | *x1* | *x2* | *x3* | *x4* | *x5* | *x6* | *R Source* |
| 280993 | -0.15 | -0.26 | -0.03 | -0.19 | 0.14 | -0.03 | 0.37 |
| 2809932 | -0.15 | -0.24 | -0.03 | -0.19 | 0.14 | -0.04 | 0.35 |
| 2809933 | -0.16 | -0.24 | -0.01 | -0.18 | 0.14 | -0.04 | 0.36 |
| Average | -0.15 | -0.25 | -0.03 | -0.19 | 0.14 | -0.04 | 0.36 |
| 95% confidence level | -0.15 ±0.01 | -0.25 ±0.02 | -0.03 ±0.02 | -0.19 ±0.01 | 0.14 ±001 | -0.04 ±0.01 | 0.36± 0.02 |
| Calculation of R | 0.40 | 0.38 | 0.38 | Mean R | | 0.39±0.02 | |
| Actual distance = (Mean R)±x | 0.23 | 0.63 | 0.36 | 0.57 | 0.53 | 0.42 | 0.39 |

| Angles | | | | | |
|---|---|---|---|---|---|
| | | | Calculation of 'x' | -0.31 | -0.31 |
| | | | Mean 'x' | -0.31±0.005 | |
| Bearing | | Altitude | Calculation of 'y' | -0.18 | -0.18 |
| ø | θ | α | Mean 'y' | -0.18±0.003 | |
| 155° | 143° | -53 | Calculation of 'z' | 0.09 | 0.08 |
| | | | Mean 'z | 0.09±0.004 | |

*Table 6.14 - Calculations for source within array half distance*

| Comparison of Measured Distances and Experimentally Determined Distances | | | | |
|---|---|---|---|---|
| Microphone distance | Calculation using x=-0.29 y=-0.19 z=0.09 (Tape measured values of coordinates) [1] | Distance using measured 'R' ( = 0.36 ) plus measured difference in distances xn. See Table 6.14 [2] | Distances found from Table 6.14 (Mean R=0.39) plus measured difference in distances xn [3] | Distances measured with tape [4] |
| d1 | 0.20 | 0.20 | **0.23** | 0.20 |
| d2 | 0.60 | 0.60 | **0.63** | 0.59 |
| d3 | 0.32 | 0.33 | **0.36** | 0.31 |
| d4 | 0.55 | 0.54 | **0.57** | 0.54 |
| d5 | 0.50 | 0.50 | **0.53** | 0.50 |
| d6 | 0.39 | 0.40 | **0.42** | 0.39 |
| Source | 0.35 | 0.36 | **0.39** | 0.34 |
| x | -0.29 | -0.29 | **-0.31** | -0.29 |
| y | -0.18 | -0.17 | **-0.18** | -0.19 |
| z | 0.08 | 0.08 | 0.09 | 0.08 |
| Diagonal XY | 0.34 | | | 0.32 |
| Diagonal XZ | 0.30 | | | 0.30 |
| Diagonal ZY | 0.20 | | | 1.20 |
| ø | 156° | 154° | 155° | 155° |
| α | -56° | -53° | -53° | -58° |
| θ | 146° | 143° | 143° | 148° |

*Table 6.15- Comparison of results when source is within the array half distance*

| | | | | |
|---|---|---|---|---|
| **Separation of microphones** | 0.28 m | **Distance 'R' between source and reference microphone** | 0.34m | |
| **'X' co-ordinate** | -0.29 m | **Time interval in 20μS intervals between mo & S** | | |
| **'Y' co-ordinate** | -0.19 m | **Interval between m1 and S** | -22 | |
| **'Z' co-ordinate** | 0.09 m | **Interval between m2 and S** | -37 | |
| **Temperature at which measurements occurred** | 20 ° C | **Interval between m3 and S** | -5 | |
| **Velocity of sound** | 343.41 m/s | **Interval between m4 and S** | -29 | |
| | | **Interval between m5 and S** | 21 | |
| | | **Interval between m6 and S** | -6 | |
| **Calculation of 'R'** | | **Calculation of 'x'** | | |
| For x1 and x2 | 0.34 | For x1 | -0.29 | |
| For x3 and x4 | 0.35 | For x2 | -0.29 | **Mean 'x' = --0.29 Error 'x'=0.23%** |
| For x5 and x6 | 0.36 | **Calculation of 'y'** | | |
| Mean value of 'R' | 0.35 | For x3 | -0.18 | |
| % error | 1.2% | For x4 | -0.18 | **Mean 'y' = --0.18 Error 'y' =2.5%** |
| **Calculation of Angles** | | **Calculation of 'z'** | | |
| θ | 146 ° Error 0.8% | For x5 | 0.08 | |
| ø | 156 ° Error 0.6% | For x6 | 0.08 | **Mean 'z' = -0.08 Error 'z' = 4.1%** |

*Table 6.16 - Time intervals from measured coordinates*

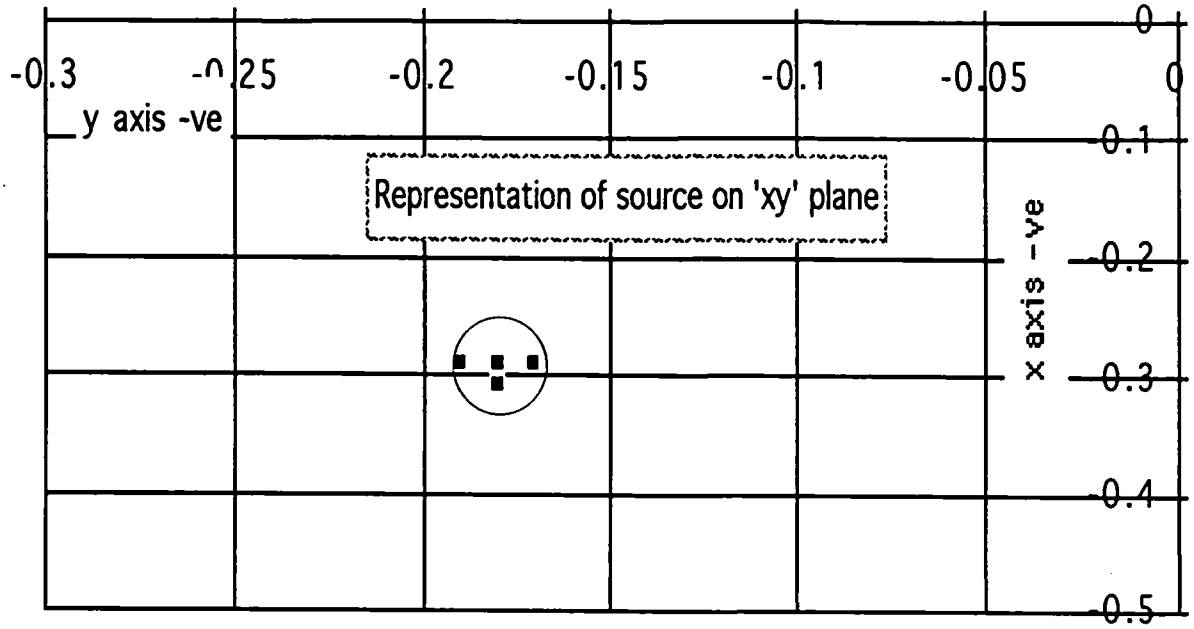


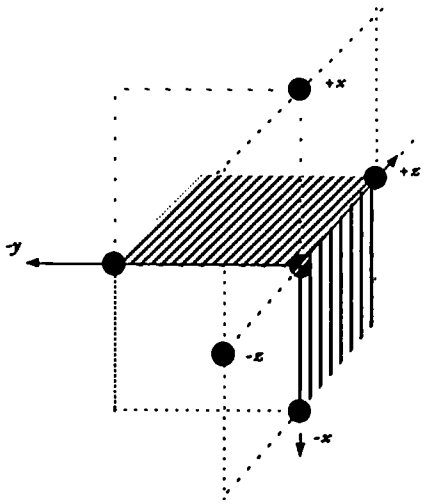


The charts are located in the negative 'x' and 'y' plane and in the positve 'z' plane. The source is within the 0.28 m distance of microphones $m_6$ and $m_3$

*Figure 6.10 - location of source within array half-length, 'd'*

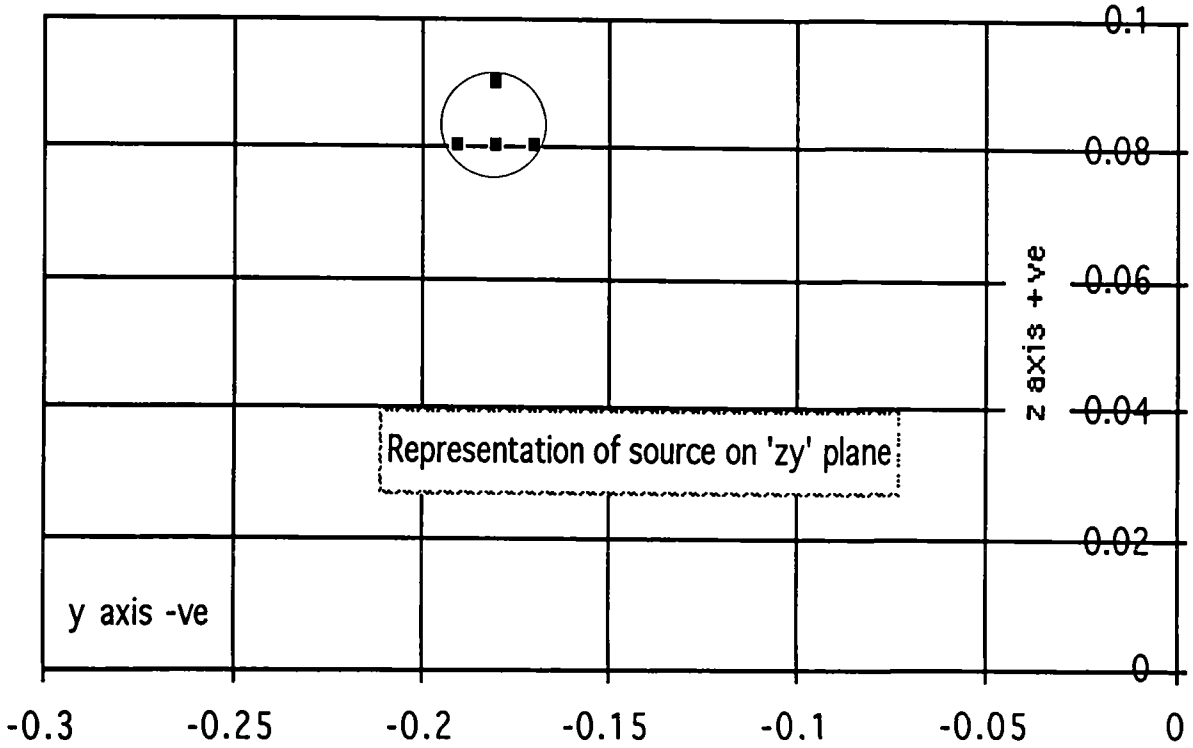

# Multiple sources -

**Experimental Programme - Section 5**

If the sound from a point source, such as a loudspeaker, is transmitted through a partition, the source of the sound on the receiving side becomes the partition rather than the loudspeaker. Where there is a weak part to the construction of the partition, such as a small hole that allows a leakage of sound, all other parts of the partition would be radiating sound so that the final signal pulse is a complex mixture of the original source pulse. A number of experiments were performed to discover how successfully the signal from a multiple source could be analysed to determine the location of the individual sources. The experiment performed used a number of identical loudspeakers, with the same magnitude signal coming from each source. There are two sets of results. One set is where there were two sources relatively close together and the second is where there were three sources. Where a small time sample is used in the correlation calculation, typically 10 samples, each of 20 $\mu$S time intervals, then a good correlation is obtained. In this context a good correlation is regarded as the normalised coefficient being greater than 0.7. For the multiple source, the correlation gave the position of the source nearest the receiving microphone, with the correlation for the second source being the next largest correlation coefficient. The result is somewhat obscure, as there are a number of other peaks very close to the same value. (See figure 6.11). If the number of samples is increased, (the example shows 100 samples being averaged), the value of the correlation coefficient decreases and the position of maximum correlation changes. (See figure 6.11 and figure 6.12). Where a larger sample is used to correlate, the correlation chart only indicates the nearer source, the second source is lost as its correlation falls to a low value comparable with the correlation of the noise in the sample.

The processing of signals to extract information is not covered in this work. The technology associated with radar and sonar are obvious examples of such technical development. In this instance the signals being analysed are transmitted rather than reflected signals, but much of the theory remains appropriate. In the paper by Goff[25], where he is using an electronic correlator, comparison of the amplitude of the correlated signals is used to measure the transmission loss of a panel. In other words, the value of the correlation function depends upon the amplitude of the received signals. In the experiment performed by Goff, the apparatus was calibrated by finding the time interval from the correlation between the source signal and the

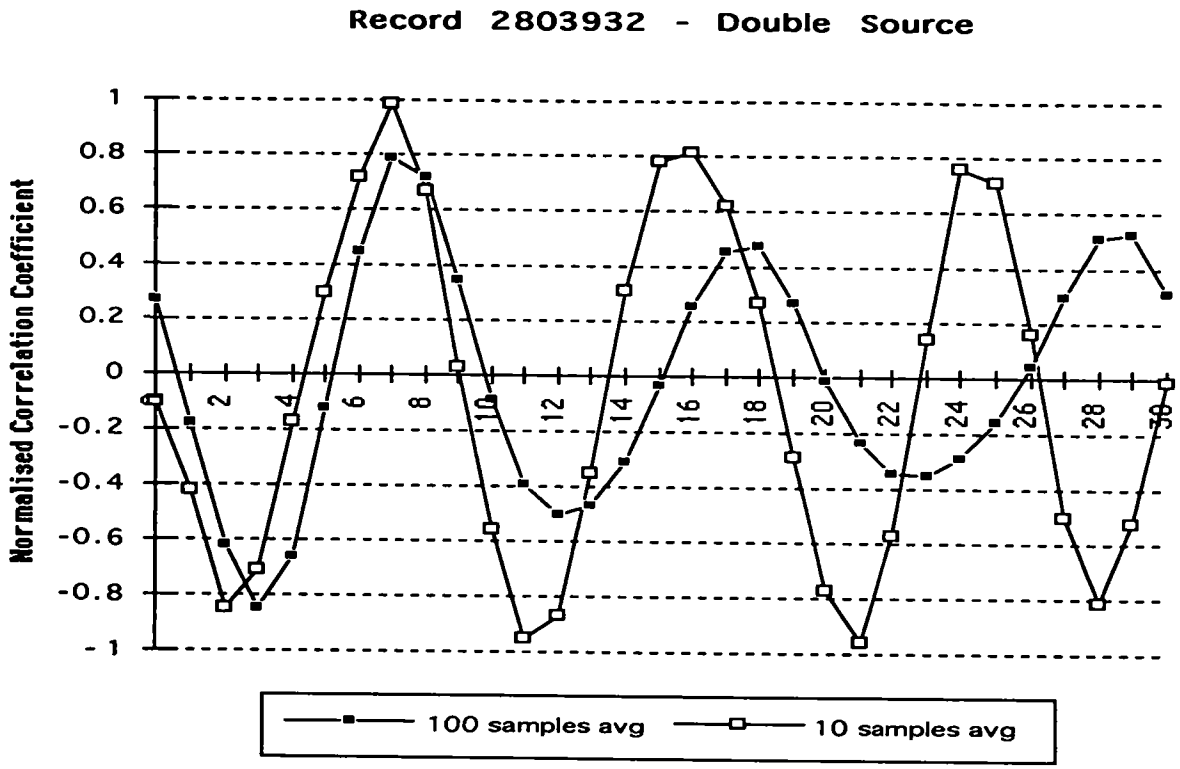


*Figure 6.11*

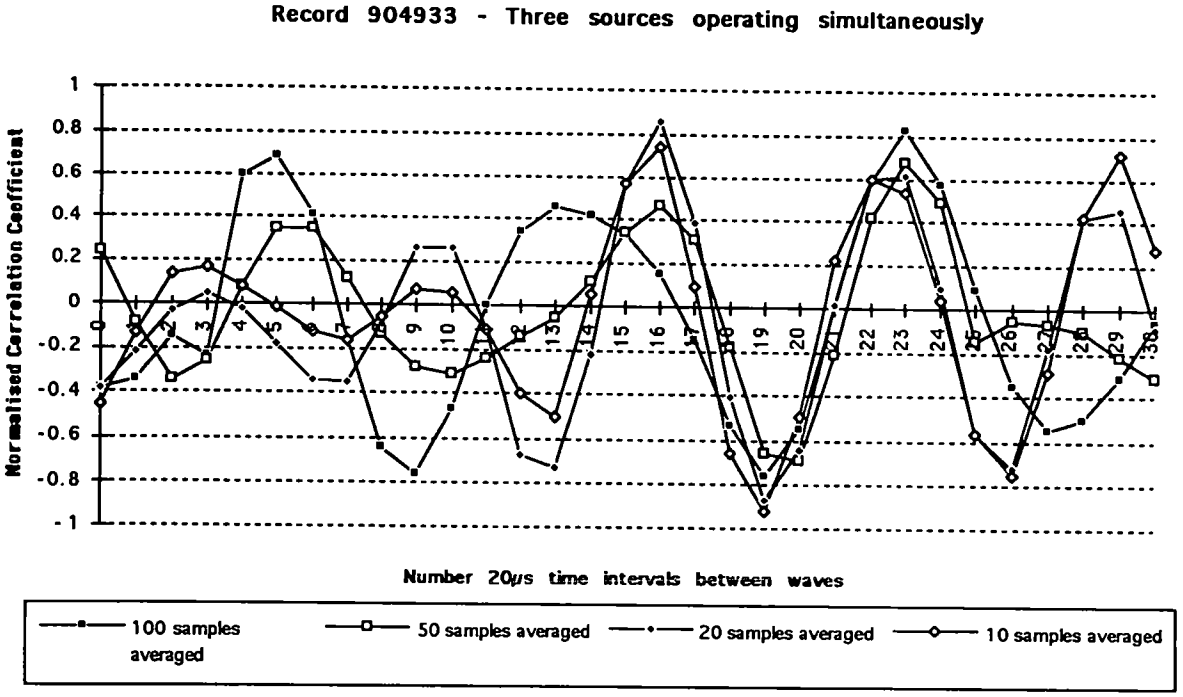


*Figure 6.12*

received signal with no partition in place and noting the amplitude of the correlation function, (not the normalised correlation coefficient). When a partition is placed between the source and the receiver, the correlation function at the same time interval is measured, and the amplitudes of the functions compared and expressed in decibels. By this technique, Goff was able to distinguish between the direct transmission and the flanking transmission purely because of the difference in the time interval between the flanking signals and the direct signals reaching the receiver. For instance, if two signals, '$x$' and '$y$' are cross correlated,

$$x = A\sin(\omega t + \phi) \qquad \text{and} \qquad y = B\sin(\omega t + \phi')$$

the result is,

$$R_{xy}(t) = \frac{1}{2}AB\cos(\omega t + \phi - \phi')$$

The technique used by Goff relied upon a electro-mechanical analogue arrangement. Similar experiments could be performed in digital format with the array. In fact, from the dimensions of the partition, it is possible to calculate the time delay for the signals coming from different parts of the surface. By selecting the number of samples used in the correlation process, an average signal value could be computed to indicate the amount of noise passing through different areas.

The graphs illustrating the effect of the number of data points being sampled are shown in Figures 6.11, 6.12 and 6.13. Through only using ten data points in determining the correlation coefficient, the value for the normalised coefficient is close to unity at the time interval corresponding to the calculated time separation of the waves for the source closest to the receiving microphones. A second correlation occurs corresponding to the second source, but the coefficient is slightly lower (See Figure 6.13).

For the correlation using microphone one and the reference microphone, (Figure 6.11), the first correlation occurs at the 7 x 20$\mu$S interval with a correlation coefficient of 0.99. The second correlation occurs at 21 x 20$\mu$S intervals with a correlation coefficient of 0.96. These results compare with the predicted results shown for the calculation based upon the tape measured coordinates of x = 0.56, y = 0.46 and z = 0.96 for the upper loudspeaker, with x = 0.10, y = 0.46 and z = 0.96 for the lower loudspeaker (See Table 6.17). The higher coefficient corresponds with the lower or nearer loudspeaker. The lower speaker is the speaker closer to microphones $m_1$ and $m_2$. The correlations with microphone $m_2$ also show comparable correlations to the

results predicted by the calculation. Figure 6.13 shows that for microphone $m_6$, the situation is not as clear. The main correlation occurs at 40 x 20$\mu$S intervals, as predicted for the lower source, but the second correlation does not conform to prediction, the highest of the second values being a 0.9 at 45 x 20$\mu$S time intervals when 10 data samples are considered. If the sample number is increased to 15 intervals, then the correlation occurs at 38x 20$\mu$S intervals with a coefficient of 0.94, and a second correlation at 34 intervals with a coefficient of 0.89. When the sample is increased to 20 intervals the correlation occurs at 38 intervals with a coefficient of 0.88 and at 34 with a coefficient of 0.87. It follows that for some reason the correlation with only 10 samples gives a false result which suggests that the selection of the optimum number of samples requires more interpretation. As the sample numbers increase then the difference between the correlation coefficients decreases and eventually, the second correlation effectively disappears. The disappearance is due to the correlation coefficient becoming comparable to the values at other time intervals.

A further anomaly occurs with microphone $m_6$, the main correlation occurs at 40 x 20$\mu$S and the secondary correlation occurs at 36 x 20$\mu$S, which does not conform to any of the calculated predictions. This result occurs for all sample numbers from 10 to 100. Unlike the predictions, the time intervals for microphone 6 is greater than for microphone 5.

The results of the experimental work are shown in Table 6.18. It is observed that the maximum correlation can switch from one source to the other depending upon the relative distance of the source to the receiving microphones. The calculated results have therefore been omitted, since it would be necessary to know which results belong to which source before the calculation could be made.

| Separation of microphones | *0.28 m* | |
|---|---|---|
| | *Upper* | *Lower* |
| 'X' co-ordinate | 0.56m | 0.10 m |
| 'Y' co-ordinate | 0.46 m | 0.46 m |
| 'Z' co-ordinate | 0.95 m | 0.95 m |
| Temperature at which measurements occurred | 20 ° C | |
| Velocity of sound | 343.41 m/s | |
| | | |
| **Calculation of 'R'** | | |
| For x1 and x2 | 1.28 | 1.01 |
| For x3 and x4 | 1.22 | 1.02 |
| For x5 and x6 | 1.09 | 1.25 |
| Mean value of 'R' | 1.20 | 1.09 |
| % error | 0.19% | 3.24% |
| **Calculation of Angles** | | |
| θ | 62 ° Error 0.6% | 85° Error 0.4% |
| ø | 65 ° Error 0.7% | 64° Error 0.9% |

| Distance 'R' between source and reference microphone | *Upper* *1.19m* | *Lower* | |
|---|---|---|---|
| Time interval in 20$\mu$S intervals between mo & S | | | |
| Interval between m1 and S | 22 | 9 | |
| Interval between m2 and S | 15 | -2 | |
| Interval between m3 and S | 19 | 22 | |
| Interval between m4 and S | 11 | 13 | |
| Interval between m5 and S | 34 | 37 | |
| Interval between m6 and S | 30 | 35 | |
| **Calculation of 'x'** | | | **Upper** |
| For x1 | 0.55 | 0.11 | **Mean 'x' = 0.55 Error 'x'=0.23%** |
| For x2 | 0.56 | 0.09 | **Mean 'x' = 0.97 Error 'x'=2.8%** |
| **Calculation of 'y'** | | | **Upper** |
| For x3 | 0.45 | 0.49 | **Mean 'y' = 0.45 Error 'y' =2.5%** |
| For x4 | 0.45 | 0.48 | **Mean 'y' = 0.48 Error 'y' =5.0%** |
| **Calculation of 'z'** | | | **Upper** |
| For x5 | 0.96 | 0.97 | **Mean 'z' = 0.95 Error 'z' = 0.05%** |
| For x6 | 0.94 | 0.98 | **Lower Mean 'z' = 0.97 Error 'z' = 2.4%** |

## *Calculation from measured coordinates for two sources*

## *- Table 6.17*

| Results for two sources operating simultaneously - Record 2803932 | | | | |
|---|---|---|---|---|
| **Distance between source and microphone (dx)** | **Calculated time intervals (20$\mu$S) for upper loudspeaker Table 6.17** | **Calculated time intervals (20$\mu$S) for lower loudspeaker Table 6.17** | **Time intervals determined from microphone array** | **Time intervals determined from microphone array.** |
| | ***Source 1*** | ***Source 2*** | ***1st correlation maxima*** | ***2nd correlation maxima*** |
| d1 | 22 | 9 | 7 | 21 |
| d2 | 15 | -2 | -2 | 20 |
| d3 | 20 | 22 | 17 | 21 |
| d4 | 12 | 13 | 13 | 17 |
| d5 | 34 | 37 | 38 | 34 |
| d6 | 30 | 35 | 40 | 36 |

***Table 6.18***

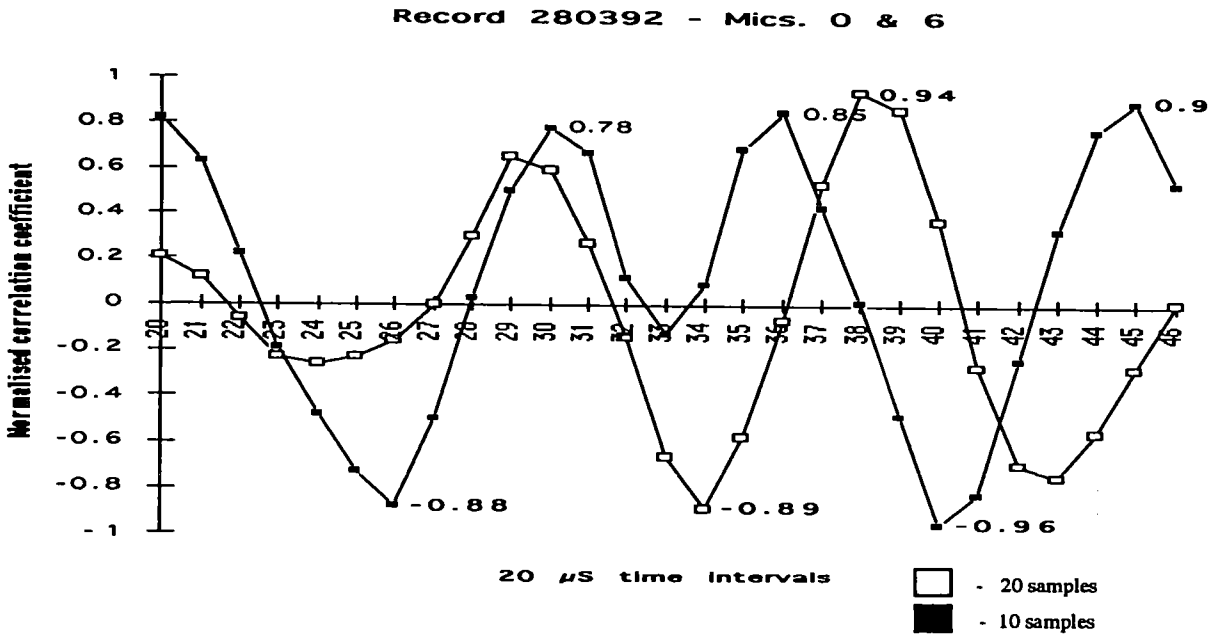


*Figure 6.13*

# Single source and a two microphone system

**Experimental Programme - Section 6**

All the practical evidence leads to the conclusion that data can be successfully collected by the sequential collection of data. If this is the case, then there is only a need to employ two microphones. One of the microphones would be the reference microphone and the other would act as the collection microphone in all other positions in turn. The equations derived require time differences to be measured, therefore the guaranteed location of the reference microphone and the positively known separation of the two microphones is an essential requirement. There is indication that in a two microphone system, provided the distance is such that the received waves do not tend to be parallel, it would be sufficient to rotate the microphone with respect to the reference microphone until the difference in the time between the wave arrivals at the reference and location microphone is zero. If a line be drawn, normal to the line joining the two microphones, it would be pointing towards the source. This would determine the line in which the source exists, but could not distinguish whether the source was in front of, or behind the microphone line. Two other directions could be found by rotating the microphone line through 90°, first to locate the other positions where the time difference in wave arrival is zero, and then to locate the position where the time difference is a maximum. This setup would only work if the source of the noise remained constant in space. It would also rely upon a finite burst of signal to avoid the effect of the environment upon the transmitted wave pattern. The arrangement would have the advantage that with only two signals to analyse and store, the possibility of results being obtained in 'real time' is quite feasible. The major draw back is that a mechanical joint is required that can lock movement in one or two planes while allowing free movement in the third plane.

The alternative arrangement of equipment will be dealt with in more detail under the discussion.

*Chapter 7*

# Discussion

# Discussion of findings.
# The pulsed source

The early experimental work used the continuous output from a loudspeaker and analysed data from various parts of the stored waveform. It was found that the cross correlation technique gave results that could not be related to the arrangement under investigation using the processing mathematics that had been developed. This difficulty was attributed to the confusion of data associated with standing waves and multiple reflections. As soon as a short tone burst was used, and the analysis concentrated upon the first part of the signal, then the analysis provided information that could be related to the experimental arrangement.

The choice of the pulse length was governed by the technique of producing it. By using a mechanical switch, a long pulse was produced when compared with the time window of the data capture. When the pulse width was reduced by introducing an electronic switch, it was found that the amount of energy contained in the tone burst was too small to generate a detectable signal in the collection transducers. A compromise had to be selected. The pulse must be long enough to drive the speaker and to create a signal at least 10 dB above the background, but short enough to be able to identify it as a pulse. In fact, the length of the pulse becomes less critical if the analysis is confined to the start of the wave only. The length becomes critical if the start and the end of the pulse are used to identify the separate directions of wave travel through the propagating medium. As the screen display is 256 pixels wide, then the maximum time that a pulse can last and be displayed in one screen width is $256 \times 20 \times 10^{-6}$ seconds or 5 ms. To be able to compare the beginning and the end of a pulse on the computer, especially if the comparison is to be between two pulses from different microphones, the length of the pulse should be nearer 2.5 ms. This size pulse would be much shorter than the reverberation time of the room and is therefore an impractical proposition.

The signal was a randomly generated sine wave with a frequency content filtered between 20 Hz and 20 kHz. The signal was further modified by the filters in the collection amplifiers. The main interest in the value of the frequency content arises when this work is related to the field of Building Acoustics and the requisite 'British Standards' documentation.

# The Potential Errors in the System

The results of all the practical work undertaken, is summarised briefly in Table 7.1. The table compares the values for the coordinates obtained from the experimental procedure with the results of the tape measurements. The difference between them is shown as a percentage. As was indicated in the descriptions of the experiments, a number of points became clear as a consequence of the practical work. From the Table, it is clear that most of

| *Description* | | *R* | *'x'* | *'y'* | *'z'* |
|---|---|---|---|---|---|
| Source in all positive octant | Calculated | 1.18 | 0.54 | 0.45 | 0.93 |
| | Measured | 1.22 | 0.56 | 0.47 | 0.96 |
| | % Difference | -3.2% | -3.57% | -4.26% | -3.12% |
| Random placement of source | Calculated | 1.24 | -0.31 | 0.59 | -1.02 |
| | Measured | 1.29 | -0.35 | 0.62 | -1.08 |
| | % Difference | 3.8% | -11.43% | -4.84% | -5.56% |
| Source in all negative octant | Calculated | 1.32 | -0.25 | -0.72 | -1.07 |
| | Measured | 1.22 | -0.27 | -0.62 | -1.04 |
| | % Difference | 8.2% | -7.41% | 16.13% | 2.88% |
| Source within array half distance | Calculated | 0.39 | -0.31 | -0.18 | 0.09 |
| | Measured | 0.34 | -0.29 | -0.19 | 0.09 |
| | % Difference | 14.7% | 6.90% | -5.26% | 0.00% |
| Multiple source (lower) | Calculated | 1.17 | 0.07 | 0.5 | 1.06 |
| | Measured | 1.07 | 0.1 | 0.47 | 0.96 |
| | % Difference | | -30.00% | 6.38% | 10.42% |
| Multiple source (upper) | Calculated | 1.18 | 0.07 | 0.5 | 1.06 |
| | Measured | 1.21 | 0.56 | 0.47 | 0.96 |

***Summary of results - Table 7.1***

the calculated results are within 5% of the measured results, but there are some significantly worse values. For instance, the value of '*x*' with the randomly placed source has a difference of 11% between calculated and measured values. The 'y' coordinate in the all negative octant experiment, differs by 16% from the measured value. For the multiple source, the calculation of '*x*' is 30% different.

The design of the wheelbrace array has particular limitations. From the mathematical analysis and the summary of equations, the determination of a set of coordinates for the source of a sound depends upon the difference in time the sound wave takes to travel between pairs of microphones, that is, for example, between $m_2$ and $m_0$ together with $m_1$ and $m_0$ in the '*x*' axis direction. This difference enables the source to reference microphone distance to be calculated, which in turn is used for the 'x,y,z' evaluation. If the situation is visualised where the source is placed on the 'z' axis, that is, both 'x' and 'y' are zero, as in the last row of table 7.2, then the determination of 'R' is impossible for the microphones on the 'z' axis. Because the microphones are placed symmetrically about the 'z' axis, the difference in the time intervals for the microphones on the 'x' and 'y' axis, although equal, must be of opposite sign. The time intervals

| **True (measured) values** | **Calculated values using equations of Table 4.1 and keeping values of 'x' as 0.50 and 'z' as 0.95 m** | | | | | | | | | |
|---|---|---|---|---|---|---|---|---|---|---|
| | Microphone Separation, [mx- m0] in 20$\mu$S intervals | | | | | | True | Calculated | | |
| **y** | **1** | **2** | **3** | **4** | **5** | **6** | **R** | **R1** | **R2** | **R3** |
| 0.5 | 21 | 13 | 21 | 13 | 34 | 31 | 1.18 | 1.18 | 1.18 | 1.43 |
| 0.4 | 21 | 13 | 18 | 10 | 35 | 32 | 1.15 | 1.18 | 1.26 | 1.28 |
| 0.3 | 22 | 14 | 15 | 6 | 36 | 33 | 1.12 | 1.15 | 1.21 | 0.90 |
| 0.2 | 22 | 14 | 12 | 2 | 37 | 34 | 1.09 | 1.15 | 1.10 | 0.96 |
| 0.1 | 23 | 14 | 9 | -2 | 37 | 34 | 1.08 | 1.00 | 1.02 | 0.96 |
| 0 | 23 | 14 | 5 | -5 | 37 | 35 | 1.07 | 1.00 | 1.13 | 1.33 |
| | when both x and y = 0 | | | | | | | | | |
| 0 | 6 | -6 | 6 | -6 | 41 | 41 | 0.95 | NA | 0.94 | 0.94 |
| | *When both 'x' & 'y' are zero, only two solutions for 'R' are possible* | | | | | | | | | |

***Table 7.2 - 'y' tends to zero***

along the 'z' axis, so long as the source is at a distance greater than the microphone separation, have the same value and sign, irrespective of the position of the source. The calculation of 'R', using the time differences from the microphones along the 'z' axis, together with the derived equations of Table 4.1, is infinity. The difference in the time interval between the arrival of the

waves at the microphones on the 'z' axis is a maximum - the time taken to travel between the two in-line microphones in the end-fire configuration. The information that can be derived from the array in this arrangement, is that the source is somewhere along the 'z' axis at a distance that can be determined from the microphones on the other axes. If the source of the sound is coming from a structural element, then the source would be on the surface of the element to which the 'z' axis is pointing. The result is the same for a source placed on either the 'x' or 'y' axis. If the source is placed at a point $x_s,y_s,z_s$ not on any of the axes, then, as the distance to the source increases and the angle of bearing or elevation becomes small, the value of 'R' calculated from one of the three pairs of microphones tends to infinity as the time differences used to calculate $R_x$ become smaller, until they eventually become equal. This is illustrated in Table 7.2 when the value of 'y' becomes zero. The difference for microphones $m_5$ and $m_6$ falls to two measurement periods. This causes the determination of the value of 'R' to differ considerably from the two other values for 'R'. In the details of the analysis of the practical work, the value of 'R' is always taken as the mean of the three readings. In practice there is a limit to the validity of this assumption. Table 7.3 takes the example further. The value of 'z' is varied whilst the values of 'x' and 'y' are kept constant. By the time the 'z' axis value equals 2.5 m, the time differences used to calculate R3, are equal. If the time measurement window were smaller, then the difference could be detected for a greater distance as shown in Table 7.4 but for a given time window, an ultimate point is reached where the value obtained for R3 has little meaning.

By reference to Figure 7.1 it is possible to illustrate this. The graph shows the plots for the time difference for the six microphones as the value of 'x' and 'y' are kept constant (0.5 for 'x' and 0.46 for 'y') and the value of 'z' is increased. What is shown clearly, is that a time difference between microphones five and six ceases to exist after quite a short distance, within 2.5 m. For the arrangement where the microphones are separated by a distance of 0.28 m, the microphones on the 'z' axis indicate that the source is at an indeterminate distance when the value of 'z' becomes 2.5 m. From reference to table 7.2 the mean value of 'R' exceeds the 'true' value of 'R' from the distance of 1m. The further the source moves away by increasing the value of 'z', the closer the values of 'R' become to the distance 'z'. The actual maximum calculated value of 'R' cannot exceed 11.5 m which is equivalent to a time separation of 1 period or 20$\mu$S. Anything less than this makes the value zero and 'R' becomes infinite. This occurs when 'z' reaches 8 m.

| Variation in accuracy of calculated values for the distance between source and reference microphone 'R' with distance of the 'z' co-ordinate x = 0.50 and y = 0.46 metres | | | | | | | | | | |
|---|---|---|---|---|---|---|---|---|---|---|
| Time intervals [mx-m0]- 20 μS units | | | | | | | Distance in metres | | | |
| z | *1* | *2* | *3* | *4* | *5* | *6* | *R1* | *R2* | *R3* | True 'R' |
| **0.25** | 31 | 23 | 30 | 20 | 20 | 6 | 0.8 | 0.71 | 0.71 | **0.72** |
| **0.5** | 28 | 19 | 26 | 17 | 28 | 19 | 0.84 | 0.91 | 0.84 | **0.84** |
| **1** | 20 | 13 | 19 | 11 | 35 | 32 | 1.37 | 1.23 | 1.28 | **1.21** |
| **1.5** | 15 | 9 | 14 | 8 | 38 | 36 | 1.74 | 1.77 | 1.08 | **1.65** |
| **2** | 12 | 7 | 11 | 6 | 39 | 38 | 2.17 | 2.19 | 1.38 | **2.11** |
| **2.5** | 10 | 6 | 9 | 5 | 39 | 39 | 2.76 | 2.78 | #### | **2.59** |
| **3** | 8 | 5 | 8 | 4 | 40 | 40 | 3.73 | 2.81 | #### | **3.08** |
| **3.5** | 7 | 4 | 7 | 4 | 40 | 40 | 3.76 | 3.76 | #### | **3.57** |
| **4** | 6 | 4 | 6 | 3 | 40 | 40 | 5.66 | 3.78 | #### | **4.06** |
| **4.5** | 6 | 3 | 5 | 3 | 40 | 40 | 3.78 | 5.69 | #### | **4.55** |
| **5** | 5 | 3 | 5 | 3 | 40 | 40 | 5.69 | 5.69 | #### | **5.05** |
| **6** | 4 | 2 | 4 | 2 | 41 | 40 | 5.71 | 5.71 | 0.31 | **6.04** |
| **7** | 4 | 2 | 3 | 2 | 41 | 41 | 5.71 | 11.45 | #### | **7.03** |
| **8** | 3 | 2 | 3 | 2 | 41 | 41 | 11.45 | 11.45 | #### | **8.03** |
| **9** | 3 | 2 | 3 | 1 | 41 | 41 | 11.45 | 5.73 | #### | **9.03** |
| **10** | 3 | 1 | 2 | 1 | 41 | 41 | 5.73 | 11.48 | #### | **10.02** |
| **12** | 2 | 1 | 2 | 1 | 41 | 41 | 11.48 | 11.48 | #### | **12.02** |
| **14** | 2 | 1 | 2 | 1 | 41 | 41 | 11.48 | 11.48 | #### | **14.02** |
| **16** | 2 | 1 | 2 | 1 | 41 | 41 | 11.48 | 11.48 | #### | **16.01** |
| **18** | 1 | 1 | 1 | 1 | 41 | 41 | #### | #### | #### | **18.01** |
| **20** | 1 | 1 | 1 | 1 | 41 | 41 | #### | #### | #### | **20.01** |
| **30** | 1 | 0 | 1 | 0 | 41 | 41 | 11.49 | 11.49 | #### | **30.01** |
| **50** | 1 | 0 | 0 | 0 | 41 | 41 | 11.49 | #### | #### | **50** |
| **100** | 0 | 0 | 0 | 0 | 41 | 41 | #### | #### | #### | **100** |

***Table 7.3 - Microphone intervals and distance 'z'***

**The # symbol indicates that there is no difference between the time intervals and 'R' cannot therefore be calculated. The time differences cannot be identified in a 20μS time window.**

If Table 7.3 is consulted, the figures show that as the distance increases for 'z', there is a large range where the difference in the time interval between microphones '1,2' and '3,4' equals 2 x 20$\mu$S. After this point, it is of little value to calculate 'R'. That is, the ability to determine the 'x,y,z' values beyond a certain point is prevented because of the lack of resolution in the time window for the data capture. From the data in table 7.3, the third pair of time difference values gives erroneous information for the calculation of 'R' from 1m.

For the microphone configuration described here, the source should not be greater than 1m away on any axis. Figures 7.2 and 7.3 illustrate the restricted range over which the mean value of 'R' corresponds with the 'true' value of 'R'.

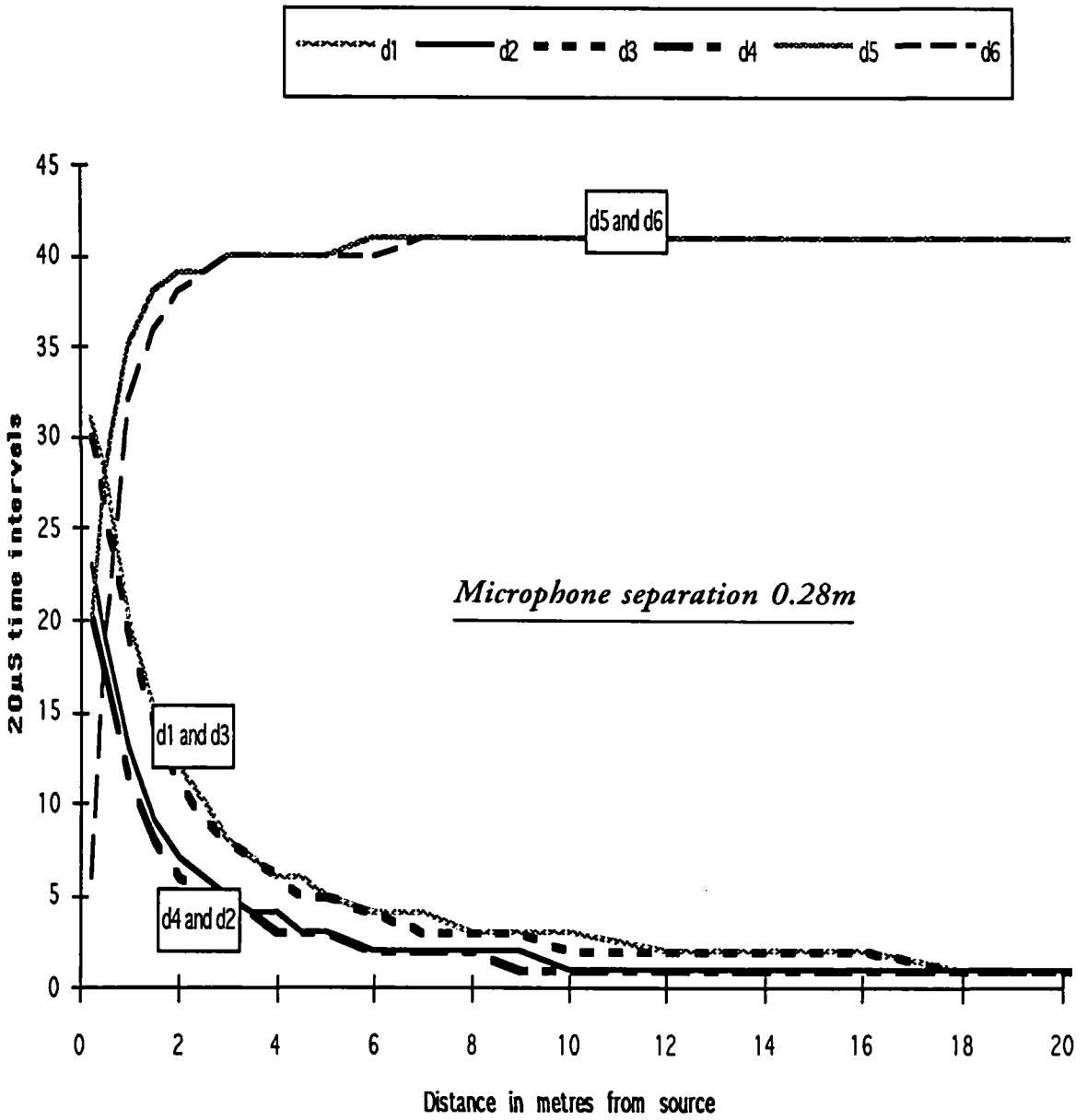


*Figure 7.1*

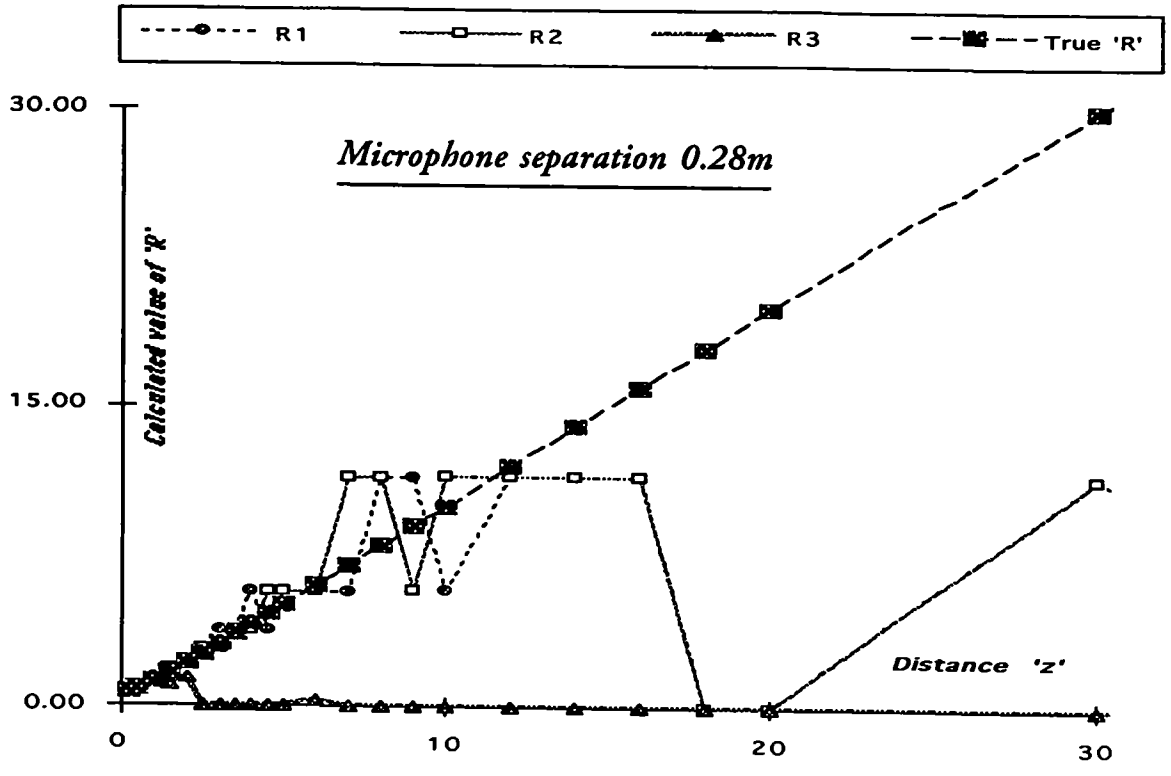


*Figure 7.2 - Variation in the value of 'R' as the distance of the 'z' coordinate increases*

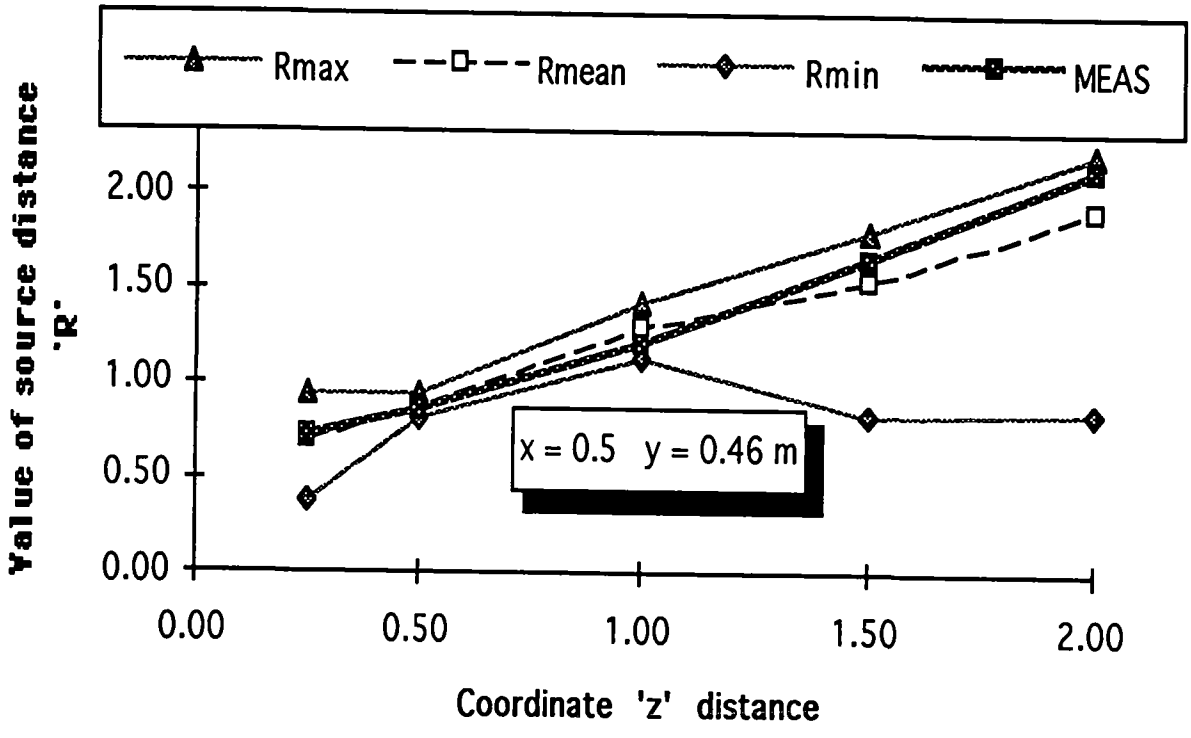


*Figure 7.3 Comparison of calculated 'R' and 'true R'*

The discussion has referred to measurements based upon the coordinates 'x' = 0.50 m and 'y' = 0.46 m. The value of 'z' has been varied to find the effect upon 'R', of the measured and calculated distance between the source and the reference microphone. The measured or **'true'** distance has been determined from the geometric analysis and calculated from

$$R = \sqrt{(x^2 + y^2 + z^2)}$$

The calculated value of 'R' has come from the derived equations relating 'x,y,z' and the time intervals between the signals reaching the respective microphones. A similar situation will occur in any octant for any of the coordinates.

Maximum resolution within the limits stated will occur when the altitude and bearing are at 45°. In this situation, x = y = z. Minimum resolution will occur when the value of 'R' tends to equal any of the coordinate values. If R = 'x' or 'y' or 'z' then the source will lie on that axis and the time differences along that axis will be the time taken to travel the distance separating the microphones.

The problem of the accuracy in determining the coordinates is associated with the fact that the data capture occurs at 20$\mu$S time intervals. There are two alternatives to the problem. Either the time window must be reduced - say, to 2 $\mu$S - or the separation of the microphones must be increased. To test this hypothesis, calculations were made based upon a separation of 2.8 m for the microphones and compared with the values obtained for a difference of 0.28 m. (Table 7.3). The value for the 'x' and 'y' coordinates were kept at 0.5 and 0.46 m and the range of 'z' values used were also the same as used for the 0.28 m separation. From figures 7.5 and 7.6 it is clear that the distance that the source can be in front of the array increases from 1 m to 1.8m. when the microphone separation is increased tenfold, to 2.8 m. When comparing the two microphone arrangements for a distance 'z' of 1 m, the 95% confidence levels for the calculated coordinates, illustrate the magnitude of the difference in reliability of the results.

| Microphone separation 0.28 m | Microphone separation 2.80 m |
|---|---|
| 'x' =0.53 ± 0.07 | 'x' = 0.497 ± 0.02 |
| 'y' = 0.48 ± 0.06 | 'y' = 0.458 ± 0.02 |
| 'z' = 1.06 ± 0.21 | 'z' = 0.997 ± 0.01 |

The measured value for R was 1.209 m

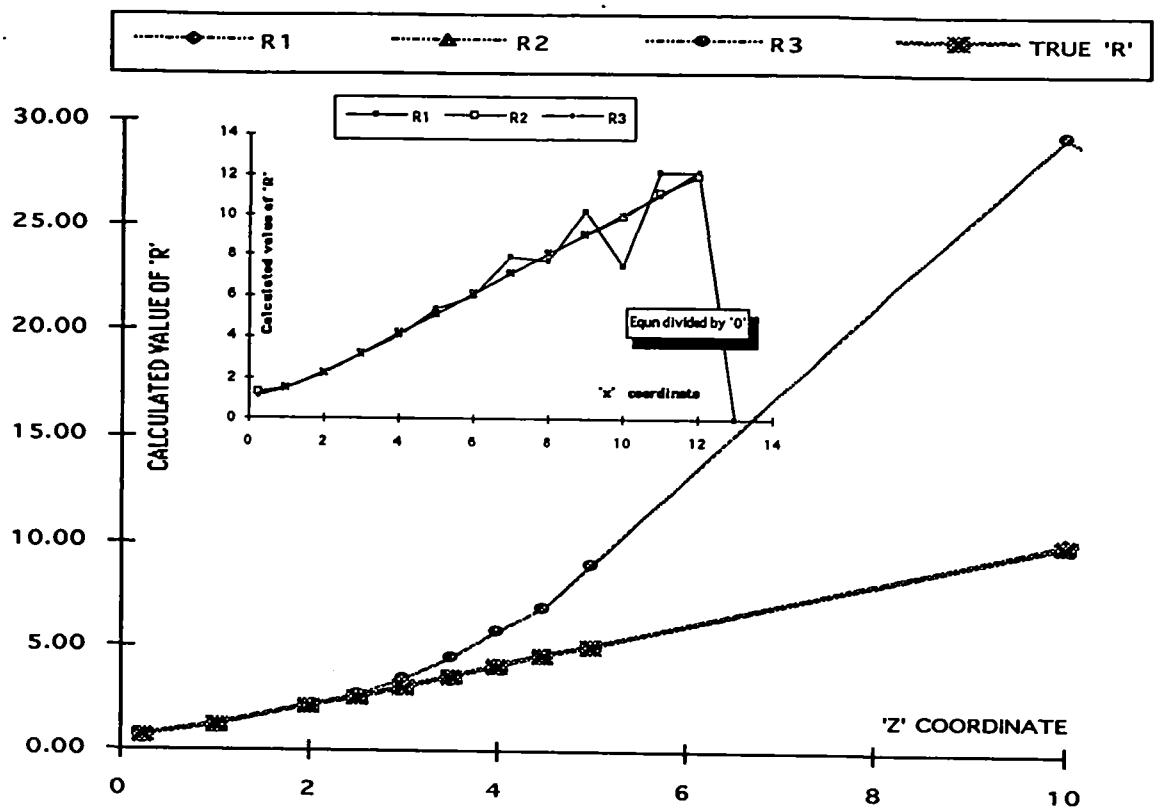


See P.145 in the Appendices for the full sized graphs of 'R' v 'x' and 'y'

*Figure 7.4*

***The variation between the three values for 'R' determined by the combinations of $'x_1,x_2'$; $'x_3,x_4'$; $'x_5,x_6'$***

| Variation in the accuracy of the calculated values of 'R' with the coordinate distance 'z' when microphone separation is 2.8 m | | | | | | | | | | |
|---|---|---|---|---|---|---|---|---|---|---|
| | Time interval in 20$\mu$S periods | | | | | | Distance in metres | | | |
| z | d1 | d2 | d3 | d4 | d5 | d6 | R1 | R2 | R3 | TRUE 'R' |
| 0.25 | 381 | -238 | 376 | -245 | 350 | -279 | 0.75 | 0.75 | 0.75 | **0.72** |
| 1 | 330 | -195 | 326 | -202 | 386 | -104 | 1.24 | 1.24 | 1.24 | **1.21** |
| 2 | 258 | -141 | 254 | -147 | 398 | 155 | 2.15 | 2.14 | 2.19 | **2.11** |
| 2.5 | 229 | -122 | 225 | -127 | 401 | 269 | 2.63 | 2.63 | 2.73 | **2.59** |
| 3 | 205 | -107 | 201 | -111 | 402 | 345 | 3.11 | 3.12 | 3.49 | **3.08** |
| 3.5 | 184 | -94 | 181 | -98 | 403 | 377 | 3.63 | 3.62 | 4.52 | **3.57** |
| 4 | 167 | -84 | 164 | -88 | 404 | 390 | 4.12 | 4.11 | 5.78 | **4.06** |
| 4.5 | 153 | -76 | 150 | -79 | 405 | 396 | 4.6 | 4.61 | 6.9 | **4.55** |
| 5 | 140 | -69 | 137 | -72 | 405 | 399 | 5.12 | 5.13 | 9 | **5.05** |
| 10 | 75 | -36 | 74 | -38 | 407 | 406 | 10.17 | 10.08 | 29.29 | **10.02** |
| 20 | 38 | -18 | 38 | -19 | 407 | 407 | 20.48 | 20.12 | #### | **20.01** |

***Table 7.4- Variation in calculated 'R' for 2.8m microphone separation***

All these values were calculated on the basis that each time difference reading could vary by ±1 x 20$\mu$S time intervals. The coordinates for both calculations were the same, but the set of results with the microphone separation at 0.28 m, gives a greater variation in the result for the 'z' coordinate. With the larger separation between the microphones, all the coordinates are more accurately predicted. The conclusion must be that the maximum distance of the source from the microphone acting as the reference point for measurements, should not exceed the values indicated in Figure 7.8. The charts in Figures 7.5 and 7.6 show how the values of the difference in distances travelled by the signal, change with the greater value of the 'z' axis. The greater the value of $z_s$, the smaller becomes the difference in the distances travelled and the more critical is the size of the window for data capture.

The disadvantage of increasing the microphone separation is that the overall space required by the microphone array is considerably increased. For a separation of 2.8 m, the array dimension becomes 5.6m. The size of the apparatus would cause problems in many investigations and a compromise solution is be needed between the distance from the source and the separation distance chosen for the array. The indications from Figures 7.5, 7.6 and 7.8 is that the increase in the microphone separation does not alter the maximum distance at which the value of 'R' can be adequately calculated.

The poor results obtained for the experiment where the source was in the all negative octant can be explained because of the value of 'z'. It has been demonstrated that if the 'z' axis is greater than 1m, there is a large error in the calculation of the mean value for 'R'. In this particular test (see Table 6.10 page 91), the 'z' coordinate was measured as -1.04 m and the 'y' coordinate was measured as -0.72 m. Although the angle of bearing was 235°, the value of the 'z' coordinate was over 1m and the value of the calculated 'R' ranged between 0.9 and 1.8, thus overestimating the calculated mean value of 'R' and giving a 16% error in the estimation of the 'y' coordinate. In the other practical tests, where the coordinates were under 1m from the source, the achieved accuracy was that much greater.

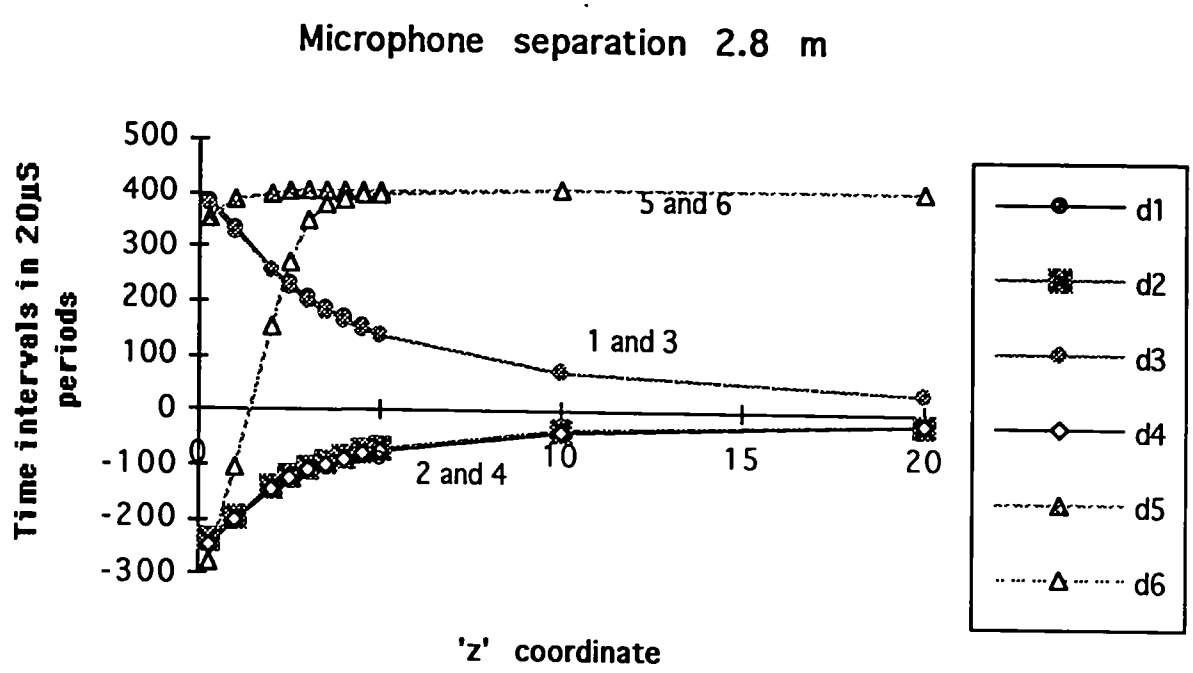


*Figure 7.5*

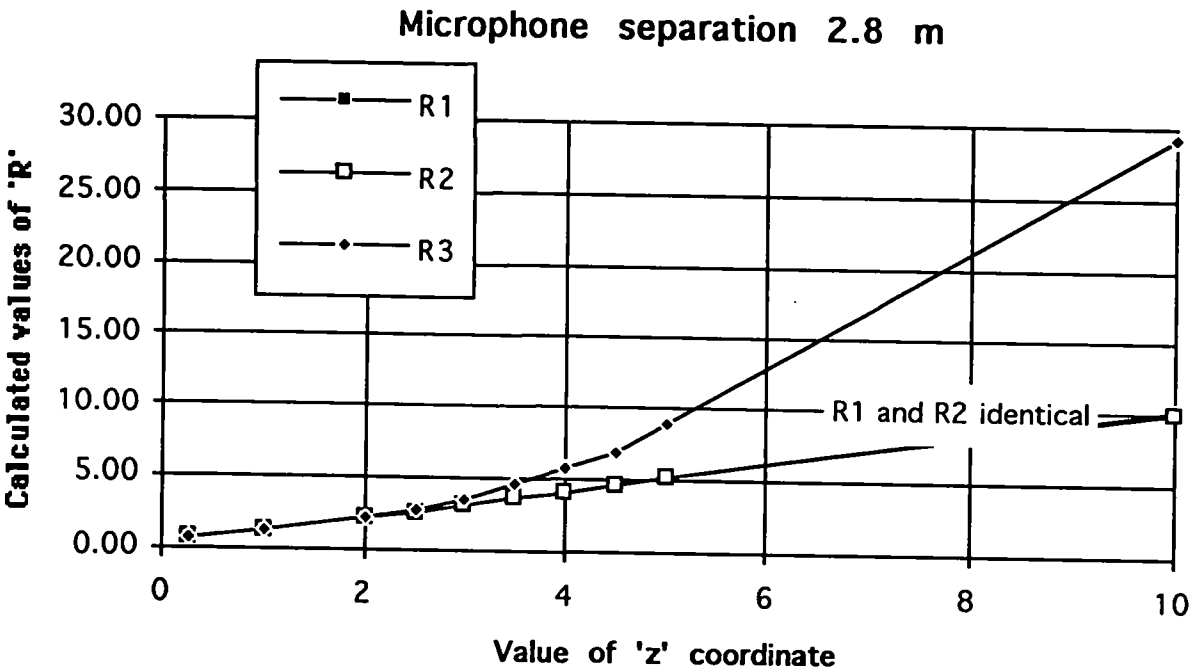


*Figure 7.6*

From the previous discussion, the reliability of the calculation of 'R' depends upon the value of 'z' Using a diagram based upon figure 4.7 it is possible to produce a mathematical relationship between the time differences 't', recorded for the appropriate microphones, in this case $m_5$ and $m_6$, the separation between the microphones 'd', the distance between the source and the reference microphone, 'R', and the size of the data recording window, 'T'.

**T - R** = the difference in distance travelled by the waves going from the source to the reference microphone, $m_o$, and the microphone, $m_5$.

**R - Q** = the difference in distance travelled by the waves going from the source to the reference microphone, $m_o$, and the microphone, $m_6$.

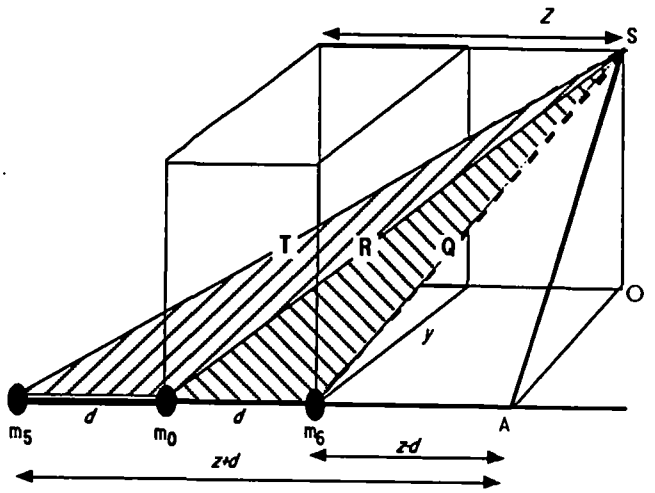


*Figure 7.7 (based upon figure 4.7)*

*illustrating variation of 'R' and 'z'*

Let $AS^2 = AO^2 + OS^2$

$$T^2 = (z+d)^2 + AS^2$$

$$R^2 = (z^2 + AS^2)$$

$$Q^2 = (z-d)^2 + AS^2 \quad \text{.....54}$$

$$R^2 - Q^2 = z^2 + AS^2 - \left[(z-d)^2 + AS^2\right]$$

$$R^2 - Q^2 = 2zd - d^2$$

$$(R-Q)(R+Q) = 2zd - d^2$$

$$(R-Q) = \frac{2zd - d^2}{(R+Q)} \quad \text{.....55}$$

$$T^2 - R^2 = (z+d)^2 + AS^2 - z^2 - AS^2$$

$$T^2 - R^2 = 2zd + d^2$$

$$(T-R) = \frac{2dz + d^2}{(T+R)} \quad \text{.....56}$$

The value calculated for 'R' ceases to be reliable when the measured differences become equal, that is when R-Q = T-R

If $R - Q = T - R$

then $T = 2R - Q$

or $T + R = 3R - Q$ .....57

By making equation [55] equal equation [56] and using the expression for T + R of equation [57], the following expression can be derived:

$$(R+Q)(2zd+d^2)=(3R-Q)(2zd-d^2)$$

$$2Rzd+Qd^2+2Qzd+Rd^2=6Rzd+Qd^2-2Qzd-3Rd^2$$

$$4Qzd+4Rd^2=4Rzd$$

$$Rd^2=Rzd-Qzd$$

$$d=\frac{z}{R}(R-Q)$$

$$\text{or } z=d.\frac{R}{(R-Q)} \qquad \text{.....58}$$

The quantity (R - Q) is the difference in distance travelled. It can be substituted by the combination of the size of the time window, the time interval and the velocity of sound.

$$(R-Q)=Tc\tau$$

Where c = velocity of sound,

T = time window or 20μS

and $\tau$ = the time interval in 20μS periods measured by the microphones

$$z=d.\frac{R}{Tc\tau} \text{ when } (T-R)=(R-Q) \qquad \text{.....59}$$

*Figure 7.8 Graph of 'z' against 'R'*

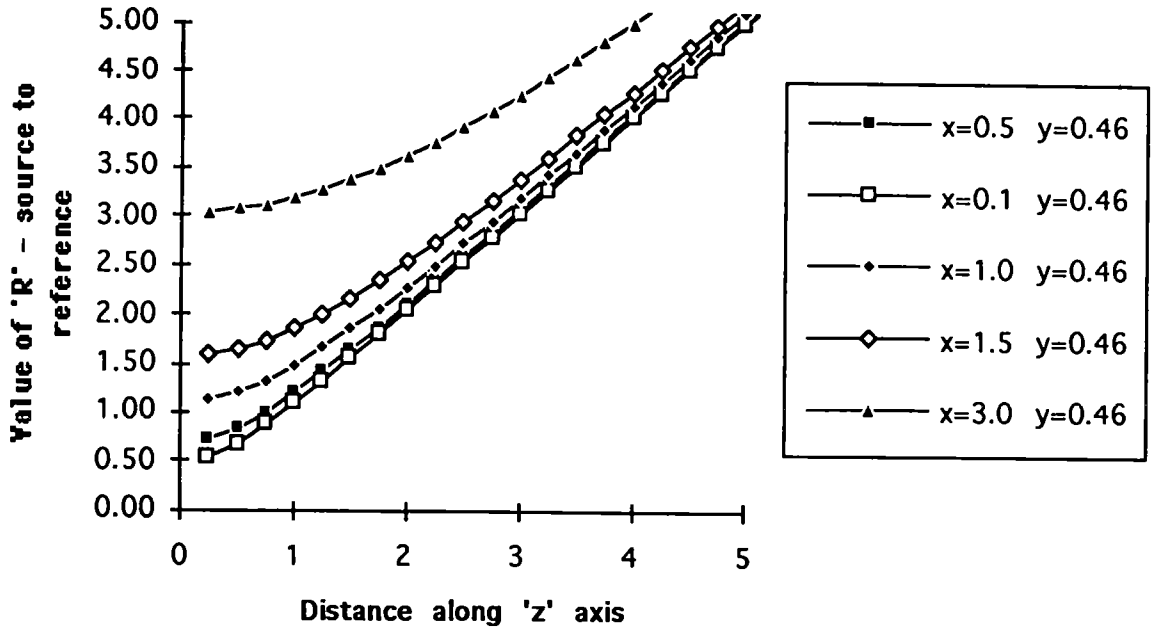

Figures 7.8 to 7.9b are to illustrate the significance of the equation

$$z = d.\frac{R}{Tc\tau}$$

Figure 7.8 shows that as the value of the time interval gets greater and the value of the distance 'z' increases, the various curves representing different time intervals, tend to converge. The convergence indicates that there is little difference in the value of 'R' with either the angle of incidence or the increase in 'z' beyond a certain distance. The angle of incidence is determined by the values of 'x' and 'y'. (See figure 7.7). This point is further emphasised by figure 7.9a, where the value of (R-Q), the difference in the distance between source to reference and source to microphone 5, can be seen to become constant at a value just greater than 1 metre for a microphone separation of 0.28 m and at 4.5 m for a separation of 2.8 m. Further, it can be seen that the curve prior to the point where (R-Q) becomes constant, is where the change in (R-Q) rapidly decreases. Figure 7.9b illustrates that the linear relationship between 'z' and $R/Tc\tau$ only occurs when the time differences become equal. At the point where R=Q, the curves go to infinity, which is the point where the source is at 90° to the line of the microphones. Between these positions, the maximum slope of the curve indicates the region where the accuracy for the determination of 'R' will be greatest.

Errors occur in the determination of the time interval from the cross correlation of the respective waves. Figure 7.10 is a plot of the normalised correlation coefficient obtained for different numbers of records included in the correlation sampling. This is of particular significance with respect to the multiple source experiments. When there is a single source, the correlation coefficient hardly changes with the greater number of records used in a sample. The normalised coefficient always remained above 0.8 although the sample sizes varied from 10 to 150. For the multiple source experiments, not only does the size of the correlation coefficient vary with the number of samples correlated, but the position of correlation can change also. (See Figure 6.13). The graph shown in Figure 7.10 attempts to show what is happening. As the number of samples increases from 10 to 60, the normalised coefficient peaks at 15 samples. The values used to produce the curve were subjected to a number of linear regression analyses. The result suggested that a cubic relationship existed between the correlation coefficient and the number of data samples. Finding the coefficient values with low sample numbers, showed that analysis with 3 samples was the lowest sample number to produce normal correlation. Below this, the correlation coefficient becomes either +1 or -1 for all samples, including the

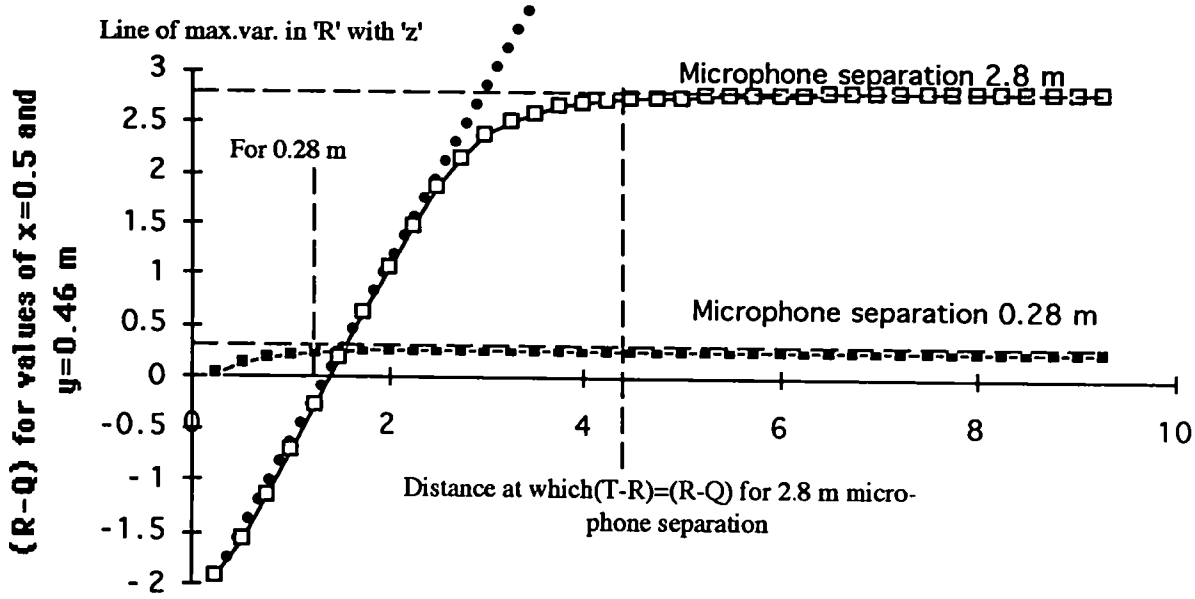


*Figure 7.9a - Relationship between 'R' and 'z'*

| Distance along 'z' axis | R | Q | (R-Q) = Tct | R/Tct |
|---|---|---|---|---|
| 0.25 | 0.72 | 0.68 | 0.044 | 16.5 |
| 0.5 | 0.84 | 0.714 | 0.129 | 6.518 |
| 0.75 | 1.01 | 0.826 | 0.186 | 5.445 |
| 1 | 1.21 | 0.99 | 0.219 | 5.51 |
| 1.25 | 1.42 | 1.184 | 0.238 | 5.967 |
| 1.5 | 1.63 | 1.396 | 0.23 | 6.58 |
| 1.75 | 1.88 | 1.619 | 0.258 | 7.551 |
| 2 | 2.11 | 1.849 | 0.268 | 8.084 |
| 2.25 | 2.35 | 2.084 | 0.266 | 8.82 |
| 2.5 | 2.59 | 2.322 | 0.269 | 9.488 |
| 2.75 | 2.89 | 2.585 | 0.271 | 10.45 |
| 3 | 3.08 | 2.824 | 0.272 | 11.39 |
| 3.25 | 3.38 | 3.047 | 0.274 | 12.14 |
| 3.5 | 3.67 | 3.291 | 0.274 | 12.99 |
| 3.75 | 3.83 | 3.286 | 0.275 | 13.85 |
| 4 | 4.08 | 3.782 | 0.276 | 14.71 |
| 4.25 | 4.3 | 4.088 | 0.276 | 15.38 |
| 4.5 | 4.55 | 4.274 | 0.277 | 16.43 |
| 4.75 | 4.8 | 4.581 | 0.277 | 17.38 |
| 5 | 5.05 | 4.769 | 0.277 | 18.2 |

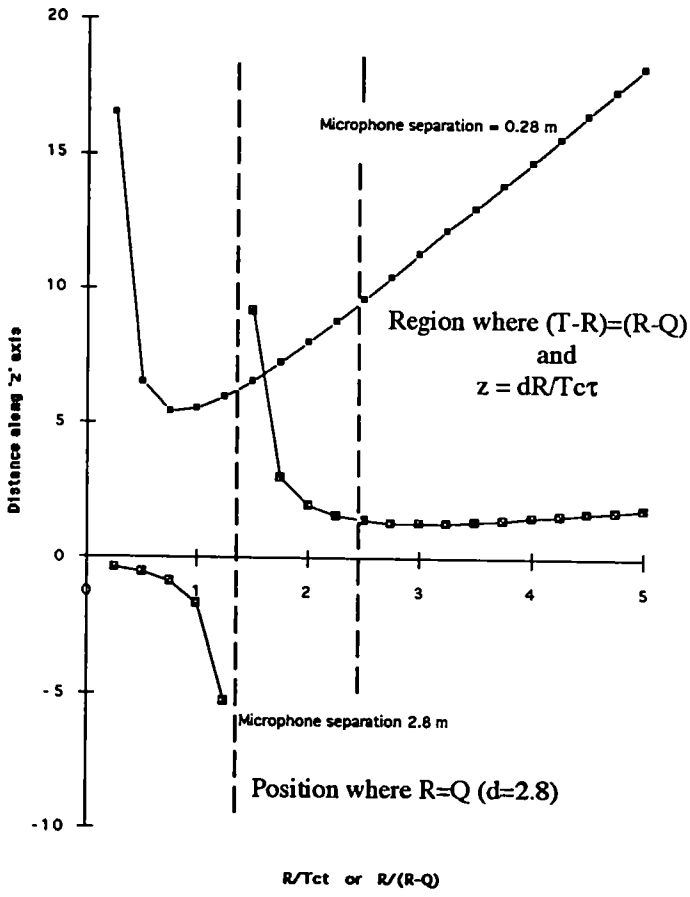


*Figure 7.9b - the effect of increasing microphone separation*

noise before the start of the signal. Similarly, taking results with between 20 and 60 samples does not produce the smooth curve of the cubic equation. However, the cubic expression fits sufficiently well to make the equation an attractive proposition to predict the optimum number of samples to use. (See insert to Figure 7.10)

In the collection of the data by the A to D conversion, the possible error in the equipment is ±1 period of 20$\mu$S. Taking the example of the experiment where the source was randomly placed, then for the distances between microphones $m_1$, $m_2$ and the reference microphone $m_o$, the values recorded were -0.041 and -0.095. Using these figures to calculate 'x' gives -0.319 and - 030. Changing the values by adding and subtracting one time period, the maximum difference in the distances becomes -0.05 and -0.10 with the minimum being -0.03 and -0.085. These values give a maximum value of 'x' of -0.40 and a minimum value of 'x' of -0.217. The percentage difference between the values is 81%. This example shows the magnitude of the difference that can occur when the correct time difference is between two integers. This occurs in the experiment for the all positive octant. The table of values - Table 6.5 - on page 82 shows the significant change in the accuracy of the readings due to the alteration of one time period for one microphone pair. Wherever the readings have been averaged, there is a probability of error and because of the size of the time window, the error can produce quite large deviations from the correct results. In the practical examples, the errors have been quoted in terms of the variability in the calculated answers from the different equations. If the variation in the possible errors were included, the range of differences would be quite large.

As indicated earlier, the size of the array becomes excessively large for the greater resolution by increasing the microphone separation. Also, as indicated, once the distance to the source gets very large, then the errors associated with the time window require that an alternative approach be used. Referring to the paper by Broadhurst[8], the use of an array can enable the system to be focused and individual areas of a surface monitored. The number of elements in the array governs the resolution of the array. Broadhurst suggests a cubic array with a minimum of 125 microphones. The advantage of the array is that it is steered electronically and an acoustic focus is possible. This enables the separation of signals from different parts of a partition. The wheel brace array offers a capability with a modest number of microphones, which, provided the limitations of the system are taken into account, can provide the same information as the more complicated systems. There are now available PC cards that will

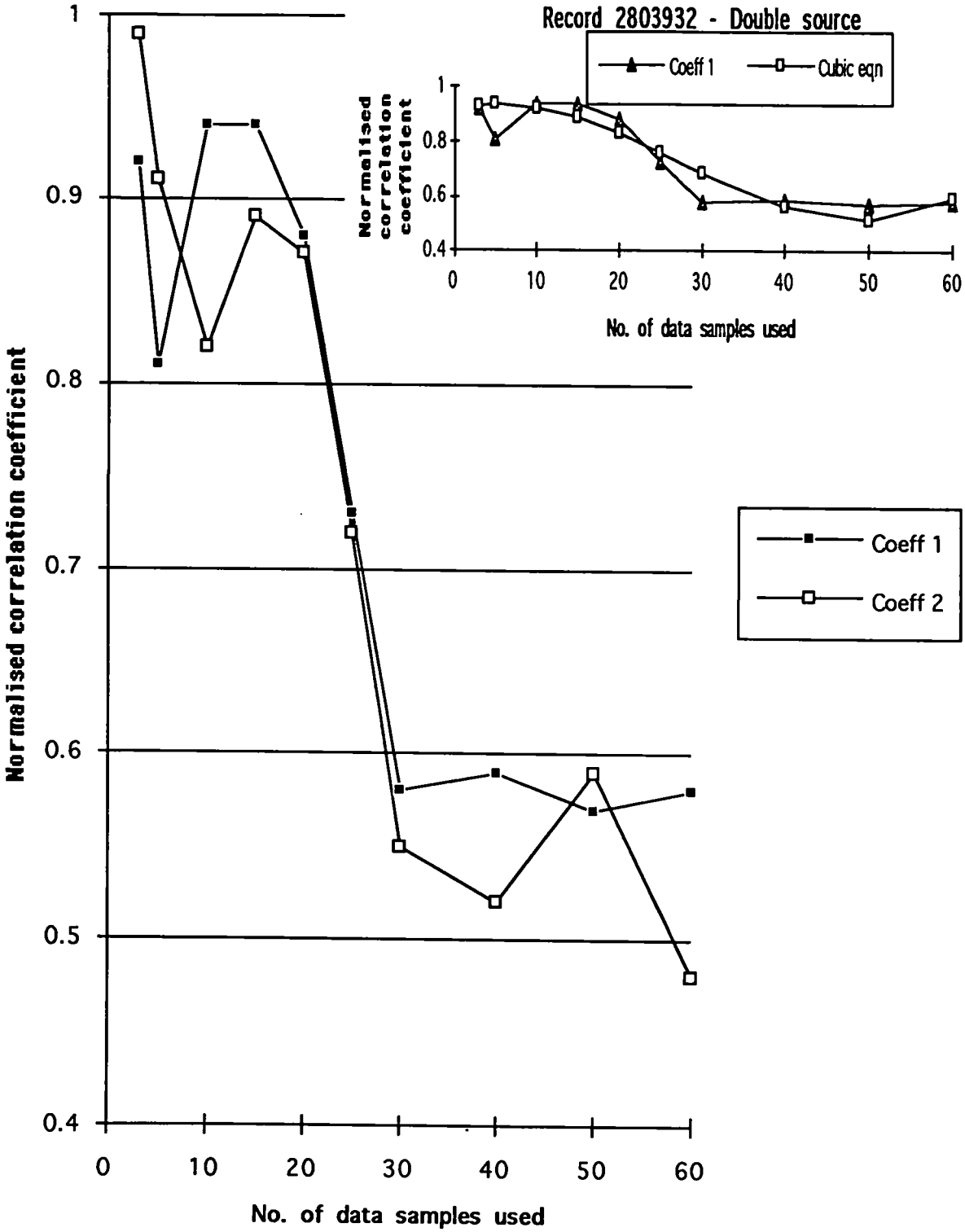


$$y = A_1x + A_2x^2 + A_3x^3 + C$$

where $A_1$ = 0.067 $A_2$ = -0.0033 $A_3$ = 0.00004

and the constant C = 0.56

*Variation in correlation coefficient - Figure 7.10*

capture data in 1/10th of a microsecond. This facility would provide a high degree of resolution for small microphone separation.

*Chapter 8*

# Uses in the Built Environment

**Use of the array in the built environment.**

The array enables a number of building acoustic measurements to be undertaken. As explained earlier, the sound transmission coefficient can be measured. Again, by selectively scanning the surface of a partition using a time-delay technique, then the surface weaknesses in a partition can be investigated. If the pulsed sound is replaced with a swept pure tone, the absorption coefficients of different surfaces within the environment can be measured and related to frequency. The system is easily adaptable for the measurement of reverberation time. In fact, because of the number of samples collected, the reverberation slope can be computed over any part of the decay range with frequency analysis included.

The use of this type of array will be largely applicable to sources in the near field, where the approximate location of the source is known. It should be appropriate for dealing with leakage of sound through ventilation systems, finding gas flues in party walls or hidden chimney breasts. The size of the imperfection that it will detect is limited to relatively large areas probably of at least 500 mm square.

The importance of techniques for on-site measurement of the acoustic properties of buildings has changed over the years. The current Building Regulations, Approved Document E(1992 Edition), page 26, gives a single figure for the sound insulation of a party floor in a multiple dwelling as 48 dB, (Building Regulations: Table 2, INDIVIDUAL VALUE, which means that only one floor was tested). It is measured as $D_{nT,W}$, the standardised level difference (reference BS 5821: Part 1 :1984) . If 'deemed to satisfy' construction techniques are used, the control of sound insulation is regarded as adequately dealt with and the construction will pass the Building Regulations. Should complaints arise subsequently about the adequacy of the sound insulation, field tests may be carried out that show a single figure sound insulation value less than 48 dB. Because the building was built as a 'deemed to satisfy' construction, then the fact that the measured values do not reach the minimum criteria does not invalidate the building conforming to the Building Regulations. In fact, there is a specific 'let-out' clause in the Building Regulations, paragraph 3.8 page 26, entitled "Limits on use of test evidence". This paragraph contains the statement "A failure of a new construction to achieve the values in the Table is not in itself evidence of a failure to comply with the requirements of the Regulations".

When a block of flats is designed, the cost implications often dictate the type of construction employed for sound insulation. Although this need not be synonymous with the cheapest option, it does seem to correlate with using the 'deemed to satisfy' construction that meets the minimum requirements. This in turn is usually the construction that is most marginal in achieving the sound insulation regarded as desirable by the occupiers of the flats. In 1988, the Building Research Establishment produced a series of digests on the results of testing a number of structures built under the deemed to satisfy category. In Digest 334, p.5 it is stated "hollow beam or beam and hollow block floors are usually designed to satisfy the Building Regulations minimum requirements by having a mass of not less than 220 kg/m$^2$". In Table 1. - 'Sound insulation of main types of floor', the value for the insulation of this type of floor, measured as $D_{nT,W}$ is 47 dB within the 95 percentile. This is 1 dB below the recommended minimum value.

It would be appropriate and helpful for any architect using a 'deemed to satisfy' design to have some means whereby the structure can be tested during construction. It is in this context that the equipment described in this research should be of particular application. The ability to detect the source of a sound could be used during construction stages to confirm that the floor construction was homogeneous and that the sound transmission was meeting the projected design criteria. The earlier a fault is detected, the more likely a solution can be found that is viable to implement. The equipment used in this research was designed as a laboratory experiment. In the discussion, suggestions have been made for the modernisation of the equipment that would be used for field measurements. These include the use of a portable computer with attached analogue to digital conversion system. With such a device, measurements could be taken, analysed and presented within 30 minutes.

Work has been undertaken to produce a simplified procedure for the determination of the sound insulation value. A paper by Robin K. Mackenzie, was presented on 'The development of a short test method for the measurement of airborne sound insulation in buildings, Proc.I.O.A. Vol. 8 Part 3 1986'. This paper described the results of a working group associated with the International Standards Organisation engaged to produce a draft standard for the procedure and

the criteria for accuracy in a simplified test method. The equipment suggested for the simplified test consisted of a special noise source and integrating sound level meters. A switch is incorporated to change the noise when the room under measurement is either occupied or unoccupied.

It is considered that the equipment developed and described in this thesis, could be included in such a simplified test procedure. The acoustic array would succeed in providing a greater amount of detail, allowing diagnosis of faults as well as determination of a simple pass or fail, with respect to the Building Regulations.

Measurements taken by the array described in this research suggest that the repeatability of results is good. The experimental work with the array does indicate that the use of a pulsed noise source could eliminate the problems associated with the amount of absorption present in the receiving room during a transmission loss test. The received waves are the direct waves, so that the transmission loss measurement would not include any build-up of sound due to multiple reflection in the receiving room. This would eliminate the need to modify the sound source, depending upon whether the room is occupied or unoccupied.

The graph in Figure 8.1 shows that provided the 'x', 'y' and 'z' coordinates are equal - which corresponds to the optimum accuracy when using the array - the values of the coordinates can be determined within an 8% accuracy using a 20 $\mu$s data capture system and a 0.28 m microphone separation at distances of (10 x microphone separation). This is equivalent to a microphone/source separation of :-

$$= \sqrt{(10 \times 0.28)^2 \times 3} = 4.84 \quad \text{meters}$$

from the expression $R = \sqrt{x^2 + y^2 + z^2}$

An additional potential source of error arises since the velocity of sound in air is a function of the room temperature. The significance of the variation of 5°C in the room temperature is illustrated in Figure 8.1

If the separation of the microphones is increased, or if the rate of sampling the data is increased by a factor of 10, then the distance is proportionally increased. Since the equipment that would

be developed with the now available A to D capture systems easily allows a 2 $\mu$s time interval for data capture, considerably improved accuracies can be obtained. In Figure 8.2 the percentage errors are calculated for an array with a microphone separation of 0.56 m and with

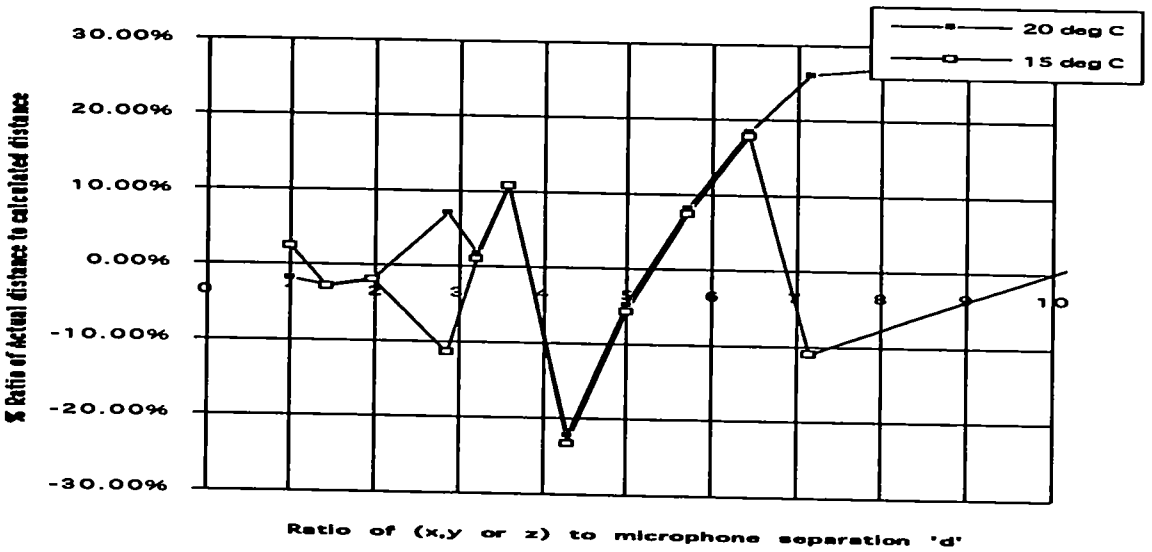


*Figure 8.1 - Effect of temperature on calculation*

time windows of 20 and 2 $\mu$s. The 2 $\mu$s time window allows distances of up to 10 m to be measured to within a ± 50 mm.

To demonstrate the possible field application of this array, the following example is included. Consider a room 20 m long by 10 m wide and 6 m high. If the wheel-brace array is placed in the middle of the floor at a height of 1.5 m and the spacing of the microphones was set at 0.56 m (double that used in the laboratory experiments) with a time window of 2 $\mu$s, (using a modern data capture system with a time window 1/10th of the size used in this research) the error in measurement is 0.5%. With a sound source occurring at the corner of the room in the all positive octant, then for the 95 percentile, the coordinates derived from the calculation are:

$$x_s = 6.1 \pm 0.12 \text{ m}$$

$$y_s = 5.1 \pm 0.10 \text{ m}$$

$$z_s = 10.2 \pm 0.20 \text{ m}$$

Thus, converting these numbers into practical terms and with a 95% confidence limit, the

source of the sound entering the room can be located within an area of 0.05 square metres of the wall. This is equivalent to 1.5 bricks or 0.5 blocks. The measurement is from a distance of 10 m away. By moving the array closer to the source, the location of the noise entry can be

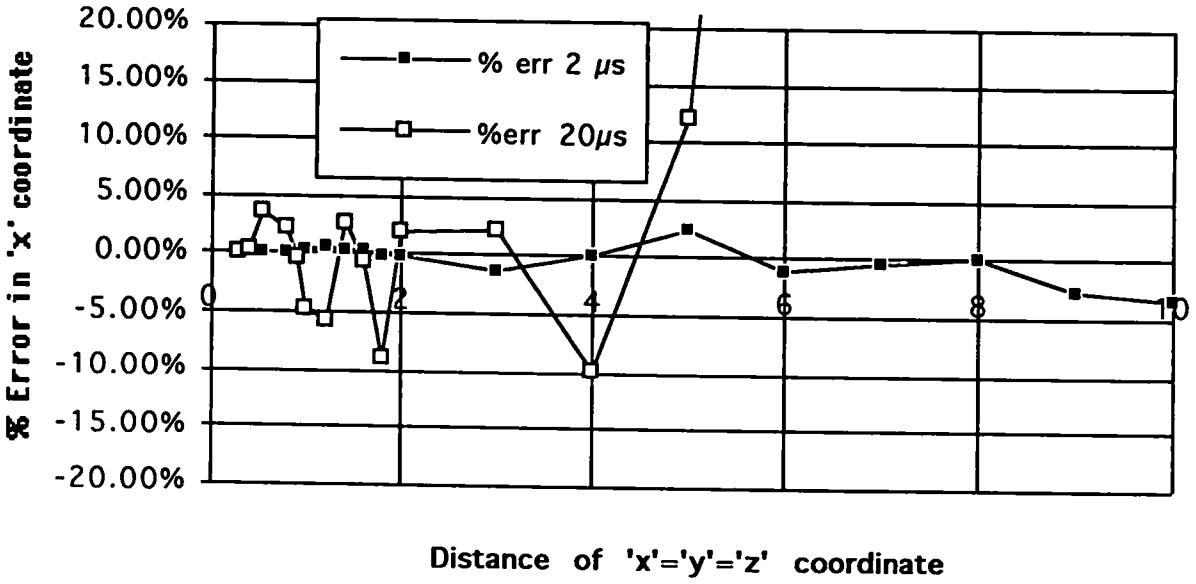


*Figure 8.2 - % error when microphone separation is 0.56m and time interval is 0.2 μs*

more precisely determined. As shown by M.E. Hopkins [76], when studying the sound insulation in a new build tenement and the identification of the flanking paths, the noise breakthrough into a room can have a number of points of entry. The sound pressure level from adjacent sources can be quite different and the distance between the entry points may be metres apart. This research has attempted to deal with this problem by investigating the resolution of two noise sources producing identical sound pressure levels at a separation of 0.10 m. The analysis shows that the cross correlation technique could separate these sources, although difficulty is experienced in attributing the coordinates to the source. The use of autocorrelation and cepstrum analysis suggest that this problem can be resolved. Figure 8.4 is the cepstrum of figure 8.3. The cepstrum can locate an echo - the echo in the case described here is a simultaneous signal from a second loudspeaker 0.46 m below the first loudspeaker. The cepstrum converts the periodicity of the autocorrelogram into a series of rahmonics with a spacing corresponding to the delay time of the echo. (B&K Technical Review No.3 - 1981, p.16-17). In figure 8.4, the spacing between the start of the trace and the first spike is the time delay of the first echo.

Finally, it is worth emphasising that the proposed equipment is portable, can investigate and analyse the acoustic problems of a room in near real-time measurements with minimum need to alter the original equipment placing, even in the relatively large room used in the above example.

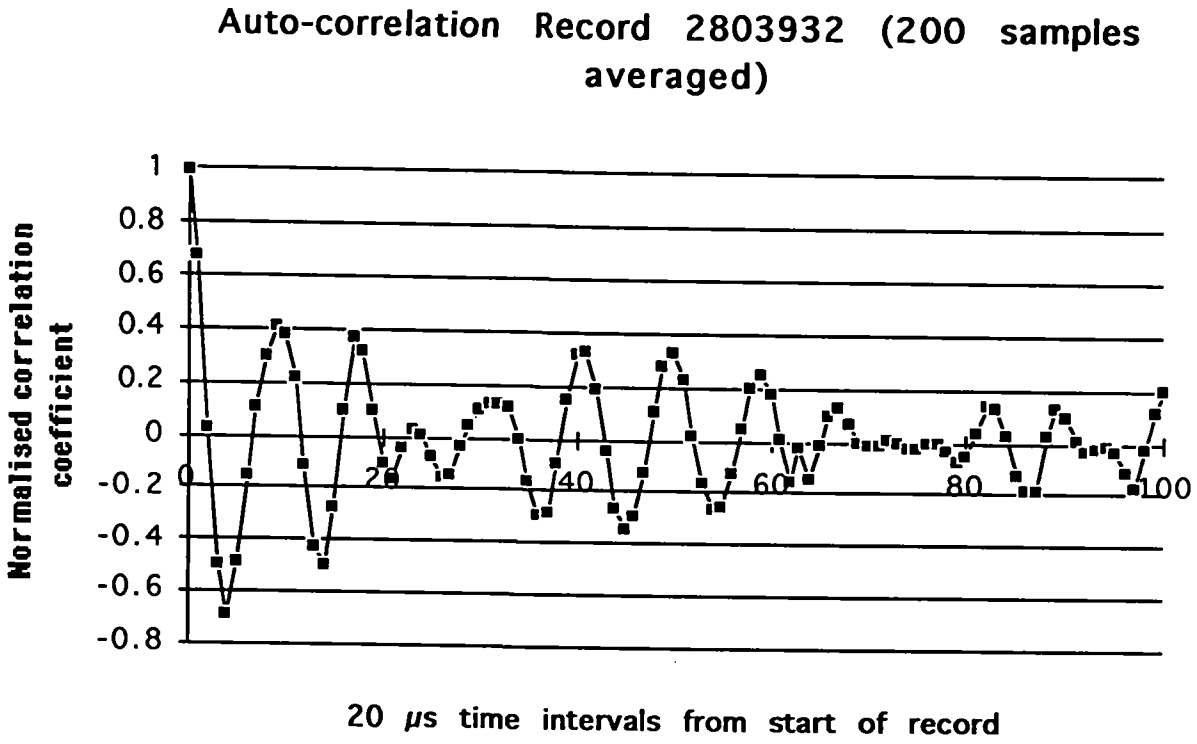


*Figure 8.3 - Autocorrelation - double source*

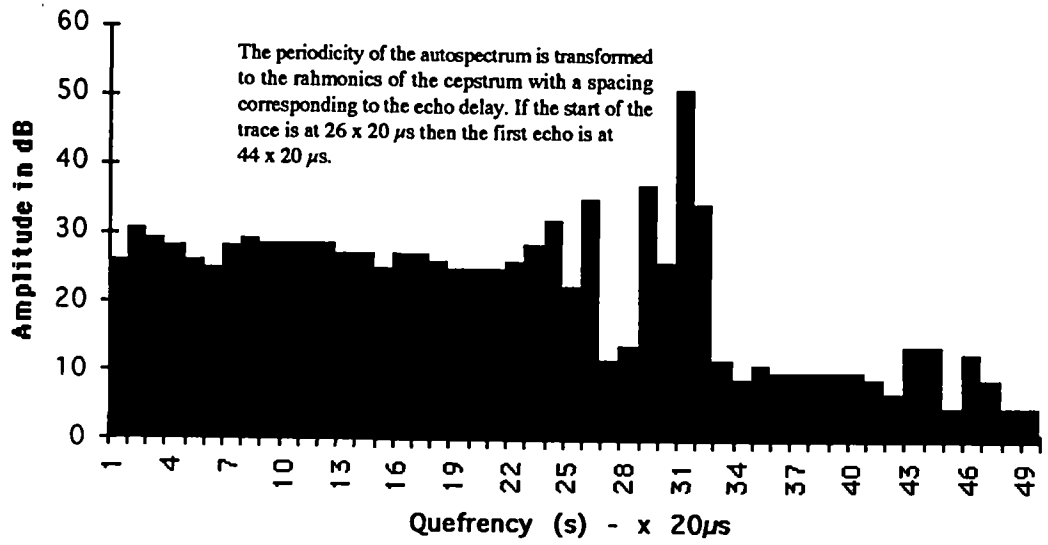


*Figure 8.4 Cepstrum showing two spikes with harmonics*

*Chapter 9*

# Conclusion

# Conclusion

The work described in this thesis has taken place over a period of seven years. During that period many advances have occurred in the field of electronics. In particular, the transition to computer based instrumentation has made vast strides. The equipment that has been demonstrated in this work, can now be contained on an 'add-on board of a personal computer'. By the selection of the right computer, the entire practical work could be performed on a single portable microcomputer with the only external components being the microphone array.

The microphone system used in the research was chosen because of its track record of reliability. Initially, the practical work had to find the areas where erroneous results were occurring. Using standard, high quality equipment, enabled confidence to be maintained in the detection side of the system and allowed the area of the problem to be reduced. At the conclusion of the work, the weak points can be identified as the preamplifiers and conditioning amplifiers. This was largely due to the age of the equipment used - it was twenty years old and already well used when it joined this project. The results of the research suggest that modern miniature microphones, such as the Knowles FET capacitance microphones, are perfectly adequate. The type of preamplifiers and conditioning amplifiers can now be selected from add-on cards for different computer makes. For instance, Laplace Instruments advertise an A to D card with a single channel that has a sampling rate of 0.1 $\mu$S to 12 bit accuracy. The same firm advertises a card with eight channels operating on 12 bits with a sampling rate of 3 $\mu$S. Both systems would give a significant improvement in resolution over the apparatus used in this research, together with being contained in a single computer. Bearing in mind that portable computers are now available that accept add-on boards, a modern system becomes an extremely portable device. Provided the computer has sufficient on-board memory - and these days this is usually a minimum of 8 megabyte - and a large enough hard disk, then with programs advertised by National Instruments, real time display of analysed data is feasible. For instance, using LabView and the analysis software suite, eight cross

correlations could be displayed within 1 second. This enables the scanning of a surface and the presentation of the results on screen to be quick enough to allow the data capture to provide the information for setting up the microphone array and with instant analysis of the collected data.

With these advances in mind, then the research that has been carried out shows that a seven microphone wheelbrace array can give valuable information about the source of noise within buildings. The correlation technique can be used to measure transmission loss in any environment, because the system can identify the time/signal relationship. In this respect it is analogous to Time Delayed Spectrometry. The apparatus can selectively assess the absorption coefficients of room surfaces, again by using the knowledge of the time delay of short wave bursts from the acoustic source. The research has established that source location can be achieved, albeit, under fairly restricted circumstances, but with the development of suitable algorithms, the equipment described shows considerable potential. Cross correlation has been shown again, to be a powerful tool in comparing coherent wave data and determining the time separation between waves travelling over different paths. Mathematical relationships have been established to relate the time differences in the reception of a signal, to the polar coordinates of the source. The realistic development of the equipment is dependent upon the use of high speed data sampling and analysis to achieve adequate resolution for the source location at positions close to any of the axes. Where the source is close to an axis, there is a finite distance before the time differences between the microphones along that axis and the reference microphone become equal. This distance is related to the separation of the microphones and to the resolution of the data capture window, that is, the minimum time between successive records. Beyond this distance, the array would serve as a direction seeking device by determination of the zero time difference along two axes and maximum time difference along the third axis, which equates to one axis of the array pointing towards the source whilst the other two axes are normal to the source. The advantage of maintaining a minimum of seven microphones is that the data collected is vectorial, that is the array can detect the sound from any direction. There is no requirement for movement of any of the parts, so that once the array is constructed, there should be little requirement for checking the structure. For source location exercises, the microphones sensitivity is not critical, but if sound transmission loss and similar

measurements are made, then unless comparative measurements can be taken, a built-in calibrator would be needed to check pressure sensitivity and phase relationship of the transducers.

The fact that the system could be reduced to two microphones, with the microphones being positioned so that one record is collected at the reference microphone, $m_0$, and the other records from a second microphone placed at the equivalent of $m_2$, $m_4$ and $m_6$ positions respectively, has certain appeal. The potential for errors in the measurement of the distance between the various microphone locations makes it less attractive, especially when one considers that this requires mechanical movement and that with two closely coupled microphones one has an acoustic intensity measuring device which is capable of higher resolution and accuracy than the near field two element array.

The aim stated for the research, of developing a mathematical model to locate a source from the time difference in the arrival of a signal at a set of microphones arranged in the form of a wheel brace array, has been achieved. The mathematical model is capable of determining the distance provided it is supplied with information that can be positively identified as coming from the same source at the same time. This research avoided the problem of the comparison of waves to find the common origin by using clearly defined pulses of sound for the signal. The second aim of testing the mathematical model produced a lot of information relating to the practical problems of the instrumentation. The overall conclusion was that the practical work verifies the mathematical model. It also indicates that there is a need to consider certain points when taking the measurements in order to obtain maximum accuracy from the equipment. The third aim, to develop a computer program for the collection of data and the evaluation of the information proved to be the least difficult. The program for the control of the hardware is enclosed in the appendix. The program for the calculation of the coordinates is shown as examples of prepared spreadsheets which use information from processing programs. These processing programs were based upon the calculation of a cross correlation. The program was developed to improve the user friendliness of the package and to enable it to be used by anyone, without difficulty . The component programs have not been integrated because they were used across a variety of incompatible hardware. If the system were developed for a specific device,

the integration of the software would not be difficult.

The final aim, to consider an optimal package for a portable system, is limited only by financial constraints. A portable computer capable of being fitted with full size add on cards would cost at least £2000. The analogue to digital conversion system with a 0.1 microsecond response, or window, would be about the same cost. The construction of the microphone array and associated amplifiers would add at least another £2000. It can be concluded that for an expenditure of £10,000 a fully operational and portable system could be assembled from units available in the present market. It is probable that the system could be produced for half that price by selective purchase.

From the literature produced over the last fifty years, there is evidence that a number of devices have been considered worthy of development for use in the built environment. Apart from the Acoustic Intensity system - notably that of B&K Ltd. - there is no sign of any of the devices being adopted. Whether the option of a compact portable system based upon a computer would change that approach remains to be seen; but what is clear, is that the acoustic array can give a lot of useful information quickly and accurately. In the developing requirement for quality control and the need for more on-site testing of buildings to meet EEC requirements, then this research has shown that a small acoustic array could be considered for site use.

# Appendices

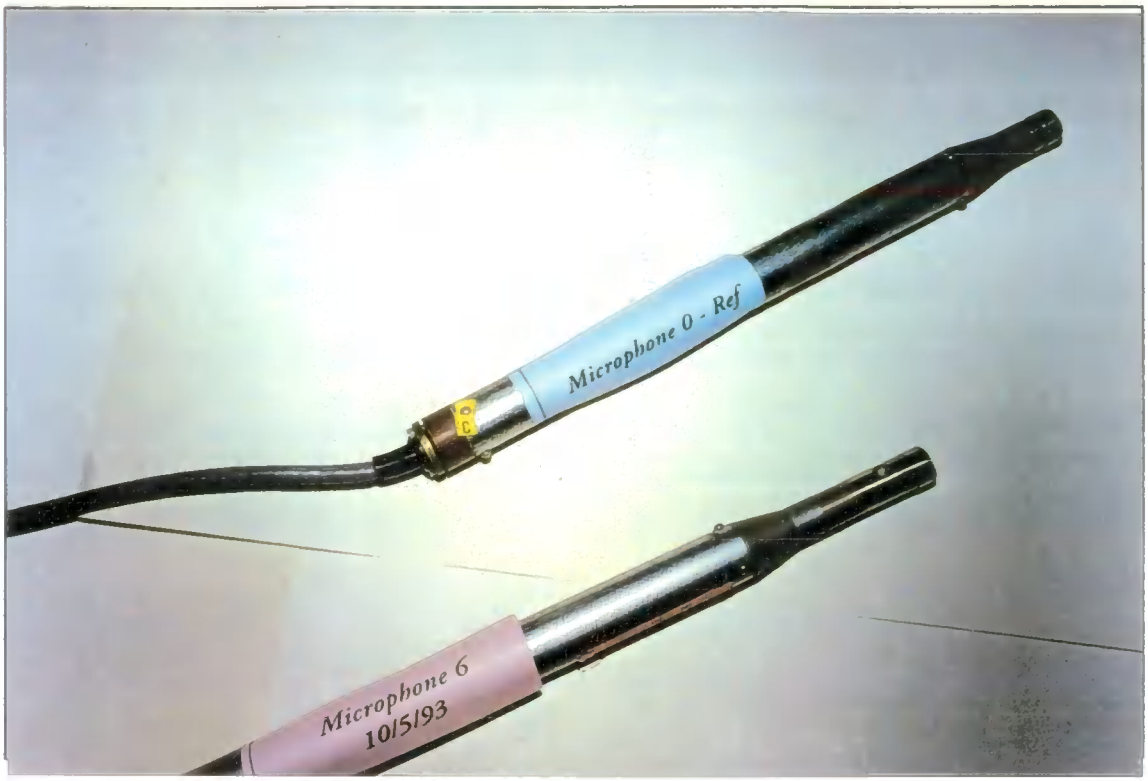


## Photographs

Above - microphone and preamplifiers used in array and labelled for identification.

Below - Small loud-speaker with plumb line used to measure the 'y' coordinate

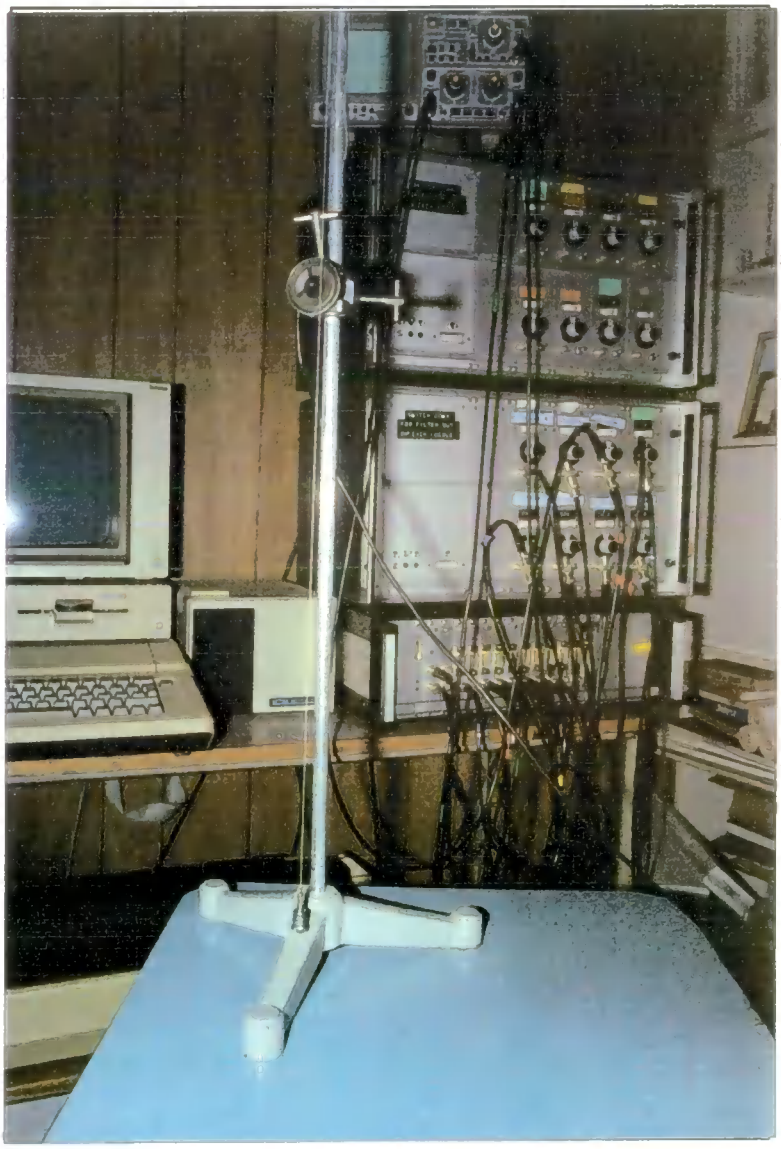

## Photographs 2

Above - The amplifier rack with the digital storage oscilloscope on top.

Below - the analogue to digital capture system.

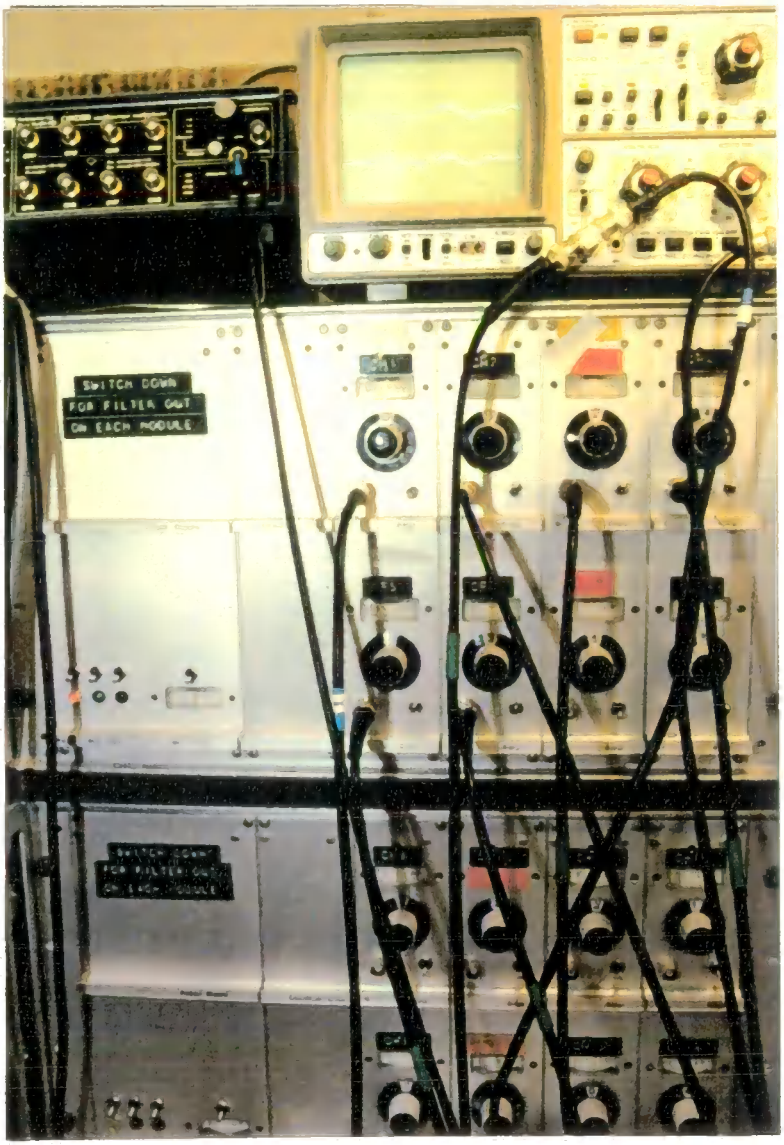


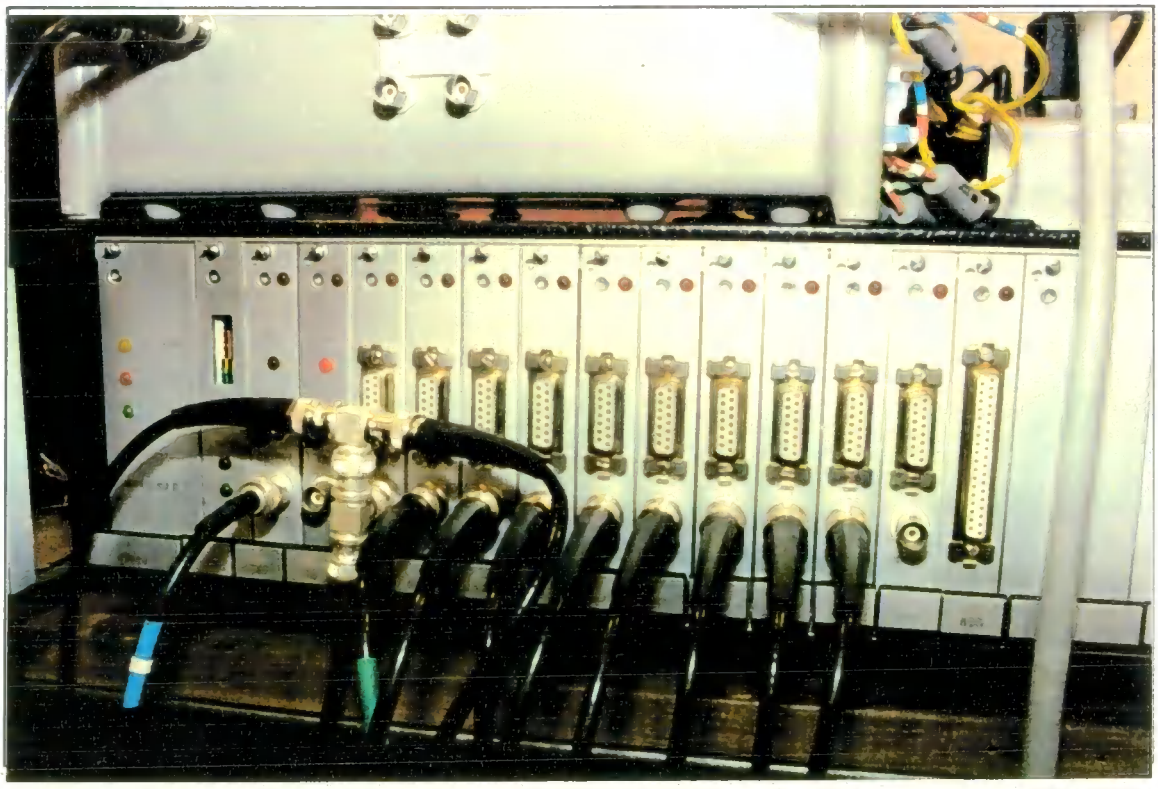

## Photograph 3

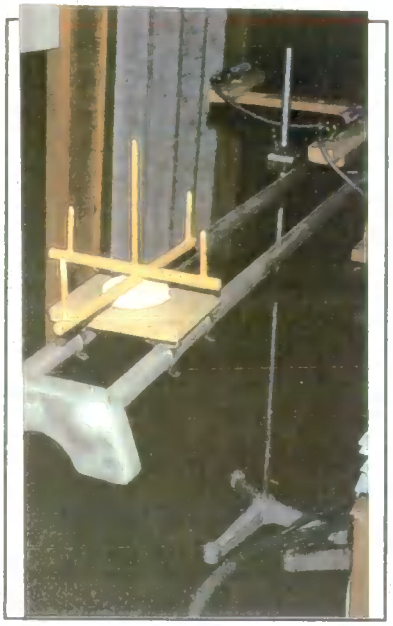

Above - The jig used to align tape measurements in the determination of the 'x,y,z' coordinates

Below - the wooden framework used to support the microphone assemble

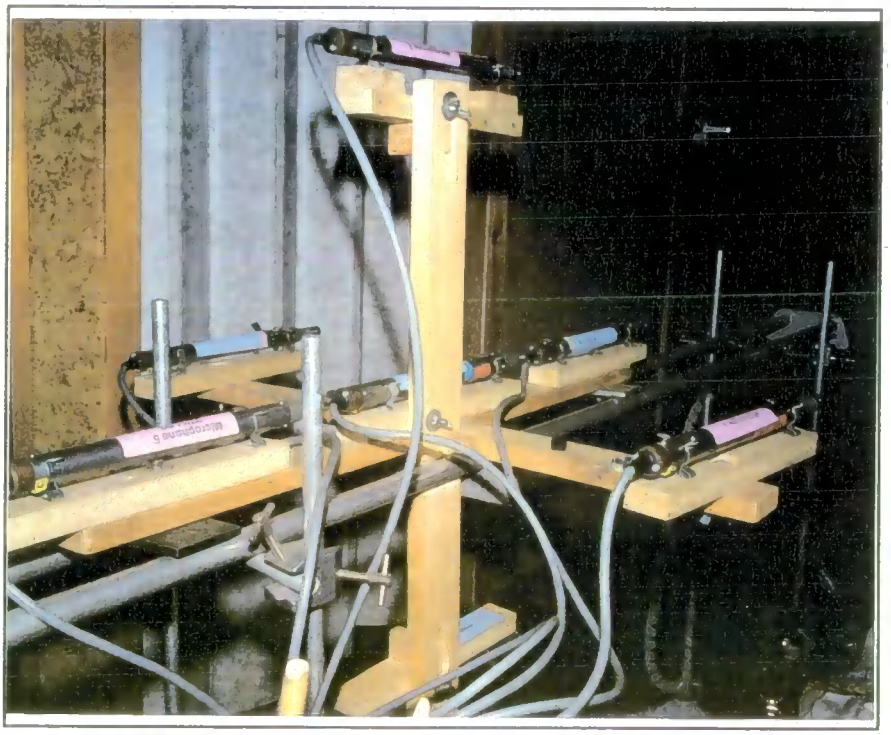

# Computer program for collection of data.

```
]LIST

20 TEXT
3999 HOME : TEXT : REM *********PLOT.IT************
4000 HOME : VTAB 5: HTAB 5: PRINT "This routine will plot TWO graphs on the Screen":::PRINT"To
   continue, [press RETURN":GET A$
4020 A$ = CHR$ (13)
4500 HGR
5000 HOME
5030 X = FRE (0)
5040 HCOLOR= 3
5050 D$ = CHR$ (4)
5060 DIM CX(256): DIM CY(256)
5070 PRINT D$;"MON C,I,O"
5080 REM ****************************
5090 VTAB 22
5095 INPUT " MICRO FILE NUMBER = ";CODE$
5096 INPUT "Trace No. 1 <can be from 1 to 8> ";N: INPUT "Trace No. 2 <again from 1 to 8> ";NN
5097 INPUT "WHICH DRIVE <1/2>";NO
5099 PRINT "Select Magnification <0 TO 100>": INPUT MG:MG = 409.6 / MG
5100 GOSUB 5320
5110 FOR K = 0 TO 512 STEP 2
5120 CX(K / 2) = PEEK (20998 + K) * 256 + PEEK (20998 + K + 1)
5140 NEXT
5150 GOSUB 11000
5155 GOSUB 5500
5158 C = 0
5160 GOSUB 5340
5170 GOSUB 5240
5180 GOSUB 5360
5192 GOSUB 7000: GOSUB 5100: GOSUB 5340: GOSUB 5240: GOSUB 5360
5230 REM ****************************
5240 FOR K = 0 TO 512 STEP 2
5250 CY(K / 2) = PEEK (20998 + K) * 256 + PEEK (20998 + K + 1)
5270 NEXT
5280 RETURN
5290 REM ************************
5300 END
5310 REM ****************************
5320 PRINT D$;"BLOAD MICRO.";N;".";CODE$;",V254,D";NO
5330 RETURN
5340 PRINT D$;"BLOAD MICRO.";NN;".";CODE$;",V254,D";NO
5345 RETURN
5350 REM ****************************
5360 HPLOT 0,100
5365 FOR K = QT TO QR STEP 2:CY = PEEK (20998 + K) * 256 + PEEK (20998 + K )
5366 VTAB 24: PRINT K / 2,CY / 4096
5370 CV = CY - 4096
5375 CV = SQR (CV * CV)
5376 IF C < 1 THEN GOSUB 18000
5377 PTY = (CV / MG) - EZ
5378 IF PTY < 1 THEN PTY = 0
5379 IF PTY > 159 THEN PTY = 159
5380 HPLOT TO C,PTY
5385 C = C + Q
```

```
5387 IF C > 275 THEN GOTO 5400
5390 NEXT
5400 RETURN
5410 REM ****************************
5500 PZ = 275 / Q * 5
5501 PT = Q * 5
5502 FOR PW = 0 TO PZ - 1
5504 HPLOT PT,155 TO PT,159
5506 PT = PT + (5 * Q)
5507 IF PT > 275 THEN RETURN
5508 NEXT
5530 RETURN
5580 REM ******************************
7000 HOME : VTAB 24: PRINT "Do you want to insert a cursor? <Y ?N>": GET A$
7010 IF A$ = "Y" THEN GOSUB 19000
7050 IF A$ = "N" THEN GOTO 8070
8070 GOSUB 12000
11000 HGR : HCOLOR= 3
11010 HOME : VTAB 22
11020 C = 0
11030 INPUT " LOWEST NUMBER ? ";QT:QT = QT * 2
11040 QR = QT + 512
11045 HPLOT 0,0 TO 279,0 TO 279,159 TO 0,159 TO 0,0
11050 HPLOT 0,80
11055 VTAB 21: HTAB 30: PRINT "Micro.";N;"";CODE$;" and Micro.";NN;"";CODE$
11058 PRINT "PRESS RETURN TO CONTINUE  ": GET A$
11059 VTAB 24: HTAB 15
11060 INPUT "SEPARATION BETWEEN POINTS <1,5,10>  ";Q
11070 FOR K = QT TO QR STEP 2:CX =  PEEK (20998 + K) * 256 +  PEEK (20998 + K)
11080 VTAB 24: PRINT K / 2,CX / 4096
11090 CV = CX - 4096
11095 CV =  SQR (CV * CV)
11098 IF C < 1 THEN GOSUB 17000
11099 PTX = (CV / MG) - EX
11100 IF PTX < 1 THEN PTX = 0
11105 HPLOT  TO C,PTX
11110 C = C + Q
11112 IF C > 275 THEN GOTO 11230
11120 NEXT
11230 RETURN
12000 PRINT "SEND DATA TO PRINTER? <Y/N>": GET Y$
12010 IF Y$ = "Y" THEN GOSUB 14500
12020 RETURN
14500 HOME : TEXT
14510 HOME : VTAB 24: PRINT "CURSOR POSN.1 = ";CURS(1);"  CURSOR POSN.2 = ";C)
14520 PRINT "THIS IS A TRACE OF MICRO.";N;".";CODE$;" AND MICRO.";NN;".";CODE$
15000 PR# 1:X$ =  CHR$ (9)
15001 PRINT X$;"15L": PRINT X$;"G,E,T,X"
15002 PRINT X$"15L"
15003 PRINT "CURSOR POSN.1 = ";CURS(1);"  CURSOR POSN.2 = ";CURS(2)
15004 PRINT "THIS IS A TRACE OF MICRO.";N;".";CODE$;" AND MICRO.";NN;".";CODE$
15005 PRINT "Start of the trace was -  ";QT / 2;"and the end was - ";(QT / 2))
15006 PRINT : PRINT : PRINT "The number of calibration marks = ";275 / Q,
15007 PRINT " and the distance between the marks corresponds to ";5 * Q;" 20 "
15050 PRINT X$;"Y"
15060 PR# 3
16000 HOME : VTAB 22: PRINT "PRINTER OR REPEAT <1/2>": INPUT ZC
16010 IF ZC = 1 THEN GOTO 8070
16020 IF ZC = 2 THEN GOTO 3999
16030 END
17000 EX = (CV / MG) - 50
```

```
17010 RETURN
18000 EZ = (CV / MG) - 100
18010 RETURN
19000 HOME : VTAB 24: PRINT "State position of cursor ": INPUT CURS
19005 HCOLOR= 3
19010 CS = CURS - (QT / 2):CS = CS * Q: HPLOT CS,0 TO CS,159
19020 PRINT "Replace the position of the cursor? <Y/N>": GET Y$
19021 PRINT A$
19028 IF CURS(1) > 1 THEN GOTO 19070
19030 IF Y$ = "Y" THEN HCOLOR= 0
19035 IF Y$ = "N" THEN GOTO 19048
19040 HPLOT CS,0 TO CS,159: HCOLOR= 3
19045 GOTO 19000
19048 CURS(1) = CURS
19050 PRINT "Do you want to place a second cursor? <Y/N> ": GET Y$
19055 IF Y$ = "Y" THEN GOTO 19000
19070 IF Y$ = "N" THEN GOTO 19080
19072 IF Y$ = "Y" THEN HCOLOR= 0
19075 HPLOT CS,0 TO CS,159
19076 GOTO 19050
19080 CURS(2) = CURS
19083 PRINT "Any more cursors? <Y/N>": GET Y$
19084 IF Y$ = "Y" THEN GOTO 19000
19085 HOME : VTAB 24: PRINT "CURSOR POS.1 = ";CURS(1);"  CURSOR POSN.2 = ")
19090 RETURN
```

]

Program to collect data from A to D system

```
0 HOME
1 GOTO 100
2 REM PULSES SPECIFIED LINE
4 REM RUNS WITH MACHINECODE5
5 N = 8
6 PA = 7:LI = 32
8 CALL 20480: REM CLEAR BUS
10 SA = 25
14 REM CLEAR BUFFERS
16 FOR I = 1 TO 8:BUFFER(I) = 0: NEXT
18 REM SET LINE
20 FOR I = 1 TO N
22 IF LI > I * 4 GOTO 30
24 L = 4 * I - LI
26 X = 2 ^ L
28 BUFFER(I) = X: GOTO 32
30 NEXT I
31 GOSUB 3000
32 REM SEND DATA
50 HOME : VTAB 10: PRINT "RUN PROGRAM AGAIN? <Y/N>": GET Y$: PRINT A$
55 PRINT A$
60 IF Y$ = "N" THEN GOSUB 12000
100 D$ = CHR$ (4):A$ = CHR$ (13)
110 CALL 20480
115 INPUT "CODE FOR THIS RECORD IS = ";DC
120 INPUT "NUMBER OF CHANNELS IN SYSTEM = ";NM
122 PRINT : PRINT
124 PRINT "50% TRIGGER IS ALWAYS 0 VOLTS"
125 PRINT : PRINT "STATE TRIGGER LEVEL <1 TO 100>": INPUT TX
126 PRINT "50% TRIGGER IS ALWAYS 0 VOLTS"
130 TEXT
140 HCOLOR= 3
170 XN = 0
```

```
180 PRINT D$;"MON C,I,O"
190 TEXT
200 GOSUB 10630
220 PRINT "TRIGGER EDGE  - POSITIVE<+>"
235 SA = 8:PA = 7:N = 2:VS = VO + 8:TR = 128 + TX
240 GOSUB 2000
270 PRINT
280 GOSUB 10500
310 N = 1:G = R: GOSUB 2500
320 HOME : VTAB 10: INVERSE : PRINT "MICROLINK TRANSIENT CAPTURE": PRINT : NO
330 PRINT "TRIGGER EDGE  - POSITIVE<+>"
360 PRINT "THERE ARE ";NM;" CHANNELS IN THE SYSTEM"
370 PRINT "SAMPLE INTERVAL PERIOD - 20 MICRO.SEC"
382 PRINT "TRIGGER LEVEL -  ";TX;"%    ";VG$
385 PRINT : PRINT "GAIN = ";CZ: PRINT : PRINT "VOLTAGE RANGE =  ";5 * 1000 /"
386 PRINT : PRINT : PRINT
387 GOSUB 11000
390 SA = 9:N = 7:SR = 1:SX = 2:SY = 0:PT = 7
410 GOSUB 2600
460 GOSUB 5000
470 GOTO 2
1999 REM *******SET BYTES*****************
2000 BYTE(1) = VS:BYTE(2) = TR: GOSUB 3000
2010 RETURN
2099 REM *************************
2500 SA = 12: FOR J = 1 TO NM
2510 BYTE(1) = G: GOSUB 3000:SA = SA + 1: NEXT
2520 RETURN
2599 REM ***********************&**
2600 BYTE(1) = SR:BYTE(2) = SX:BYTE(3) = SY:BYTE(4) = PT:BYTE(5) = 1:BYTE(6) =0
2605 GOSUB 3000
2610 FOR X = 0 TO 100: NEXT
2620 BYTE(6) = 1: GOSUB 3000
2630 RETURN
2999 REM ******************************
3000 REM  SUBROUTINE TO SEND N BYTES ************************
3010 REM  TO DEVICE WITH PRIMARY ADDRESS 7
3020 REM  AND SECONDARY ADDRESS SA
3030 POKE 20993,N
3040 POKE 20994,64: REM  SLOT 4
3050 POKE 20995,(32 + PA): REM  PRIMARY ADDR
3060 POKE 20996,(96 + SA)
3070 POKE 20997,255: REM  END OF ADDRS
3080 B = 20998
3090 FOR I = 1 TO N
3100 POKE B,BYTE(I)
3110 B = B + 1
3120 NEXT I
3130 CALL 20543: REM  SEND ROUTINE
3140 RETURN
3199 REM ******************************
3999 REM  SUBROUTINE TO COLLECT  DATA ********************
4000 VZ =  INT (16384 / 256)
4010 VX = 255 - VZ
4020 POKE 20994,64
4030 POKE 20995,(64 + PA)
4040 POKE 20996,(96 + SA)
4050 POKE 20993,VX
4060 POKE 20992,VZ
4070 CALL 20660
4080 B = 20998
```

```
4090 SA = SA + 1:XN = XN + 1
4100 RETURN
5000 SA = 12: FOR J = 1 TO NM
5010 GOSUB 4000
5020 PRINT D$;"BSAVE MICRO.";XN".";DC;",A"20998;",L";4096;",D2"
5030 NEXT
5040 RETURN
10500 PRINT "INPUT THE GAIN OF THE SYSTEM?": PRINT : PRINT : PRINT "1.  GAIG
10510 PRINT A$
10520 IF CG = 1 THEN R = 4
10530 IF CG = 2 THEN R = 5
10540 IF CG = 3 THEN R = 6
10550 IF CG = 4 THEN R = 7
10560 IF R = 7 THEN CZ = 50
10570 IF R = 6 THEN CZ = 10
10580 IF R = 5 THEN CZ = 5
10590 IF R = 4 THEN CZ = 1
10600 RETURN
10610 REM
10620 REM
10630 PRINT "INPUT VOLTAGE RANGE FOR THE TRIGGER": PRINT : PRINT : PRINT "1  G
10640 IF VG = 1 THEN VO = 4
10650 IF VG = 2 THEN VO = 5
10660 IF VG = 3 THEN VO = 6
10670 IF VG = 4 THEN VO = 7
10680 IF VO = 4 THEN VG$ = "+/- 5.0 VOLTS"
10690 IF VO = 5 THEN VG$ = "+/- 1.0 VOLTS"
10700 IF VO = 6 THEN VG$ = "+/- 0.5 VOLTS"
10710 IF VO = 7 THEN VG$ = "+/- 0.1 VOLTS"
10720 RETURN
11000 PRINT D$;"OPEN TEXT.";DC;",D2"
11010 PRINT D$;"DELETE TEXT.";DC
11020 PRINT D$;"OPEN TEXT.";DC
11030 PRINT D$;"WRITE TEXT.";DC
11040 PRINT "TRIGGER EDGE - POSITIVE"
11050 PRINT "THERE ARE ";NM;" CHANNELS"
11070 PRINT "THE TRIGGER LEVEL IS ";TX;"% ";VG$
11080 PRINT "GAIN = ";CZ;"  VOLTAGE RANGE = ";5 * 1000 / CZ;" MV"
11085 PRINT D$;"CLOSE TEXT.";DC
11090 RETURN
12000 PRINT D$;"RUN HELLO,D1"
12010 END

]
```

# Spreadsheet calculation to predict time differences

| Calculations from Geometry | Selected Values |
|---|---|
| Separation of microphones = | 0.28 |
| 'X' co-ordinate = | 0.59 |
| 'Y' co-ordinate = | 0.46 |
| 'Z' co-ordinate = | 0.95 |
| Temperature at which measurements occurred = | 20.00 |

**Derived values**

| | |
|---|---|
| Velocity of sound | 343.414 |
| **Diagonals of imaginary cube** | |
| 'R'- source to reference [OS] | 1.209 |
| XY diagonal [cS] | 0.748 |
| XZ diagonal [aS] | 1.118 |
| ZY diagonal [Ob] | 1.056 |

Distances to microphones along axes

| x - d | x + d |
|---|---|
| 0.31 | 0.87 |
| y - d | y + d |
| 0.18 | 0.74 |
| z - d | z + d |
| 0.67 | 1.23 |

Name of Record

*Mean of ten records*

Positive Octant

| Distance between microphone and the source - 'mx to S' | Distance in metres | Time in 20μS equiv. to distance | Time in 20 μS between mics | to nearest 20μS |
|---|---|---|---|---|
| m0 to S | 1.209 | 176.1 | | |
| m1 to S | 1.368 | 199.2 | 23.1 | 23 |
| m2 to S | 1.100 | 160.2 | 15.9 | 16 |
| m3 to S | 1.341 | 195.2 | 19.2 | 19 |
| m4 to S | 1.133 | 164.9 | 11.1 | 11 |
| m5 to S | 1.440 | 209.6 | 33.6 | 34 |
| m6 to S | 1.004 | 146.2 | 29.8 | 30 |
| **Angles to source** | Degrees | | | |
| Ø | 64.2 | | | |
| θ | 60.8 | | | |

| Separation of microphones | Diff. in distance travelled |
|---|---|
| [1 - 0] = x1 | 0.158 |
| [0 - 2] = x2 | 0.110 |
| [3 - 0] = x3 | 0.130 |
| [0 - 4] = x4 | 0.076 |
| [5 - 0] = x5 | 0.234 |
| [0 - 6] = x6 | 0.206 |
| Calculated angle - øc | 64.6 |

| Equation 1 | Calculation of 'R' |
|---|---|
| For 'x1' & 'x2' | 1.246 |
| For 'x3' & 'x4' | 1.220 |
| For 'x5' & 'x6' | 1.089 |
| Mean for 'R' | 1.185 |
| % error | -2.03% |

| Equation 2 | Calculation of 'x' |
|---|---|
| For 'x1' | 0.573 |
| For 'x2' | 0.583 |
| Mean | 0.578 |
| % error | -2.01% |

| Equation 3 | Calculation of 'y' |
|---|---|
| For 'x3' | 0.443 |
| For 'x4' | 0.449 |
| Mean | 0.446 |
| % error | -3.04% |

| Equation 4 | Calculation of 'z' |
|---|---|
| For 'x5' | 0.945 |
| For 'x6' | 0.936 |
| Mean | 0.941 |
| % error | -0.98% |

| Calculation of Angles | |
|---|---|
| Ø | 64.63 |
| % error | 0.7% |
| θ | 60.8 |
| % error | -0.0% |

# Spreadsheet calculation to calculate 'x,y,z' coordinates

| | A | B | C | D | E | F | G | H | I |
|---|---|---|---|---|---|---|---|---|---|
| 1 | Calculation of Co-ordinates from the equations ( [Vel.sound * 20 *x/1000] | | | | | | | | |
| 2 | Record | Actual readings taken from computer graph plotter | | | | | | Source | |
| 3 | 622 | 645 | 606 | 641 | 611 | 656 | 592 | 446 | |
| 4 | | DELAY TIME INTERVAL - 20 μS | | | | | | mo to S | |
| 5 | Record no. | 23 | 16 | 19 | 11 | 34 | 30 | 176 | |
| 6 | mean of 10 | | | | | | | | |
| 7 | | Distances in mm's between m0 and other microphones | | | | | | mo to S | |
| 8 | | 0.157 | 0.109 | 0.130 | 0.075 | 0.232 | 0.205 | 1.200 | |
| 9 | | | | | | | | | |
| 10 | | x 1 | x 2 | x 3 | x 4 | x 5 | x 6 | R(meas) | |
| 11 | Diff. dis | 0.157 | 0.109 | 0.130 | 0.075 | 0.232 | 0.205 | 1.200 | |
| 12 | Dist. to | 1.36 | 1.09 | 1.33 | 1.13 | 1.43 | 1.00 | meas R | |
| 13 | Dist. mx | 1.36 | 1.10 | 1.33 | 1.13 | 1.44 | 1.00 | calc R | |
| 14 | | 0.007 is Dist. travelled in 1 x 20μS | | | | | | | |
| 15 | Max diff | 0.16 | 0.12 | 0.14 | 0.08 | 0.24 | 0.21 | | |
| 16 | Min diff | 0.15 | 0.10 | 0.12 | 0.07 | 0.23 | 0.20 | | |
| 17 | | x | x | y | y | z | z | | |
| 18 | | 0.498 | 0.534 | 0.385 | 0.423 | 0.823 | 0.823 | | |
| 19 | 95% confidence | 0.595 | 0.595 | 0.455 | 0.448 | 0.993 | 0.986 | | |
| 20 | is betwe | 0.46 | 0.65 | 0.36 | 0.49 | 0.71 | 1.10 | | |
| 21 | lax & Mi | 1.22 | 1.21 | 1.01 | | | | | |
| 22 | "R" | 1.30 | 1.26 | 1.23 | | | | | |
| 23 | | Max 'x' 0.60 | | Max 'y' 0.46 | | Max 'z' 0.99 | | Max 'R' 1.30 | |
| 24 | | Min 'x' 0.50 | | Min 'y' 0.39 | | Min 'z' 0.82 | | Min 'R' 1.01 | |
| 25 | | Mean 'x' 0.56 | | Mean 'y' 0.43 | | Mean 'z' 0.91 | | Mean 'R' 1.20 | |
| 26 | | | | | | | | Std Dev 0.10 | |
| 27 | Calc. of | 1.26 | 1.23 | 1.12 | Mean R | 1.20 | θ | α | |
| 28 | Calculation of 'y | | Calculation of 'z | | Calculation of ' | | 61.03 | 28.97 | |
| 29 | 0.447 | 0.453 | 0.953 | 0.945 | 0.579 | 0.588 | øc | ø | |
| 30 | Mean 'y' | 0.450 | Mean 'z | 0.949 | Mean 'x | 0.583 | 64.54 | 64.54 | |
| 31 | ± | 0.06 | ± | 0.19 | ± | 0.10 | | | |
| 32 | | | | | | | | | |
| 33 | | | | | | | % error based upon distances | | |
| 34 | Measured error allowing ±20μS to each | | | | | | from geometric | calculation | |
| 35 | value of x,y,z and R | | | | | | x | -0.27 | #### |
| 36 | x | 16.37% | | | | | y | -0.62 | #### |
| 37 | y | 14.00% | % | | | | z | -1.04 | #### |
| 38 | z | 20.26% | | | | | | | |
| 39 | | | | | | | | | |
| 40 | | | | | | | | | |

# Collected wave data from plotter output

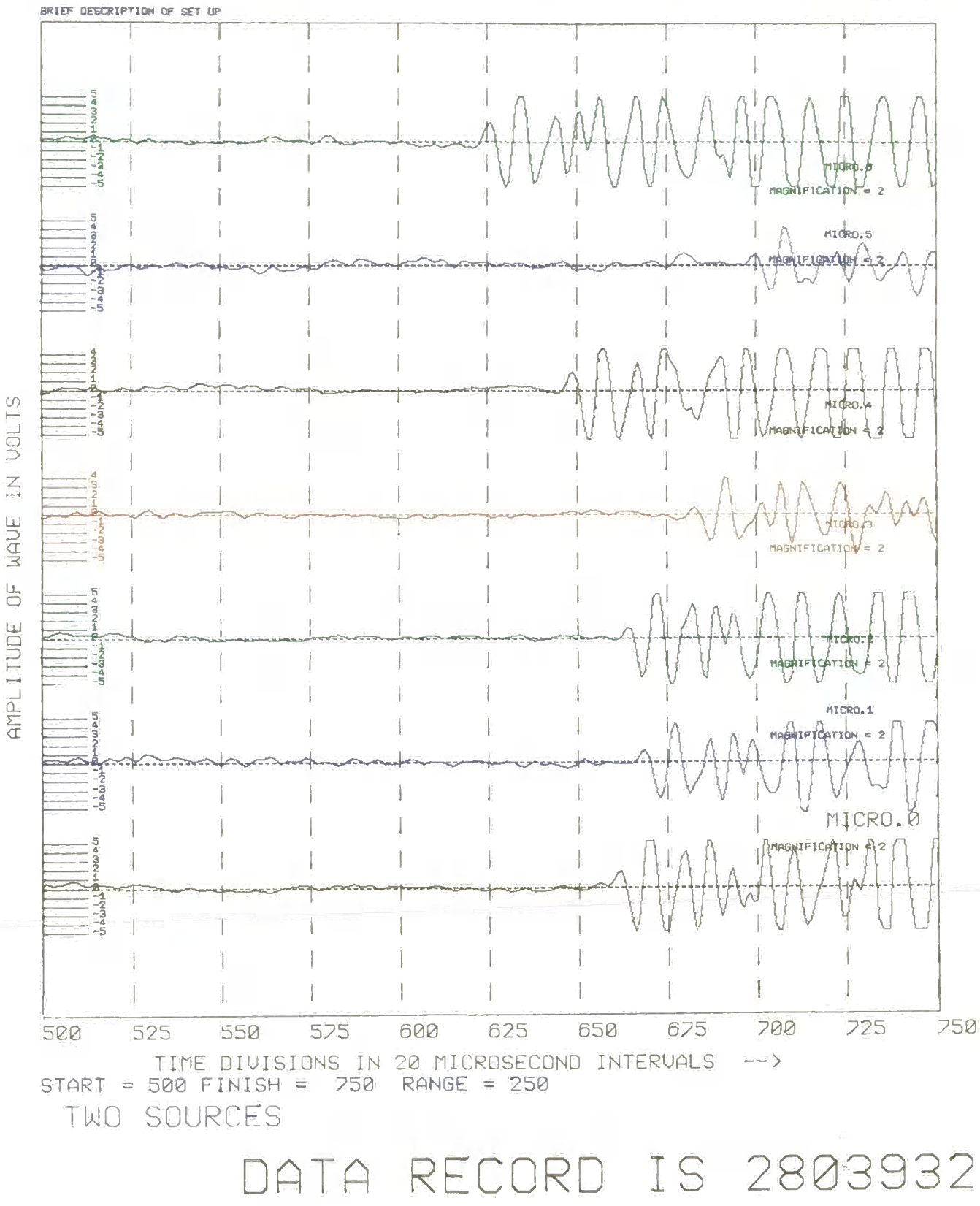

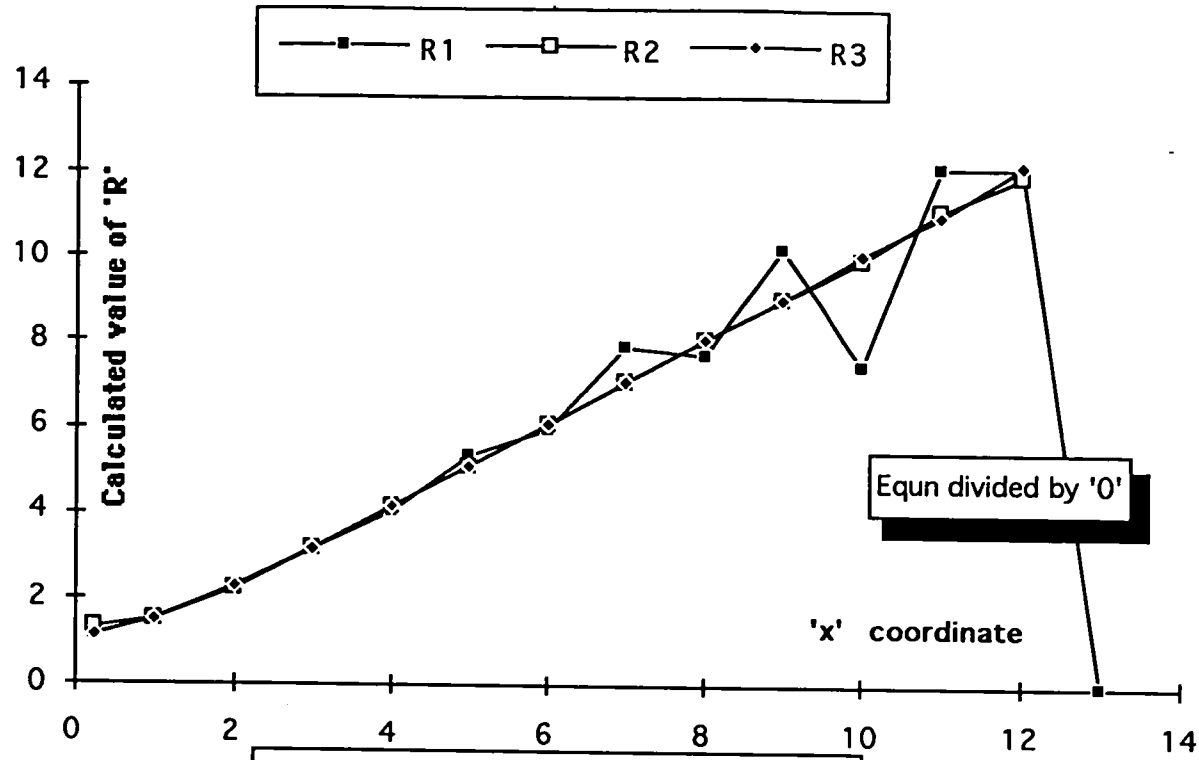


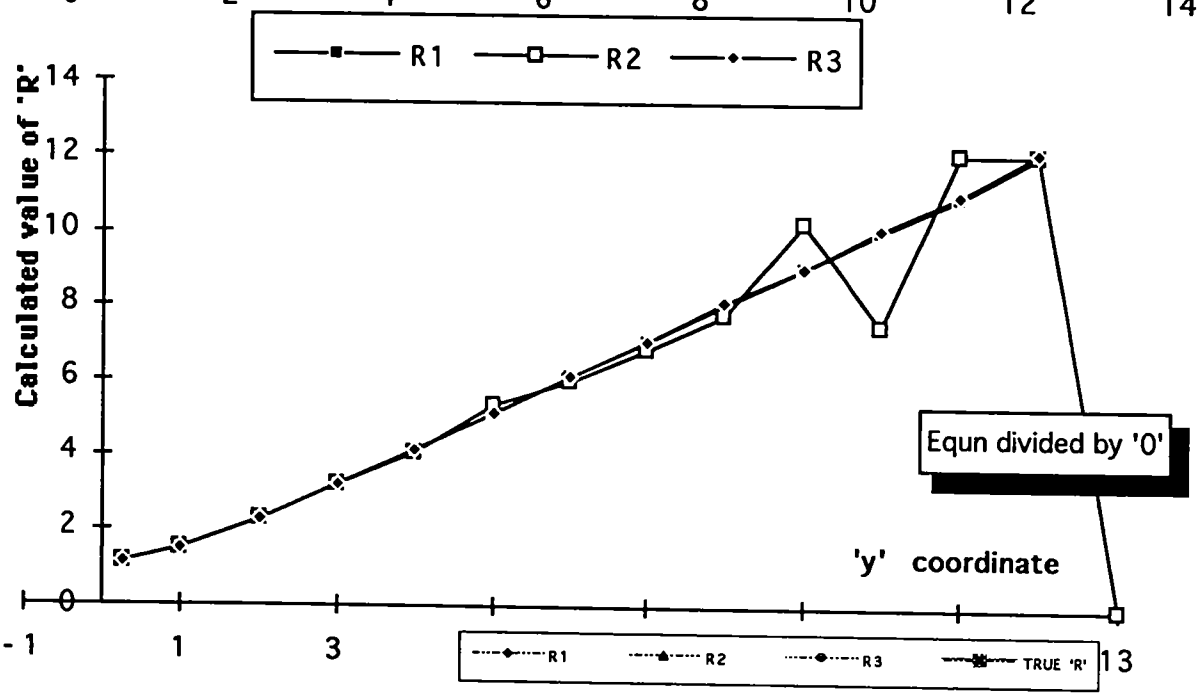


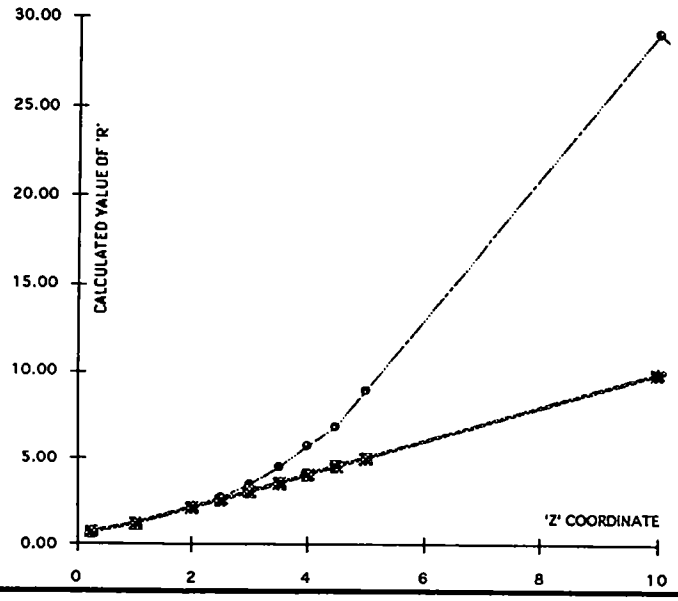


The divergence of the value for $R_1$ with 'x' varying and $R_2$ with 'y' varying, is not as great as for $R_3$ with 'z' varying. The start of the unreliable values is similar, starting when the variable coordinate is approximately 5 metres

# Bibliography & References

1 B&K TECHNICAL REVIEWS
No2 1979, No2 1980, No3 1981, No3,4 1982,No1,2 1984, No4

2 Barger James.E
Noise Path Diagnostics in Dispersive Structural Systems using Cross Correlation Analysis
Noise Control Engineering May-June 1976

3 Beauchamp, Yuen
Digital Methods for Signal Analysis
George Allen & Unwin 1979

4 Bendat, J.S
The Hilbert Transform and application to correlation transforms.
B&K 1985

5 Berman A, & Clay C.S.
Theory of Time-Averaged-Product Arrays
J.Acoust.Soc. of America Vol 29,No.7 July 1957805-812

6 Billingsley J. and R.Kinns
The Acoustic Telescope
J. of Sound & Vibration.(1976)48(4),485-510

7 Boone Marinus M. and A.J.Berkout
Theory and Applications of a High Resolution Synthetic Acoustic Antenna for Industrial Noise Measurement
Noise Control Engineering J. Vol 23 No.2 Sept-Oct 1984

8 Broadhurst A.D.
Applications of Acoustic Telescopes
Acustica Vol.43 1979

9 Brown, Robert Grover
Introduction to Random Signal Analysis and Kalman Filtering
John Wiley and Son, New York 1983

10 Bryant James and Lew Counts
Ask the applications engineer
Analog Dialogue 24-2 1990

11 Bucker Homer,P.
Cross-sensor beam forming with a sparse line array
J.Acoust.Soc.of America Vol.61 No.2 Feb 1977

12 Bullen R and F.Fricke
Time-distribution of impulse noise in an enclosure
J. of Sound & Vibration(1982)80(1),25-30

13 Carter Clifford, G
Variance bounds for passively locating an acoustic source with a symmetric line array.
J.Acoust.Soc.of America Vol.62 No. 4 Oct 1977

14 Carter,G. Knapp,H. and Nuttall, A
Statistics of the Estimate of the Magnitude-Coherence Function IEEE Transactions on Audio and Electroacoustics
August 1973

15 Chen C.H.
Digital Waveform Processing and Recognition
CRC Press Inc Boca Raton, Florida

16 Chen Yaoming and Huang Zengyang
Prony's Method for processing of Data with White or Colour Noise
Chinese Journal of Acoustics Vol.2 No.2 1983

17 Cops and Minten
Comparative study between the sound intensity method and the conventional two room method to calculate the sound transmission loss of wall constructions
Noise Control Engineering Vol.22, No.3 May-June 1984

18 Cremer L.
Theory of the sound attenuation of thin walls with oblique incidence.
Akustische Zeitschrift No.3 vii May 1942 pp 91-104

19 DeNoyer L.K. & Dodd J.G.
Maximum Likelihood smoothing of data.
International Laboratory, June 1990 P.16-22

20 Dowling A.P. and J.E.Ffowcs Williams
Sound and sources of sound
Ellis Horwood Publishers 1983

21 Dym and Lang
Transmission of sound through sandwich panels.
J.Acoust.Soc. of America 1974, Nov. 56

22 Fakley, D.C.
Comparison between the Performances of a Time-Averaged Product Array and an Interclass Correlator
J.Acoust.Soc.of America Vol.31 No.10 October 1959

23 Fan H. El-Masry E.I. & Jenkins W.K.
Digital Extrapolation Beamforming
ICASSP 83 Boston CH1841-6/83/0000-0367

24 Gerretsen E.
Calculation of the sound transmission between dwellings by partitions and flanking structures.
Applied Acoustics 0003-682X/79/0012-0413

25 Goff Kenneth W.
The Application of Correlation Techniques to some Acoustic Measurements
J.Acoust.Soc.of America Vol27, No.2 March 1955

26 Gowar,N.W.,Baker,J.E
Fourier Series
William Collins & Sons 1974

27 Gridley, Doreen
Program for narrow-band analysis of aircraft flyover noise using ensemble averaging techniques.
NASA Contractor Report 165867

28 Guy J.R.F. & Davies D.E.N.
Studies of the Adcock direction finder in terms of phase-mode excitations around circular arrays
The Radio and Electronic Engineer, Vol 53 No.1 pp 33-38 Jan 1983

29 Harris, F.J
On the use of windows for the harmonic analysis with discrete fourier transform
Proc.IEEE 1978 vol 66,pp 51-83

30 Hebbert, R.S.,Leha T.Barkakati
An extension of maximum entropy beamforming to arbitrary planar arrays with statistics.
J.Acoust. Soc. of America.76(3)Sept 1984

31 Hinich Melvin J.
Processing spatially aliased arrays
J.Acoust.Soc.of America Vol.64 No.3 Sept 1978

32 Hinich Melvin J.
Passive range estimation using subarray parallax
J.Acoust.Soc.of America Vol.65 No.5 May 1979

33 Inomoto,K and Hattori,S
Prony's Method applied to estimate noise source locations and their sound powers.
J. of Sound & Vibration 1983 89(4), 509-517

34 Jacobson Melvin J.
Analysis of a Multiple Receiver Correlation System
J.Acoust.Soc.of America Vol.29, No,12 Dec 1957, 1342-1347

35 Jacobson, Melvin,J
Correlation of a Finite Distance Point Source
J.Acoust.Soc.of America Vol.31 No.4 April 1959

36 Jones Robert E.
How to accurately predict the sound insulation of partitions.
J. of Sound & Vibration June 1979

37 Jong M.T.
Methods of Discrete Signal and System Analysis
McGraw-Hill Series in Electrical Engineering

38 Kates James, M.
A generalised approach to High-Resolution Array Processing
ICASSP 83,Boston CH1841-6/83/0000-0328 1983 IEEE

39 Kinns R.
Aliasing in the Time Domain for the Estimation of Power Spectra
J. of Sound & Vibration(1973)26 (1) 121-128

40 Kino Gordon S.
Acoustic Waves - Devices, Imaging & Analog Signal Processing
Prentice-Hall Signal Processing Series - Alan V.Oppenheim Editor

41 Landers T.E. & Lacoss R.T.
Long Range Acoustic Tracking of Low Flying Aircraft
J.Acoustical Soc. of America Annual Meeting Honolulu , Hawaii Nov-dec 1978

42 Lee,Robert P.
Analysis of the errors of atmospheric sound ranging
Atmos. Sciences Lab White Sands Missile Range

43 Lockwood J.C. Thorn J.V. & Booth N.O.
Directivity index of arrays of random line arrays
J.Acoust.Soc.of America Vol.72 No.1 July 1982

44 Low Hua Kin
Prediction and measurements of airborne sound transmission through concrete structures.
Architectural Science Review March 1974, p.5-9

45 Lowenstein Carl, D. & Anderson Victor,C.
Quick Characterisation of the Directional Response of Point Array
J.Acoust.Soc.of America Vol.43 No.1 1968

46 Lyon Richard H.
Machinery Noise and Diagnostics
Butterworths

47 Maksym, J.N.
Directional Accuracy of Small Ring Arrays
J.Acoust.Soc.of America Vol.61 No.1 Jan 1977

48 Mason Warren,P & Thurston R.N. Edited by
Physical Acoustics Volume XVII
Academic Press San Diego California 1988

49 McDonald Verne, H. & Schultheiss, Peter,M.
Optimum Passive Bearing Estimation in a Spatially Incoherent Noise Environment
J.Acoust.Soc.of America Vol.46 No.1(Prt 1) 1969

50 Merrill I, Skolink
Introduction to Radar Systems
McGraw-Hill 1983

51 Mohlman,HT
Computer programs for producing single-event aircraft noise data for spec.

52 Newland D.E.
An introduction to Random Vibrations and Spectral Analysis
Longman Group Ltd.1984

53 Nilsson A.C.
Reduction index and boundary conditions for a wall between two rectangular rooms.
Acustica 1972,vol.26(pp.1-23)

54 Nuttall,A.H.,Carter,G,C and Montavon,E.M
Estimation of the two-dimensional spectrum of the space-time noise field for a sparse line array.
J.Acoust.Soc.of America Vol.55 No.5 May 1974

55 Pernet and Payne
Non-linear propagation of signals in air
J. of Sound & Vibration.(1971)17(3),383-396

56 Prasad, M.G. and Crocker, M.J
Acoustical Source Characterisation Studies.
J. of Sound & Vibration 1983 Vol.90, No.4 pp.479-490

57 Randell,R.B
Application of B&K Equipment to Frequency Analysis
B&K 1977

58 Rathe E.J.
Note on two common problems of sound propagation
J. of Sound & Vibration(1969)10(3),472-479

59 Schelkunoff S.A.
A Mathematical Theory of Linear Arrays
Bell System Technical Journal

60 Steinberg Bernard D.
Principles of Aperture and Array System Design Including Random and Adaptive Arrays
John Wiley and Son, New York 1976

61 Streit Roy, L.
Optimisation of discrete arrays of arbitrary geometry
J.Acoust.Soc.of America Vol.69(1) Jan 1981

62 Swingle Donald M.
Effects of arrival time errors in weighted range equation solutions for linear base sound ranging.

63 Vaicaitis R, M,Slazak
Noise transmission through stiffened panels.
J. of Sound & Vibration(1980)70/3,413-426

64 Willen W. & Wempson J.
FFT-Based, High Resolution Measuring technique with Application to Outdoor Ground Impedance at Grazing Incidence
Noise Contro;l Engineering Sept-Oct 1986

65 Wingle,D, Crenshaw, C & Bellucci, R
Improved Sound Ranging Location of Enemy Artillery
Army Science Conf. US Military Academy 1970

66 Youn. D.H.
Time delay estimation via coherence:An adaptive approach.
J.Acoust.Soc. of America,75(2)Feb1984

67 Faran, J.J. jnr & Hills, R. jnr
The Application of Correlation Techniques to Acoustic Receiving Systems.
Technical memo No.28, Acoustics Research Laboratory, Harvard University, Camb. Mass.(1952)

68 Cheatham, T.P.
An Electronic Correlator
R.L.E. Technical Report No.122, Research Laboratory of Electronics, M.I.T. Cambs, Mass. (1951)

69 Escudié B. and Chiollaz M.
Interferometric Acoustic Imaging of Railway Noise
J.Acoust. Soc. of America (1988( 120(2), 303-310

70 Flynn, O.E. & Kinns, R.
Multiplicative Signal Processing for Sound Source Location on Jet Engines
J.Acoust. Soc. of America(1976)46(1),137-150

71 Goff, Kenneth W.
An Analog Correlator for Acoustic Measurements
J.Acoust. Soc of America March 1955Vol 27, Number 2, 223-237

72 Redfern ,F.R. & Munson, R.D.
Acoustic Emission Source Location - A mathematical analysis
Report 8692, U.S.Dept. of the Interior, Bureau of Mines 1978

73 Kinns, R
Binaural Source Location
J.Acoust. Soc. of America (1976)44(2),275-289

74 Lai, J.C.S.
Application of Sound Intensity Technique to Noise Source Identification: A Case Study
Applied Acoustics 34(1991) 89-100

75 Attenborough, K. Heap, N. Oldham, D.J. Orlowski, R.J.
The Prediction of Sound Radiation from Buildings

76 Hopkins, M.E.
Investigation of Sound Insulation in a New Build Tenament and Identification of the Flanking Transmission Paths
Diploma in Acoustics Project, July 1987